

canadian acoustics

acoustique canadienne

Journal of the Canadian Acoustical Association - Revue de l'Association canadienne d'acoustique

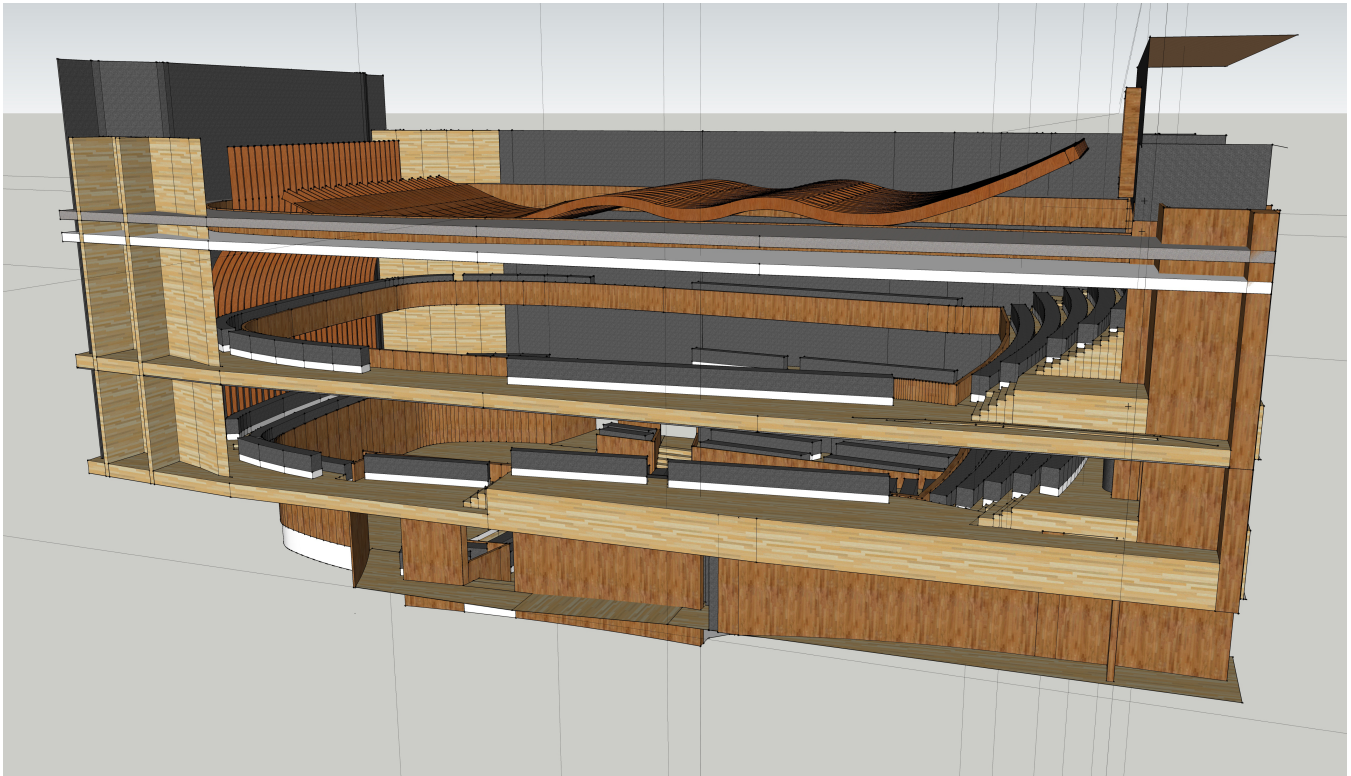
SEPTEMBER 2018

Volume 46 - - Number 3

SEPTEMBRE 2018

Volume 46 - - Numéro 3

EDITORIAL - ÉDITORIAL	3
ARCHITECTURAL ACOUSTICS - ACOUSTIQUE ARCHITECTURALE	5
HEARING CONSERVATION - PRÉSERVATION DE L'OUÏE	15
PHYSICAL ACOUSTICS / ULTRASOUNDS - ACOUSTIQUE PHYSIQUE / ULTRASONS	19
PSYCHOLOGICAL ACOUSTICS - PSYCHO-ACOUSTIQUE	29
CONSULTING - CONSULTATION	43
OTHER FEATURES - AUTRES RUBRIQUES	49



canadian acoustics

acoustique canadienne

Canadian Acoustical Association/Association
Canadienne d'Acoustique P.B. 74068 Ottawa,
Ontario, K1M 2H9

Association canadienne d'acoustique B.P. 74068
Ottawa, Ontario, K1M 2H9

Canadian Acoustics publishes refereed articles and news items on all aspects of acoustics and vibration. Articles reporting new research or applications, as well as review or tutorial papers and shorter technical notes are welcomed, in English or in French. Submissions should be sent only through the journal online submission system. Complete instructions to authors concerning the required "camera-ready" manuscript are provided within the journal online submission system.

L'Acoustique Canadienne publie des articles arbitrés et des informations sur tous les aspects de l'acoustique et des vibrations. Les informations portent sur la recherche, les ouvrages sous forme de revues, les nouvelles, l'emploi, les nouveaux produits, les activités, etc. Des articles concernant des résultats inédits ou des applications ainsi que les articles de synthèse ou d'initiation, en français ou en anglais, sont les bienvenus.

Canadian Acoustics is published four times a year - in March, June, September and December. This quarterly journal is free to individual members of the Canadian Acoustical Association (CAA) and institutional subscribers. Canadian Acoustics publishes refereed articles and news items on all aspects of acoustics and vibration. It also includes information on research, reviews, news, employment, new products, activities, discussions, etc. Papers reporting new results and applications, as well as review or tutorial papers and shorter research notes are welcomed, in English or in French. The Canadian Acoustical Association selected Paypal as its preferred system for the online payment of your subscription fees. Paypal supports a wide range of payment methods (Visa, Mastercard, Amex, Bank account, etc.) and does not require you to have already an account with them. If you still want to proceed with a manual payment of your subscription fee, please use the application form from the CAA website and send it along with your cheque or money order to the secretary of the Association (see address above). - Canadian Acoustical Association/Association Canadienne d'Acoustique/o JASCO Applied Sciences 2305-4464 Markham Street Victoria, BC V8Z 7X8 Canada - - secretary@caa-aca.ca - Dr. Roberto Racca

Acoustique canadienne est publié quatre fois par an, en mars, juin, septembre et décembre. Cette revue trimestrielle est envoyée gratuitement aux membres individuels de l'Association canadienne d'acoustique (ACA) et aux abonnés institutionnels. L'Acoustique canadienne publie des articles arbitrés et des rubriques sur tous les aspects de l'acoustique et des vibrations. Ceci comprend la recherche, les recensions des travaux, les nouvelles, les offres d'emploi, les nouveaux produits, les activités, etc. Les articles concernant les résultats inédits ou les applications de l'acoustique ainsi que les articles de synthèse, les tutoriels et les exposées techniques, en français ou en anglais, sont les bienvenus. L'Association canadienne d'acoustique a sélectionné Paypal comme solution pratique pour le paiement en ligne de vos frais d'abonnement. Paypal prend en charge un large éventail de méthodes de paiement (Visa, Mastercard, Amex, compte bancaire, etc) et ne nécessite pas que vous ayez déjà un compte avec eux. Si vous désirez procéder à un paiement par chèque de votre abonnement, merci d'utiliser le formulaire d'adhésion du site de l'ACA et de retourner ce dernier avec votre chèque ou mandat au secrétaire de l'association (voir adresse ci-dessus). - Canadian Acoustical Association/Association Canadienne d'Acoustique/o JASCO Applied Sciences 2305-4464 Markham Street Victoria, BC V8Z 7X8 Canada - - secretary@caa-aca.ca - Dr. Roberto Racca

EDITOR-IN-CHIEF - RÉDACTEUR EN CHEF

Umberto Berardi
Ryerson University
editor@caa-aca.ca

DEPUTY EDITOR RÉDACTEUR EN CHEF ADJOINT

Romain Dumoulin
CIRMMT - McGill University
deputy-editor@caa-aca.ca

JOURNAL MANAGER DIRECTRICE DE PUBLICATION

Cécile Le Cocq
ÉTS, Université du Québec
journal@caa-aca.ca

COPYEDITOR RELECTEUR-RÉVISEUR

Olivier Valentin, M.Sc., Ph.D.
Université de Sherbrooke
copyeditor@caa-aca.ca

ADVERTISING EDITOR RÉDACTEUR PUBLICITÉS

Bernard Feder
HGC Engineering
advertisement@caa-aca.ca

ADVISORY BOARD COMITÉ AVISEUR

Jérémie Voix
ÉTS, Université du Québec

Frank A. Russo
Ryerson University

Ramani Ramakrishnan
Ryerson University

Bryan Gick
University of British Columbia

Contents - Table des matières

EDITORIAL - ÉDITORIAL	3
ARCHITECTURAL ACOUSTICS - ACOUSTIQUE ARCHITECTURALE	5
Development Of A Method To Realize A Uniform Sound Field In Three Dimensional Spaces Based On The RayTracing Algorithm <i>Yigang Lu, Hengling Song</i>	5
HEARING CONSERVATION - PRÉSERVATION DE L'OUÏE	15
Field Attenuation Of Individual Orchestra Shields <i>Alberto Behar, Mohammad Abdoli-Eramasaki, Stephen Mosher</i>	15
PHYSICAL ACOUSTICS / ULTRASOUNDS - ACOUSTIQUE PHYSIQUE / ULTRASONS	19
Simulation Study Of SuperResolution In Hydrophone Measurements Of Pulsed Ultrasonic Fields <i>Wahiba Djerir, Tarek Boutkedjirt</i>	19
PSYCHOLOGICAL ACOUSTICS - PSYCHO-ACOUSTIQUE	29
Perspectives On How Acoustical NonAcoustical And User Characteristics Should Be Considered In Multimodal Virtual Reality Research And Application <i>Jennifer L Campos, Darryl McCumber, Brian Chapnik, Gurjit Singh, Sin-Tung Lau, Karen Z. H. Li, Victoria Nieborowska, Kathleen Pichora-Fuller</i>	29
CONSULTING - CONSULTATION	43
True North: A Comparison of Measured vs Modelled Noise Levels with iNoise <i>Henk de Haan, Virgini Senden</i>	43
OTHER FEATURES - AUTRES RUBRIQUES	49
Call for Papers - Special Issue on Audiology and Neuroscience - Appel à soumission - Numéro spécial sur l'audiologie et les neurosciences	49
CAA Announcements - Annonces de l'ACA	53

For
Digital Recorders

Introducing

For
USB A/D Systems

PHANTOM POWER

7052PH

Measurement Mic System

7052H Type 1.5™

Titanium Diaphragm

3Hz to >20 kHz

<20 dBA > 140 dBSPL

MK224 (<14 dBA to >134 dBSPL) Optional

4048 Preamp

Superior
IEC 1094 Type 1
Long-term Stability
Temperature and Humidity
Performance

Now in Stock

**Phantom
to IEPE/ICP
Adaptor
Supplies 3-4 mA
Power
Accelerometers
Microphones**

ICP1248

A **B**
C **e**
O **g**
u **i**
S **n**
t **S**
i **w**
c **i**
S **t**
O **h**
A
C
C
O



**MATT™
Family**

Mic Attenuator

Handle Higher Sound Pressure Levels

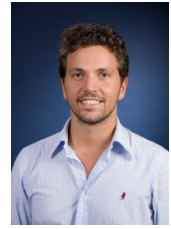
ACO Pacific, Inc., 2604 Read Ave., Belmont, CA 94002

Tel: (650) 595-8588 FAX: (650) 591-2891 E-Mail: sales@acopacific.com

Web Site: www.acopacific.com

TM

Editor's note: North-America Acoustics stops in Victoria Éditorial : L'acoustique nord-américaine s'arrête à Victoria



North-America Acoustics stops in Victoria, BC

Dear reader, welcome to the third issue of our 46th year. This issue includes articles about architectural acoustics, hearing conservation, physical acoustics, and psychological acoustics. If somebody has ever doubted about why our discipline is so amazing, please consider the broad range of topics, fields, applications, and discoveries that acoustics enables and that you will read in this issue.

While I am writing this editorial, I cannot avoid to think that the upcoming joint 176th Meeting of the Acoustical Society of America (ASA) that will be held jointly with the Acoustics Week in Canada 2018 of the Canadian Acoustical Association (CAA) in Victoria, BC, Canada, is approaching (5-9 November 2018).

I hope many CAA members will join, and will celebrate this great event in our country with our fellow friends from the States. I am glad to report that thanks to the excellent organizational committee, there will be more than usual possibilities to follow this conference, even after the conference! Speeches, unless denied by the authors, will be recorded and disseminated through ASA channels (non-attendees will be charged a fee to be able to access the recordings).

I also kindly encourage those who are members of both the ASA and the CAA to use preferably their CAA membership status while registering, and to submit their paper to the next CAA special issue. We are collecting (as usual) 2-page articles presented at the conference in our December issue. What a Christmas gift for the readers of the Canadian Acoustics journal!

Meanwhile, I wish you a pleasant reading of this issue.

Umberto Berardi,
Editor-in-chief.

L'acoustique nord-américaine s'arrête à Victoria, BC

Chère lectrice, cher lecteur, bienvenue au troisième numéro de notre 46ème année. Ce numéro comprend des articles sur l'acoustique architecturale, la préservation de l'audition, l'acoustique physique et la psychoacoustique. Si quelqu'un s'est déjà demandé pourquoi notre discipline est si formidable, il devrait considérer le large éventail de sujets, de domaines, d'applications et de découvertes que l'acoustique permet et qui vous est présenté dans ce numéro.

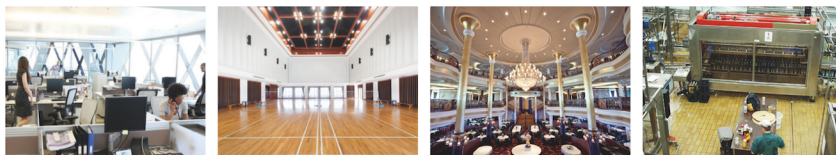
Pendant que j'écris cet éditorial, je ne peux m'empêcher de penser à la prochaine réunion conjointe de la 176e réunion de la Société d'acoustique américaine (ASA), qui se tiendra conjointement avec la Semaine de l'acoustique au Canada 2018 de l'Acoustique Canadienne (CAA), à Victoria, en Colombie-Britannique, très prochainement (du 5 au 9 novembre 2018).

J'espère que de nombreux membres de la CAA se joindront à nous et célébreront ce grand événement dans notre pays avec nos amis états-uniens. Je suis heureux d'annoncer que, grâce à l'excellent comité d'organisation, les possibilités de suivre cette conférence, même après celles-ci, seront plus nombreuses que d'habitude ! Les exposés, sauf refus des auteurs, seront enregistrés et diffusés via les canaux de l'ASA (des frais seront exigés aux non-participants pour l'accès aux enregistrements).

J'encourage également les membres à la fois de l'ASA et de la CAA à utiliser de préférence leur statut de membre CAA lors de leur inscription et à soumettre leur communication au prochain numéro spécial du journal de la CAA. Nous rassemblons (comme d'habitude) des articles de deux pages présentés à la conférence dans notre numéro de décembre. Quel cadeau de Noël pour les lecteurs du journal L'Acoustique Canadienne !

En attendant, je vous souhaite une bonne lecture de ce numéro.

Umberto Berardi,
Rédacteur en chef



CadnaR is the powerful software for the calculation and assessment of sound levels in rooms and at workplaces

Intuitive Handling

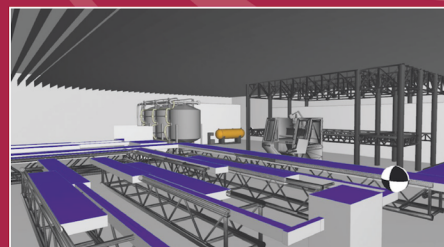
The clearly arranged software enables the user to easily build models and make precise predictions. At the same time you benefit from the sophisticated input possibilities as your analysis becomes more complex.

Efficient Workflow

Change your view from 2D to 3D within a second. Multiply the modeling speed by using various shortcuts and automation techniques. Many time-saving acceleration procedures enable a fast calculation process.

Modern Analysis

CadnaR uses scientific and highly efficient calculation methods. Techniques like scenario analysis, grid arithmetic or the display of results within a 3D-grid enhance your analysis and support you during the whole planning and assessment process.



Fields of Application

Office Environments

- Process your acoustic calculations and assessments according to DIN 18041, VDI 2569 and ISO 3382-3
- Receiver chains serve as digital "measurement path" and provide you with relevant insights into the acoustic quality of rooms during the planning phase
- Import of DWG-/DXF-/SKP-files (e.g. pCon.planner, AutoCAD, SketchUp)
- Visualization of noise propagation, noise levels and parameters for quality criteria like the Speech Transmission Index STI

Production Plants

- Calculation of the sound load at workplaces based on the emission parameters specified by the machine manufacturer according to the EC guideline 2006/42/EC while also taking the room geometry and the room design into account
- Tools for enveloping surfaces and free field simulations to verify the sound power of the sources inside of the enveloping surface
- Calculation of the sound power level based on technical parameters such as rotational speed or power



Distributed in the U.S. and Canada by: Scantek, Inc. Sound and Vibration Instrumentation and Engineering
6430 Dobbin Rd, Suite C | Columbia, MD 21045 | 410-290-7726 | www.scantekinc.com

DEVELOPMENT OF A METHOD TO REALIZE A UNIFORM SOUND FIELD IN THREE-DIMENSIONAL SPACES BASED ON THE RAY-TRACING ALGORITHM

Yigang Lu ^{*1} and Hengling Song ^{†1}

¹School of Architecture, South China University of Technology, Guangzhou, China

Résumé

Dans la présente étude, une méthode de cartographie des mouvements de rayons dans les espaces géométriques tridimensionnels a été établie théoriquement en utilisant un algorithme de radiosité (*ray-tracing*). Les chemins le long desquels se propage le rayon acoustique dans des espaces clos rectangulaires et concaves sont décrits selon l'algorithme de radiosité. La localisation et la direction du rayon acoustique à des points arbitraires sur les chemins ont été explorés. Les plus grands exposants de Lyapunov (PGEL) des systèmes de rayons dans les espaces rectangulaires et concaves ont été déterminés en utilisant l'algorithme de Wolf selon les points sur les chemins de propagation avec une longueur égale dans la série chronologique. Une nouvelle géométrie chaotique concave est produite avec un PGEL positif. Les PGEL de la dynamique de rayon entre les deux espaces géométriques ont été comparés et les résultats indiquaient que le rayon se déplace de manière régulière dans l'espace rectangulaire avec un PGEL de 0 tandis que le rayon adopte un comportement chaotique dans l'espace concave avec un PGEL positif. Les champs acoustiques dans chacun de ces espaces ont été décrits en appliquant le chaos du rayon à l'acoustique des bâtiments. La diffusion acoustique a été évaluée selon l'uniformité des niveaux de pression acoustique à différentes positions dans le champ acoustique en utilisant un logiciel d'acoustique de la salle Odeon. Les résultats ont démontré que le modèle proposé a le potentiel de simuler la dynamique chaotique des rayons acoustiques dans les espaces clos.

Mots clefs : diffusion, ray-tracing, radiosité, plus grand exposant de Lyapunov, algorithme de Wolf, acoustique des salles

Abstract

In this study, a method of mapping ray motions in three-dimensional geometrical spaces was theoretically established using the ray-tracing algorithm. The paths along which the acoustic ray propagates in enclosed rectangular and concave spaces are described according to the ray-tracing algorithm. The location and the direction of the acoustic ray at arbitrary points on the paths were explored. The largest Lyapunov exponents (LLEs) of the ray systems in the rectangular and concave spaces were determined using the Wolf algorithm based on the points on the propagation paths with equal length in the time series. A new chaotic concave geometry is produced with a positive LLE. The LLEs of ray dynamics between the two geometrical spaces were compared and the results showed that the ray moves in a regular fashion in the rectangular space with an LLE of 0 whereas the ray exhibits chaotic behavior in the concave space with a positive LLE. The acoustic fields in both of these spaces were described by applying ray chaos to the building acoustics. The acoustic diffusion was evaluated based on the uniformity of the sound pressure levels at different positions in the sound field using Odeon room acoustics software. The results showed that the proposed model has the potential to simulate chaotic dynamics of acoustic rays in enclosed spaces.

Keywords: diffusion, ray-tracing algorithm, largest Lyapunov exponent, Wolf algorithm, room acoustics

1 Introduction

Particle billiard theory is originally used in the electromagnetic field [1, 2] and in quantum mechanics studies [3–5]. However, in room acoustics, the scenario in which the sound rays bounce back and forth in an enclosed space can be analyzed by establishing the sound ray model. Tracking acoustic arrays is crucial for ocean acoustics applications such as underwater acoustic communication and ocean acoustic tomography. Li et al. [6], Brown et al. [7], and Makarov et al. [8] used the ray chaos model to investigate the effects of sound velocity on the system

dynamics behavior in underwater acoustics. The results showed that the acoustic ray system was randomly interfered underwater because of the characteristics of the inhomogeneous seawater medium. Studies on the effects of random disturbance on the characteristics of the acoustic ray system characteristics showed that the acoustic ray motions changed from regular to irregular or the original irregular motions of the acoustic rays were intensified when a random disturbance was introduced into the system and the intensity of the random disturbance was increased. In the absence of reflections underwater, the increased disturbance of the internal waves on the sound velocity resulted in a system with a positive Lyapunov exponent. This increased the chaotic motion of the acoustic rays and expanded the chaotic region [9]. Similar to the results obtained for

* phyiglu@scut.edu.cn

† shm3214974@hotmail.com

underwater acoustics, Kawabe et al. [10] found that perturbations in the sound velocity resulted in a chaotic acoustic ray propagation due to the temperature fluctuations caused by the inhomogeneous medium in the room. For example, for a two-dimensional space with an inhomogeneous medium, there were slight deviations in the acoustic ray trajectories such that the acoustic rays did not travel in a straight line because of perturbations. The acoustic ray trajectory was curved when there were temperature fluctuations in the medium. Ray chaos was observed in the domain when perturbations due to the inhomogeneity of the medium were considered in the analysis. However, for a homogeneous medium, the non-interacting rays would always propagate along a straight trajectory between the boundaries of the domain. According to the billiard theory, the chaotic behavior of acoustic rays is closely related to the geometry of the enclosed space. Koyanagi et al. [11] used the square well potential model to simulate the acoustic ray motions in a room where the absorption was uniformly distributed along the boundaries and the results showed that the square well potential model can be used to determine the reverberation time in a two-dimensional enclosed space. They computed the largest Lyapunov exponents (LLEs) and they believed that reverberation of the sound field was related to the ray chaos of the billiards in the polygons with smooth convex walls. Yu and Zhang [12, 13] used 13 acoustic ray equations to describe the acoustic ray motions in a two-dimensional semicircle stadium model and computed the Lyapunov spectrum of the ray systems using the classic Wolf algorithm. They obtained the power law of the Lyapunov exponents used in architectural acoustics in order to describe the characteristics of acoustic defects such as diffusion, flutter echoes, and acoustic focusing. Most of the studies published to date are focused on two-dimensional systems because the simplest form of classical chaos is two-dimensional. However, a three-dimensional system is a more accurate representation of the real-world system and it has more practical significance in architectural acoustics. Hence, this work is focused on investigating acoustic ray chaos in a three-dimensional enclosed space based on a two-dimensional enclosed space.

The remainder of this paper is organized as follows. The ray-tracing algorithms used to track the trajectories of acoustic rays in the geometrical space are presented in Section 2. The LLEs of ray systems in the rectangular and concave enclosed spaces were calculated and presented in Section 3, in which the chaotic characteristics for the concave geometry are derived. The ray systems are then used for building acoustics and the results are validated using Odeon room acoustics software, as presented in Section 4. Finally, the conclusions drawn based on the findings of this study are presented in Section 5 and the significance of the method proposed in this work is highlighted.

2 Method

2.1 Ray-tracing algorithm

The points in the time series used to determine the LLEs are extracted from the reflection paths in a three-dimensional geometrical space using the random ray-tracing algorithm. The ray moves in a straight trajectory with an initial direction from a source in the geometrical space and the ray then changes its direction when it encounters a surface. In this algorithm, it is assumed that only specular reflections occur and therefore, the angle of reflection is equal to the angle of incidence at each point on the surface. Figure 1 shows the ray reflections on the rigid smooth boundary of a geometrical space.

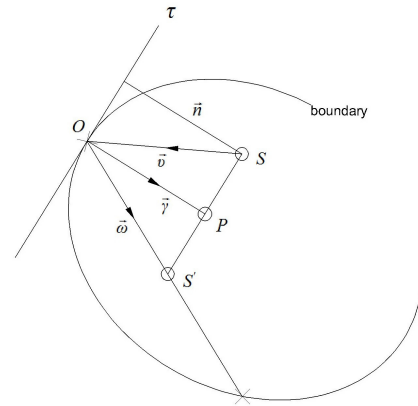


Figure 1: Specular reflections on the rigid smooth boundary of a geometrical space.

It is assumed that the acoustic ray moves in the domain (which is determined by the geometrical space) depending on the reflections at the boundaries:

$$f_i(x, y, z) = 0, \quad i \in Z^d, d \geq 1 \quad (1)$$

The launching ray \overline{SO} exerted by the source S is given by:

$$\begin{cases} x = x_0 + at \\ y = y_0 + bt, \quad t \in R_+ \\ z = z_0 + ct \end{cases} \quad (2)$$

Where $S(x_0, y_0, z_0)$ represents the coordinates of the source and $\vec{v} = (a, b, c)$ represents the directional vector of the incident ray, which is not normal to the boundary. A singularity will occur if the directional vector is normal to the boundary.

The reflection point, $O(x_0 + at_{min}, y_0 + bt_{min}, z_0 + ct_{min})$ is determined by substituting Eq. (2) into Eq. (1), where the line intersects the surface of the boundary:

$$f_i(x_0 + at_{min}, y_0 + bt_{min}, z_0 + ct_{min}) = 0 \quad (3)$$

Here, the subscript “min” stands for minimum parameter “t”, which is required for the intersection.

The normal vector across the reflection point is expressed as:

$$\vec{n} = \left(\frac{\partial f(x_{min}, y_{min}, z_{min})}{\partial x}, \frac{\partial f(x_{min}, y_{min}, z_{min})}{\partial y}, \frac{\partial f(x_{min}, y_{min}, z_{min})}{\partial z} \right) \quad (4)$$

The normal vector $\vec{\gamma}$ is determined from the projection method, as follows:

$$\vec{\gamma} = -\frac{\vec{v} \cdot \vec{n}}{|\vec{n}|^2} \vec{n} \quad (5)$$

Hence, the direction of the reflected ray $\overline{OS'}$ is confined by $\vec{\omega} = \vec{v} + 2\vec{\gamma}$.

The reflection path in a three-dimensional enclosed space is traced by successive iterations of the new reflection points and directions of the reflected rays.

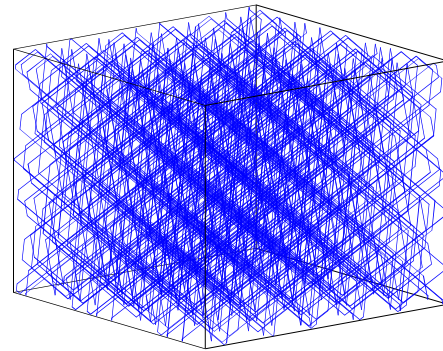
The following cases need to be avoided because they result in singularities:

- The acoustic ray hits into a corner;
- The acoustic ray is normal to the boundary surface;
- The reflected acoustic rays are all on the same plane.

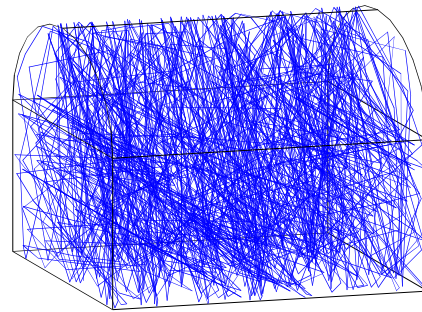
The acoustic ray will lose its consistency in the first and second cases whereas the acoustic ray has consistency in the third case, but it will not reflect on all surfaces.

Based on the above mapping procedure, the position and direction of the acoustic ray can be obtained at any arbitrary point on the propagation paths in a three-dimensional geometrical space, even for complex geometries. The time series used to compute the LLEs is derived from the points on the propagation paths. Two geometries (rectangular and concave enclosed spaces) have been widely studied in architectural acoustics. In this study, the LLEs were introduced to the ray systems in rectangular and concave enclosed spaces. Previous studies have shown that the propagation of an acoustic ray in an enclosed space is analogous to the particle trajectory in a billiard system within a high-frequency limit [10, 14]. Figure 2 shows the acoustic ray motions in the rectangular and concave enclosed spaces.

The ray-tracing algorithms were used to determine the acoustic ray motions and derive the time series in order to perform the Lyapunov exponent analysis. In the numerical simulations, the incident ray is launched from a source in the geometrical space. Many simulation runs were performed and it was found that changes in the source location and direction of the launching ray did not affect the LLE values. Because the continuity of the reflected rays is guaranteed, the method can be used to simulate motions of acoustic rays reflecting off a surface from an arbitrarily located source in various geometrical spaces. The method can also be used to simulate ray motions irrespective of the launching direction, provided that the acoustic ray is not perpendicular to the boundary surface.



(a)



(b)

Figure 2: Ray motions in the (a) rectangular and (b) concave enclosed spaces.

With the exception of the three singularities mentioned previously, it can be seen that the acoustic ray is launched from the source in the geometrical space in the direction indicated by the directional vector. It is possible to derive the directional vectors for the rectangular and concave geometries by tracing the ray propagation.

The ray has four ($2^2 = 4$) and eight ($2^3 = 8$) possible direction values for the two-dimensional and three-dimensional rectangular geometries, respectively. The base number “2” refers to the reverse directions in which the ray rebounds whereas the exponent number refers to the dimension of the space. For an initial directional vector (a, b, c) , there are eight possible directions for the acoustic ray in the rectangular geometry: (a, b, c) , $(a, -b, -c)$, $(a, -b, c)$, $(a, b, -c)$, $(-a, -b, -c)$, $(-a, -b, c)$, $(-a, b, -c)$, and $(-a, b, c)$. However, there is a large number of directions for the acoustic ray in the concave geometry. MATLAB computer aided engineering software (Release 2012b, MathWorks, Inc., USA) was used for the numerical simulations. The ray was launched from the source point $(1, 1, 1)$ in the direction of $\left(1, \tan \alpha, \tan \alpha * \sqrt{1 + (\tan \alpha)^2} \right)$, where $\alpha = 75^\circ$. This

means that the ray is inclined at angle of 75° from the vertical planes X - Y and X - Z in the geometrical space. The length, width, and height of the rectangular space are 6.80, 6.62, and 5.10, respectively. The length, width, height, and radius of the concave space are 6.80, 6.62, 3.21, and 3.00,

respectively. The elements of each directional vector refer to the ray direction from the point of origin to the vector point. The large number of directional vectors creates a vector field, which gives the directional vector of the acoustic ray at every point. Figure 3 shows the projection of the directional vectors onto the X - Z and Y - Z planes (denoted by the blue asterisks), which is obtained by substituting the y or x -coordinate of the directional vectors with 0. The acoustic ray reflects 10000 times in the concave space. The ray propagates in eight directions in the rectangular space whereas the reflected ray in the concave space propagates in different directions, where the directional vectors projected onto the X - Y and X - Z planes follow an angular distribution (Figure 3(a)) whereas the directional vectors projected onto the Y - Z plane follow a circular distribution (Figure 3(b)). There is an exponential proliferation of acoustic rays in the concave space due to the sensitivity of the ray trajectories to the initial conditions for a chaotic system.

By applying this ray-tracing model in room acoustics, the ray will propagate repeatedly in a small number of directions in the rectangular space, which produces acoustic effects because the sound waves are reflected back and forth between the parallel reflective surfaces. This phenomenon is known as “flutter echo” in room acoustics, in which strong points are generated at locations where the sound energy is concentrated in one direction.

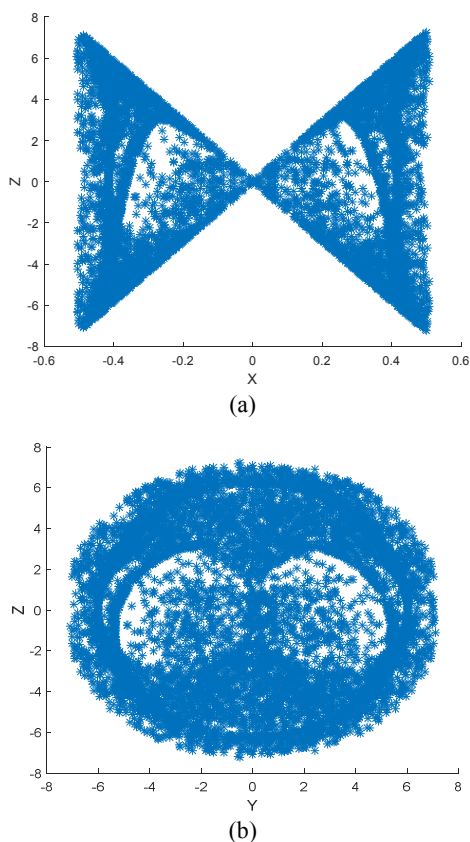


Figure 3: (a) Angular distribution of the directional vectors projected onto the X - Z plane and (b) circular distribution of the directional vectors projected on the Y - Z plane (b) in the concave space.

In contrast, the concentration of sound energy in one direction is reduced and the uniformity of the sound field is improved in a concave space because the ray propagates from various possible directions in the Y - Z plane.

Figure 4 shows the distributions of Z -values taken from 150 points on the propagation paths of equal length for the rectangular and concave spaces. In this case, equal length means that the ray is divided into length intervals (dL) of equal time t for a specific sound propagation velocity c . The Z -values were plotted against the number of points N for the ray trajectories with multiple reflections. The Z -value distributions clearly show the time series of the ray trajectories in the rectangular and concave enclosed spaces.

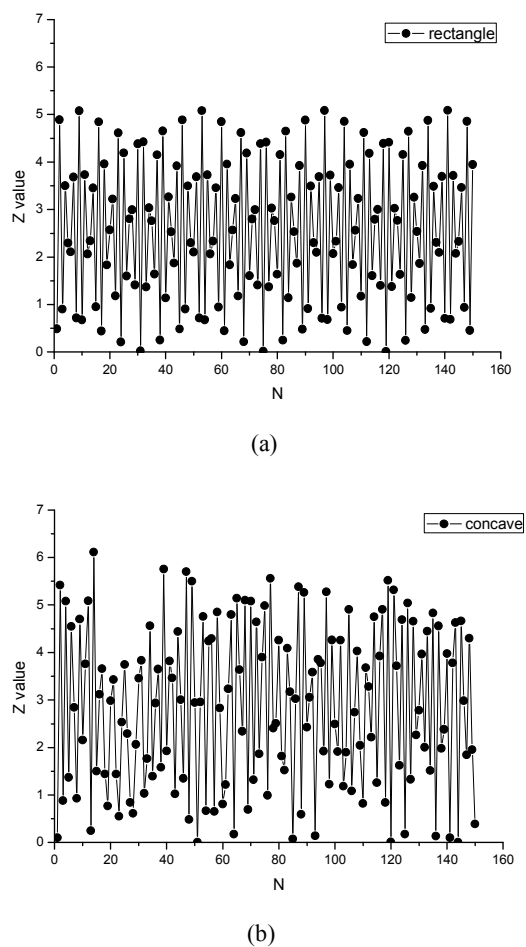


Figure 4: Distributions of Z -values taken from 150 points on the ray propagation paths of equal length for the (a) rectangular and (b) concave enclosed spaces.

2.2 Determination of the LLEs

The Lyapunov exponent is a quantity that characterizes the rate of separation of infinitesimally close ray trajectories. In other words, the ray separation is sensitive to the initial conditions of the system. The system is considered chaotic if at least one Lyapunov exponent is positive [15]. The sensitivity of the ray separation to the initial conditions of the chaotic system makes it possible to investigate the diffusive behavior of rays in various enclosed spaces.

Assuming that there are two (usually the nearest) neighboring points in the phase space at time 0 and time t , the distances of the points in the i^{th} direction are denoted as $\|\delta x_i(0)\|$ and $\|\delta x_i(t)\|$, respectively. The Lyapunov exponent is then defined by the average growth rate λ_i of the initial distance, which is given by:

$$\lambda_i = \lim_{t \rightarrow \infty} \frac{1}{t} \log_2 \frac{\|\delta x_i(t)\|}{\|\delta x_i(0)\|} \quad (6)$$

The set $\{\lambda_1, \dots, \lambda_{max}\}$ is called the Lyapunov spectrum.

Although the full Lyapunov spectrum can provide detailed information on the dynamic behavior of the system, it is not practical to compute the full Lyapunov spectrum because of the lengthy computational time. For this reason, LLEs are computed to validate a chaotic system rather than the complete Lyapunov exponents. In this study, the Wolf algorithm was used to determine the LLEs of the ray systems in the rectangular and concave spaces based on the time series.

The Wolf algorithm estimates the LLEs from a finite number of time series values by keeping the track of the exponentially divergent adjoining trajectories, as shown in Figure 5. The time series data for a single coordinate of the chaotic system (measured at equal time intervals) was considered in this study and the degree of the trajectory divergence was evaluated at regular intervals. There are five steps involved to determine the LLEs. First, select the point closest to the initial point on the fiducial trajectory at time t_0 . The distance between both of these points is denoted as $L(t_0)$. Second, let $L'(t_1)$ denote the distance between two points on the fiducial trajectory and neighboring trajectory at a later time t_1 . Next, compute the exponential ratio of $L'(t_1)$ to $L(t_0)$. Third, select the closest point at t_1 such that θ_1 is minimum and measure the distance $L(t_1)$. Fourth, repeat the second step at t_2 after time Δt and then compute the exponential ratio. Fifth, repeat the above procedure M times and compute the average exponential ratio. The LLE is defined as:

$$LLE = \frac{1}{M\Delta t} \sum_{k=1}^M \log_2 \frac{L'(t_k)}{L(t_{k-1})} \quad (7)$$

Where $\Delta t = t_k - t_{k-1}$ and M is the number of iterations. The parameters $L'(t_k)$ and $L(t_{k-1})$ are calculated from the Euclidean distance.

The LLEs for the rectangular and concave spaces were determined based on the time series points on the trajectory with equal length intervals dL , where the values on the z -coordinate are taken as its own series, as shown in Figure 6.

It can be seen that the LLE values are ~ 0 and ~ 0.3 for the rectangular and concave spaces, respectively. It is evident that there is a positive Lyapunov exponent for the ray system in the concave geometry, which indicates that chaos has truly developed.

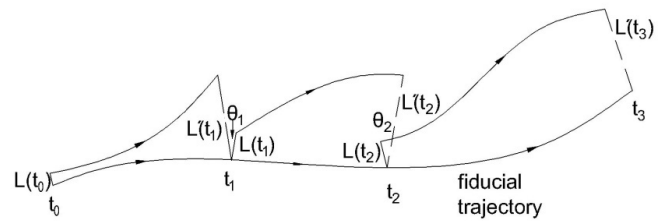
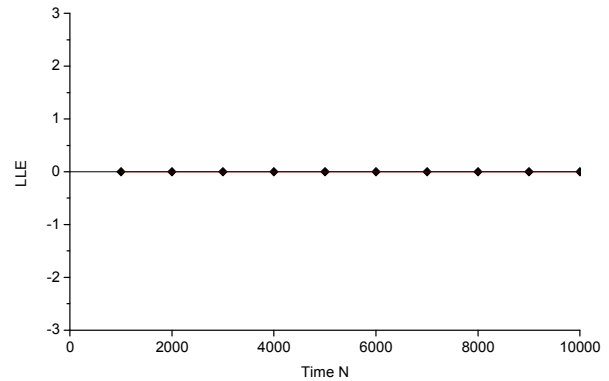
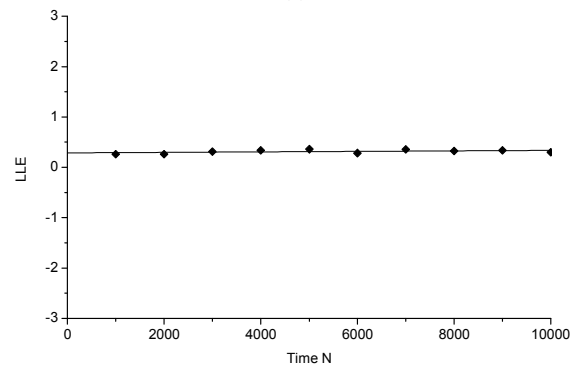


Figure 5: Procedure used to estimate the LLEs from the experimental data.



(a)



(b)

Figure 6: LLEs of the ray systems in the (a) rectangular and (b) concave enclosed spaces.

In contrast, an LLE value of 0 indicates that two nearby rays will not separate exponentially with respect to time. In other words, the ray moves in a regular fashion in the rectangular space. Nevertheless, when the LLE value is positive, the ray motion shows chaotic characteristics, such as that in the concave space. In room acoustics, a ray system with a positive Lyapunov exponent indicates the ray trajectories are sensitive to the initial conditions of the system and the rays may be diffuse [16].

3 Simulations of room acoustics using Odeon software

In room acoustics, sounds may propagate as rays at high frequencies. Ray acoustics is deemed to be a part of the ray moments in the geometrical space and therefore, it is possible to account for ray chaotic behavior in building acoustics. Empirically, a perfectly diffused enclosed space is

defined as one in which there are equal levels of sound energy at all positions and the sound energy flows equally in all directions upon excitation by a source. The definition of a diffuse field is probably adequate from a conceptual standpoint, but it does not provide much information from an operational viewpoint. At present, there are no practical direct metrics for this concept and there are no reliable methods to determine the diffusion levels in an enclosed space. Hence, it is not possible to state the diffusion level required for a given application. For this reason, most researchers attempt to create a test environment that is representative of an ideal physical scenario using mathematical models that are developed based on the current knowledge on ray theories. The diffusion levels of an enclosed space can be evaluated using either one of the following methods: (1) spatial uniformity of pressure method, which involves measuring the spatial variations of the sound pressure levels (SPLs), (2) cross-correlation analysis method, which involves measuring the degree of correlation between the sound pressure measurements at different microphone positions, (3) acoustic wattmeter method, which involves measuring the vector energy flow, (4) directional diffusion method, which involves measuring the sound levels in different directions using a directional microphone, and (5) multifractal method, which involves assessing the diffusion levels using a singularity spectrum corresponding to a monofractal signal [17–20]. At present, there are limited means to quantify the diffusion levels in an enclosed space. This work is focused on exploring the diffusion levels of sound field based on the uniformity of the SPLs in the enclosed space.

It has been shown [21] that the source directivity directly affects the uniformity of the sound field. In reality, the sources used in auditoriums, especially those produced by electro-acoustical instruments, are usually directional. Thus, studies on the uniformity of room acoustics with a directional source are of great significance to architectural researchers and designers during the early stages of design.

The acoustic diffusion was evaluated using Odeon 12.2 room acoustics software, which is a software typically used to simulate room acoustics with complex geometries [22] based on the image source and ray-tracing methods. In order to approximate the specular reflections on the rigid walls, the absorption and scatter coefficients were assigned a value of 0.01 and 0, respectively. Both the absorption and scatter coefficients were assumed to be uniformly distributed over all surfaces in the enclosed space. A directional source was used for the simulations. Because a directional source was used in the model (where the directivity of the source is at an angle), the sound transmission is more complete due to the rays coming from various directions compared to a source with stronger directivity. Even though the default line number provided in the Odeon software was 2000, many studies have shown that the directivity of the source is influenced by a line number up to 500. Thus, a suitable line number needs to be chosen for the simulations when the directivity of the source is considered. The line number should be within a range of 25–100 because the directivity of the source is at an angle. It is found in this study that a

higher line number reduces the effect of directivity whereas a line number within a range of 100–500 leads to obscure results. In contrast, the directivity of the source does not affect the diffusion of room acoustics when the line number is greater than 500. Increasing the line number may reduce dependency of the acoustic performance on the geometry of the enclosed space, but this comes at the expense of a loss of directivity. Even though increasing the line number will improve the ray distribution in both rectangular and concave enclosed spaces, the line number should be limited to a maximum of 500 to ensure that the directivity of the source is not entirely lost.

For the simulations, the line number required is available within the range in which the directivity of the source is valid. In this study, the line number and impulse response length were set at 25 lines and 5000 ms, respectively. It is found that temperature and humidity will not significantly affect the results, indicating that the sound ray still propagates in a straight trajectory within a normal range at high frequencies. Information of the directivity of the loudspeaker is provided by the CLF Group [23]. Because the software is based on geometrical acoustics, only the sample directivity balloons for selected octave bands (1000, 2000, 4000, and 8000 Hz) were chosen for this work, as shown in Figure 7.

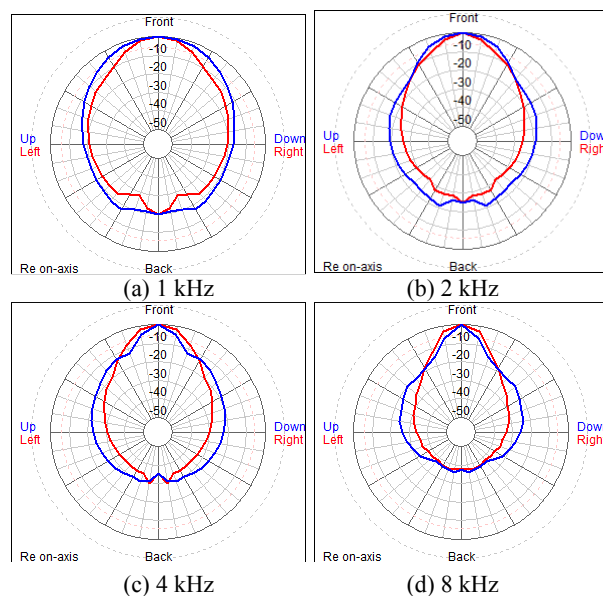


Figure 7: Directivity patterns of the “DNH-Tunnel-500” source at different frequencies [17]. The sample directivity balloons for the loudspeakers were used for validation, with the axis pointing to the left as “front” in three dimensions for the following octave bands: (a) 1 kHz, (b) 2 kHz, (c) 4 kHz, and (d) 8 kHz.

The SPLs at 20 receiver positions obtained from the simulations were compared to evaluate the status of the sound field. Figure 8 shows the top view and side view of the spatial distribution of the source and receivers. The source is positioned at one corner of the enclosed space and the receivers are positioned in a grid, as indicated by the numbered circles. These receivers are considered to occupy the whole space. The distances between the source,

receivers, and surfaces comply with the requirements of the ISO 3382 standard. The positions of the source and receivers in the rectangular and concave enclosed spaces are summarized in Table 1.

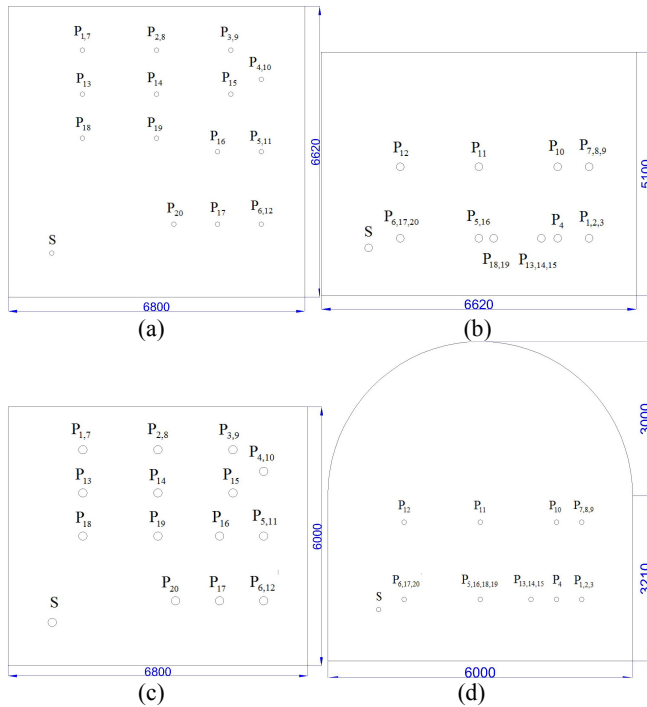


Figure 8: (a) Horizontal and (b) vertical layouts of the source and receivers in the rectangular space (length = 6800 mm, width = 6620 mm, height = 5100 mm); (c) Horizontal and (d) vertical layouts of the source and receivers in the concave space (length = 6800 mm, width = 6620 mm, height = 3210 mm, radius = 3000 mm).

4 Results and discussion

The differences of the SPLs between 20 receiver points were compared based on the range and variance, as shown in Table 2. The range represents the difference between the highest and lowest SPLs while the variance indicates the fluctuations of the SPLs in the sound field. Table 2 shows the uniformity of the sound field under excitation of the “DNH-Tunnel-500” source.

It can be seen from Table 2 that the receivers located at sites in front of the source have relatively higher SPLs, regardless whether the enclosed space is rectangular or concave. The range and variance of the SPLs are smaller for the concave space compared with those for the rectangular space for the frequency bands investigated in this work. The range is larger at higher frequency bands. The sound energy distribution is more homogeneous in the concave space because of the chaotic behavior of the acoustic rays, which is consistent with the theoretical results of ray chaos. Because the ray system in the concave space has a positive LLE, the ray separation is sensitive to the initial conditions of the chaotic system. Therefore, the ray distribution has better diffusion characteristics in a concave space.

Table 1: Positions of the source and receivers in the rectangular and concave enclosed spaces.

	Rectangle	Concave	Rectangle	Concave
S	(1,1,1)	(1,1,1)	S	(1,1,1)
P ₁	(1.70,5.62,1.20)	(1.70,5.00,1.20)	P ₁₁	(5.80,3.31,2.70)
P ₂	(3.40,5.62,1.20)	(3.40,5.00,1.20)	P ₁₂	(5.80,1.66,2.70)
P ₃	(5.10,5.62,1.20)	(5.10,5.00,1.20)	P ₁₃	(1.70,4.62,1.20)
P ₄	(5.80,4.96,1.20)	(5.80,4.50,1.20)	P ₁₄	(3.40,4.62,1.20)
P ₅	(5.80,3.31,1.20)	(5.80,3.00,1.20)	P ₁₅	(5.10,4.62,1.20)
P ₆	(5.80,1.66,1.20)	(5.80,1.50,1.20)	P ₁₆	(4.80,3.31,1.20)
P ₇	(1.70,5.62,2.70)	(1.70,5.00,2.70)	P ₁₇	(4.80,1.66,1.20)
P ₈	(3.40,5.62,2.70)	(3.40,5.00,2.70)	P ₁₈	(1.70,3.62,1.20)
P ₉	(5.10,5.62,2.70)	(5.10,5.00,2.70)	P ₁₉	(3.40,3.62,1.20)
P ₁₀	(5.80,4.96,2.70)	(5.80,4.50,2.70)	P ₂₀	(3.80,1.66,1.20)

Table 2: Uniformity of the sound field under excitation of the “DNH-Tunnel-500” source.

	1 kHz	2 kHz	4 kHz	8 kHz
	Rectangle / Concave	Rectangle / Concave	Rectangle / Concave	Rectangle / Concave
1	108.6/108.5	102.8/103.4	88.3/89.2	76.3/77.1
2	108.7/109.2	103.1/104.4	88.8/90.4	76.8/78.5
3	109.2/108.6	103.9/103.7	89.9/89.7	78.0/77.7
4	108.9/109.4	103.8/104.4	89.9/90.2	77.9/78.1
5	109.3/109.7	104.1/104.5	89.9/90.2	77.8/78.0
6	111.1/109.8	106.5/104.4	92.4/89.9	80.2/77.7
7	108.5/109.3	102.6/104.5	88.1/90.4	76.0/78.3
8	108.6/109.5	103.1/104.8	88.8/90.8	76.8/78.6
9	108.7/109.4	103.4/104.7	89.4/90.6	77.4/78.5
10	108.7/109.1	103.6/104.2	89.6/90.2	77.6/78.1
11	109.2/109.2	104.2/103.9	90.1/89.6	78.0/77.5
12	110.3/109.6	105.7/104.3	91.6/89.9	79.4/77.8
13	108.6/109.6	103.3/104.5	89.2/90.3	77.1/78.2
14	109.0/109.9	103.7/104.9	89.6/90.8	77.5/78.7
15	108.8/109.9	103.6/104.9	89.6/90.8	77.5/78.6
16	109.5/109.4	104.3/104.2	90.2/90.0	78.1/77.8
17	111.1/109.9	106.5/104.7	92.5/90.4	80.3/78.2
18	109.0/109.2	104.0/104.1	90.0/89.9	77.9/77.8
19	109.2/109.3	104.2/104.2	90.2/90.0	78.1/77.8
20	111.2/109.4	106.7/104.3	92.7/90.0	80.5/77.9
Range	2.7/1.4	4.1/1.5	4.6/1.6	4.5/1.6
Variance	0.7862/0.1457	1.5110/0.1468	1.7267/0.1760	1.5783/0.172

For an enclosed space with homogeneous medium, the ray motions are determined by the geometry of the space and the characteristics of the sound field are determined by the ray motions. In this work, the ray distribution is more diffusive in a concave space compared to that in a three-

dimensional rectangular space. In addition, the sound field is more uniform in a concave space compared to that in a rectangular space, as shown in Table 2.

In this study, the uniformity of the sound field is focused on the audience area, which is typically the lower and middle section of the room. Hence, it can be deduced that chaos theory is more valid to describe the sound ray mechanism. There are two types of mechanism for chaotic systems [24]: (1) the Sinai billiards (dispersion mechanism), where the dispersing boundary elements in the nearby trajectories diverge upon scattering and the consecutive collisions with the dispersing elements result in higher divergence and (2) Bunimovich stadium billiards (defocusing mechanism), where the nearby trajectories converge after a collision with the focusing boundary elements. The trajectories only begin to diverge after they pass through the focusing point. Provided that the free flight is sufficiently long (including reflections at the neutral boundary elements), the focusing may be overcompensated by divergence, which results in defocusing. It is worth noting that a long free flight is required for weak focusing before defocusing. The sound field is more uniform in a concave space because of the defocusing effects. A positive LLE indicates that separation of the acoustic rays is sensitive to the initial conditions of the chaotic system, which results in a higher uniformity of the sound field in the enclosed space.

It is also evident that the difference in the uniformity of the sound field is higher for intermediate and high frequency bands, regardless whether the enclosed space is rectangular or concave. This indicates that the method proposed in this work is suitable to analyze geometrical acoustics. Ray chaos theory provides a new perspective on the analysis of geometrical acoustics. The sound energy density distribution is more uniform if the acoustic rays exhibit chaotic characteristics. In this study, simulations were performed for different acoustic source (“Danley Sound Labs-SH-25”) with a different directivity. Similar results were obtained for this case, as shown in the appendix.

5 Conclusions

In this study, the kinetic behaviors of ray systems in rectangular and concave enclosed spaces were described based on LLEs. A new concave geometry with chaotic ray system was introduced by computing the LLEs of the ray system. By converting the points on the ray trajectories into a time series, the LLEs of the ray systems in three-dimensional spaces were successfully determined without the need for a kinetic equation. The Lyapunov exponent was found to be positive for the concave space, which confirms the chaotic behavior of the ray system in this geometry. A ray system with a positive LLE indicates that the rays behave in an ergodic manner whereas a ray system with an LLE of 0 indicates that the ray motions are regular. According to the ray chaos theory, the rays in a chaotic system are sensitive to the initial conditions of room acoustics, which makes it possible to obtain a uniform sound energy density distribution as in the case of the

concave space. Owing to the chaotic characteristics in the concave space, there are less fluctuations of the SPLs in this space compared with that in the rectangular space. The results indicate that the method can be used to assess the acoustic performance of a geometrical space with homogeneous medium based on the dynamics of the acoustic rays.

The method presented in this paper can be used for preliminary architectural acoustic design, especially when designing large auditoriums in which ray acoustics play a dominant role. It is possible to obtain a diffuse sound field by modifying a regular geometry into a chaotic geometry. In room acoustics, designing a ray system with positive Lyapunov exponents may be effective to realize a more uniform sound field. This method is of practical significance to designers in order to gain insight on the dynamics of acoustic rays in enclosed spaces and optimize architectural designs to obtain a satisfactory sound distribution.

Acknowledgments

This work was supported by the National Science Foundation of China (Grant nos.: 11174086 and 1157408). Odeon 12.2 room acoustics software was provided by the Architecture Acoustic Laboratory of the South China University of Technology.

Appendix

Different speakers were used for the room acoustics simulations in this study. The following results show the fluctuations of the SPLs under the excitation of “Danley Sound Labs-SH-25” directional source in the rectangular and concave enclosed spaces with the same dimensions as those used in the simulations based on the “DNH-Tunnel-500” source. These supplementary results support the key findings presented in this paper.

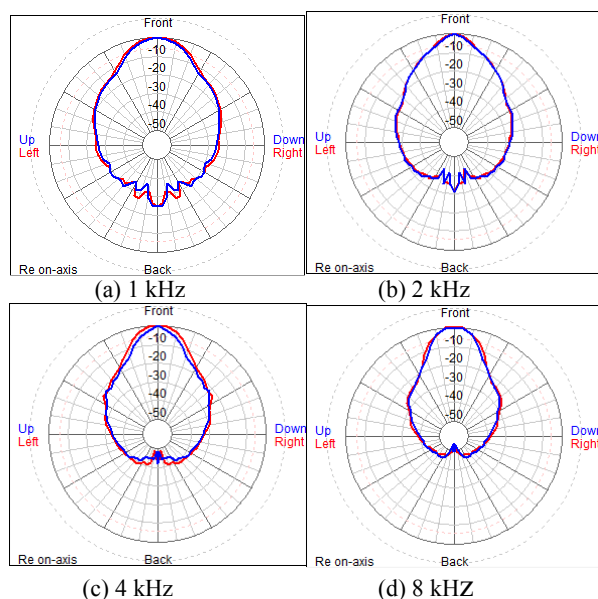


Figure 9: Directivity patterns of the “Danley Sound Labs SH25” source at different frequencies.

Table 3: Uniformity of the sound field under excitation of the “Danley Sound Labs SH25” source.

	1 kHz	2 kHz	4 kHz	8 kHz
	Slope/Sinai	Slope/Sinai	Slope/Sinai	Slope/Sinai
1	101/101.7	98/98.7	96.1/97.1	93.2/94.7
2	101.4/102.8	98.6/100.1	96.6/98.4	93.8/95.8
3	102.3/102.2	99.9/99.3	97.8/97.7	94.8/95.3
4	102.2/102.8	99.7/99.5	97.8/98.3	94.9/96.1
5	102.6/102.9	99.4/99.5	98.0/98.3	95.7/96.1
6	105.1/102.7	101.3/99.1	100.7/98	99.0/95.9
7	100.8/103.0	97.7/99.6	95.9/98.6	93.2/96.5
8	101.3/103.3	98.5/100.0	96.6/98.9	93.8/96.9
9	101.8/103.2	99.2/99.9	97.2/98.8	94.4/96.8
10	102.0/102.8	99.4/99.6	97.5/98.3	94.7/96.1
11	102.7/102.4	99.6/99.0	98.2/97.7	95.9/95.5
12	104.3/102.7	100.7/99.2	99.9/98.0	98.0/95.9
13	101.7/103.0	98.9/99.7	97.1/98.5	94.4/96.3
14	102.1/103.3	99.3/100.2	97.5/98.9	94.8/96.6
15	102.0/103.4	99.3/100.1	97.5/98.9	94.8/96.7
16	102.8/102.7	99.7/99.2	98.3/98.1	96.0/96.0
17	105.1/103.2	101.4/99.6	100.8/98.6	99.0/96.6
18	102.4/102.6	99.6/99.2	98.0/98.0	95.4/95.9
19	102.7/102.7	99.8/99.2	98.2/98.1	95.8/96.0
20	105.3/102.7	101.7/99.3	101/98.2	99.2/96.1
Range	4.5/1.7	4/1.5	5.1/1.8	6/2.2
Variance	1.8090/0.1626	1.1150/0.1674	2.2161/0.2138	3.4846/0.2830

References

[1] H.J. Stöckmann and J. Stein. “Quantum” chaos in billiards studied by microwave absorption. *Phys. Rev. Lett.*, 64(19): 2215, 1990.

[2] J. Stein and H.J. Stöckmann. Experimental determination of billiard wave functions. *Phys. Rev. Lett.*, 68(19): 2867, 1992.

[3] M.C. Gutzwiller. Chaos in classical and quantum mechanics. Springer-Verlag, New York, 1990.

[4] K. Nakamura, Quantum chaos: A new paradigm of nonlinear dynamics, Cambridge University Press, Cambridge, 1993.

[5] R. Blümel and W.P. Reinhardt, Chaos in atomic physics, Cambridge University Press, Cambridge, 1997.

[6] X. Lin, Y. Zhang, and G. Du. Influence of perturbations on chaotic behavior of the parabolic ray system. *J. Acoust. Soc. Am.*, 105 (4): 2142, 1999.

[7] M.G. Brown, J.A. Colosi, S. Tomsovic, A. Virovlyansky, M.A. Wolfson, and G.M. Zaslavsky, Ray dynamics in long-range deep ocean sound propagation. *J. Acoust. Soc. Am.*, 113(5), 2533, 2003.

[8] D.V. Makarov, M.Y. Uleysky, and S.V. Prants, Ray chaos and ray clustering in an ocean waveguide. *Chaos: Interdiscip. J. Nonlinear Sci.*, 14(1) :79, 2004.

[9] Y. Zhang and X. Xu. Influence of ocean bottom reflection on ray chaotic behaviors in underwater acoustics. *Acta Acust.*, 36(2): 221, 2011.

[10] T. Kawabe, K. Aono, and M. Shin-ya. Acoustic ray chaos and billiard system in Hamiltonian formalism (L). *J. Acoust. Soc. Am.*, 113(2): 701, 2003.

[11] S. Koyanagi, T. Nakano, and T. Kawabe. Application of Hamiltonian of ray motion to room acoustics. *J. Acoust. Soc. Am.*, 124(2): 719, 2008.

[12] X. Yu and Y. Zhang. Acoustic ray diffuse behaviors of an architectural semi-stadium model. *Int. J. Model. Simul.*, 31(4): 301, 2011.

[13] X. Yu and Y. Zhang. Ray chaos in an architectural acoustic semi-stadium system. *Chaos: Interdiscip. J. Nonlinear Sci.*, 23(1): 013107, 2013.

[14] W.J. Cavanaugh and J.A. Wilkes. Architectural acoustics: principles and practice, John Wiley & Sons, Inc., New York, 1999.

[15] H.D.I. Abarbanel, R. Brown, and M.B. Kennel. Lyapunov exponents in chaotic systems: their importance and their evaluation using observed data. *Int. J. Mod. Phys. B*, 5(9): 1347, 1991.

[16] W.B. Joyce. Erratum: Sabine’s reverberation time and ergodic auditoriums. *J. Acoust. Soc. Am.*, 59(1): 234, 1976. 58(3) (1975) 643-655.

[17] A. Kulowski. Remarks on a limit value of the sound directional diffusion coefficient in rooms. *Appl. Acoust.*, 32(2): 93, 1991.

[18] B.N. Gover, J.G. Ryan, and M.R. Stinson. Measurements of directional properties of reverberant sound fields in rooms using a spherical microphone array. *J. Acoust. Soc. Am.*, 116(4): 2138, 2004.

[19] T.J. Schultz. Acoustic wattmeter. *J. Acoust. Soc. Am.*, 28(4): 693, 1956.

[20] S.J. Loutridis. Quantifying sound-field diffuseness in small rooms using multifractals. *J. Acoust. Soc. Am.*, 125(3): 1498, 2009.

[21] L.M. Wang and M.C. Vigeant: Evaluations of output from room acoustic computer modeling and auralization due to different sound source directionalities. *Appl. Acoust.*, 69(12): 1281, 2008.

[22] J. Keränen, and V. Hongisto. Comparison of simple room acoustic models used for industrial spaces. *Acta Acust. united with Acust.*, 96(1): 179, 2010.

[23] CLF Group, Common Loudspeaker Format, <<http://www.clfgroup.org/files/index.php>>, 2018.

[24] T. Papenbrock. Numerical study of a three-dimensional generalized stadium billiard. *Phys. Rev. E*, 61(4): 4626, 2000.

40 YEARS
ANNIVERSARY

 **AcoustiGuard**[®]

WILREP LTD.

SOUND and VIBRATION CONTROL



Since 1977, AcoustiGuard – WILREP LTD. has been providing products and solutions for sound and vibration control.

We are now pleased to announce the addition of our new **ARCHITECTURAL ACOUSTICS** product line.



Exclusive Canadian Dealer for RealAcoustix
Exclusive North American Distribution of DeAmp and QuietStone

www.acoustiguard.com

1-888-625-8944

FIELD ATTENUATION OF INDIVIDUAL ORCHESTRA SHIELDS

Alberto Behar ^{*1}, Mohammad Abdoli-Eramasaki ^{†1} and Stephen Mosher ^{‡2}

¹Ryerson University, Toronto, Ontario, Canada.

²Canadian Federation of Musicians, Toronto, Ontario, Canada.

Résumé

Un test a été effectué pour mesurer l'atténuation de deux écrans acoustiques commerciaux utilisés par musiciens d'orchestres symphoniques. Trois instruments différents ont été utilisés comme sources de son. Les écrans étaient équipés de deux dosimètres, un situé en avant et l'autre derrière chaque écran. L'atténuation a été trouvée en calculant la différence entre la lecture des deux dosimètres. Les atténuations calculées étaient entre 5,8 et 10,7 dBA.

Mots clefs : boucliers acoustiques, orchestre symphonique, contrôle du bruit, protection de l'ouïe

Abstract

A test was conducted to assess the field attenuation of two commercial acoustic shields used by symphonic orchestra musicians. Three different musical instruments, were used as sound sources. The shields were equipped with two noise dosimeters each, located one in front and the other behind the shield. The attenuation was calculated as the difference between the readings of both dosimeters. Attenuations were found to be between 5.8 and 10.7 dBA.

Keywords: acoustic shields, symphonic orchestra, noise control, hearing conservation

1 Introduction

Acoustic shields are devices used in symphonic orchestras to protect musicians' hearing from high sound levels originated by players located behind them. A field attenuation study aimed to determine if shields are beneficial to orchestra players was conducted by some of the present authors¹. The attenuation was obtained as the difference between the readings of two noise dosimeters: one installed on the shield, exposed to the direct sound of the instrument generating the sound, and the second one was attached to the shoulder of the protected player. Results of the study showed that in most cases, the attenuation was negligible.

The results from the study didn't actually measure the attenuation of the shield, but only the difference between the measured sound levels. As a matter of fact, noise levels reaching any of the dosimeters are the result of sounds from several sources including musicians seated on the sides and in front of the protected musicians, reflections from lateral walls and/or ceiling, and finally those generated by the protected musician. No distinction can be made between signals from all these sources and the one generated by the musician seated behind the individual intended to be protected short of using acoustic intensity techniques.

Musicians, however, claim that they do perceive significant attenuation of sounds generated by loud instruments (e.g., brass and percussion) located on the other side of the shields. The present study was intended to

evaluate the attenuation of the shield in the same location, but only with instruments being played by the musician into the shield.

2 Attenuation measurement

2.1 Location

The testing was performed in the orchestra pit of the Four Seasons Centre for the Performing Arts, in Toronto, same location where the study of the reference was conducted.

2.2 Shields under test

The two types of acoustic shields used in the previous study, Wenger and Manhasset model 2000, were evaluated. Both shields consist of an acrylic plate mounted on a pole that allows for varying its height from the floor. The Wenger's plate dimensions are 57 cm by 43 cm. The Manhasset's plate is larger: 65 cm by 55 cm. Both plates are made of Lexan polycarbonate with a thickness of 6 mm. The density of the material is 1,200 kg/m³, the resulting surface density is 7.2 kg/m². As per the acoustic Mass Law, the transmission loss should be in the order of 20 dB at 500 Hz in absence of diffraction.

2.3 Sound sources

Three musical instruments were used as sound sources. They were chosen as being among the loudest in the orchestra and also to cover the low, middle and high portion of the sound spectrum. The instruments were a trombone, a trumpet and a flute.

* alberto.behar@psych.ryerson.ca

† m.abdoli@ryerson.ca

‡ notabother@ca.inter.net

Only one instrument was used at a time. Musicians were requested to perform a loud piece of their choice, playing for roughly one minute duration. All musical segments were extracts from Tchaikovsky - Swan Lake.

Measurement instruments and set-up

Measurements were performed simultaneously on two shields (See Figure 1): one Wenger and one Manhasset. They were located at an angle of 45° in front of the player, at a distance of around 1 m between the end of the instrument and the player. Each shield was equipped with two dosimeters B&K Type 4448, one on each side of the shield. The dosimeters were located on stands at a distance of 10 cm from the center of the shield.

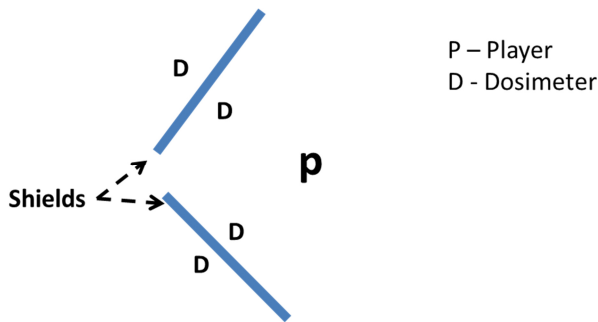


Figure 1: Measurement setup.

2.4 Procedure

Before the start of each measurement the batteries of the four dosimeters were tested and the instruments calibrated per the manufacturer’s instructions.

At the beginning of the test the four dosimeters were switched on. One of the players executed the selected piece. Then the dosimeters were switched off and their readings were recorded. The second player took the place of the first; dosimeters were again switched on at the beginning and off at the end of the playing and their readings were recorded. Same procedures were conducted for the third player.

To assess the repeatability of the results, the entire procedure with the three players was repeated. In such the attenuation of both shields was recorded twice with each instrument.

At the end of the tests, the readings from the dosimeters were extracted electronically and compared with those read directly from the dosimeters to confirm the measurement results accuracy.

3 Results of the measurements

The results of the measurements are shown in Table 1, The first column shows the test trials (1 and 2). As mentioned above, each of the three players played twice. The fifth column “Attenuations” shows the differences between the readings from the front and the back dosimeters. The last

column shows the differences between the attenuations between the first and second trials of measurements.

Table 1: Results from the measurements (Leq, dBA).

Trials #	Instruments	Shield		Attenuation*	diff. trials 1 and 2
		Front	Back		
		Manhasset			
1	Trumpet	103.5	92.8	10.7	0.6
	Flute	91.9	82.8	9.1	2.0
	Trombone	93.5	85.9	7.6	2.9
2	Trumpet	103.2	93.1	10.1	
	Flute	90.7	83.6	7.1	
	Trombone	96.1	85.6	10.5	
		Wenger			
1	Trumpet	101.2	95.0	6.2	0.6
	Flute	90.0	83.0	7.0	2.0
	Trombone	95.3	89.3	6.0	1.0
2	Trumpet	99.5	93.9	5.6	
	Flute	90.3	85.9	5.0	
	Trombone	96.2	89.2	7.0	

* Attenuation = Leq Front - Leq Back, dBA

Figure 2 shows graphically the values of the column 5 of Table 1.

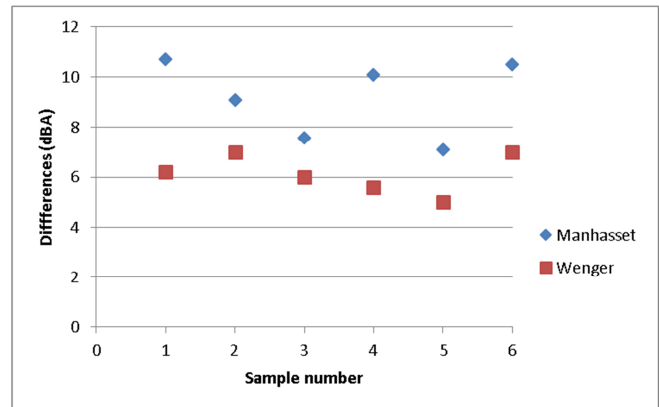


Figure 2: Scattergraph of the attenuations.

4 Discussion

4.1 Attenuation

With regard to the measured attenuations, results in Table 1 and Figure 2 show that the Manhasset shield has a larger attenuation than the Wenger. This can be explained by the Manhasset’s larger surface that reduces the diffraction of the impinging sound. Interesting enough, the spread among the individual values is larger for the Manhasset than for the Wenger. No satisfactory explanation was found for this finding.

Table 2 summarizes the results from Table 1. It shows that the average attenuation of the Manhasset shield is

3.3 dBA larger than the Wenger. This is a statistically significant difference, shown by the result of the t-Test, also shown in Table 2.

The measured attenuation is much larger than that from the referenced study. This confirms that the real attenuation by the shields is greatly reduced because of the sound generated by the surrounding instruments and by the protected player. This is shown in Table 3. As stated in the previous study, the shield cannot reduce the noise generated by the protected player as well the generated by the players surrounding him.

The present study performed using real orchestra instruments shows that the average attenuation of acrylic acoustic shields in ideal conditions (no background noise) is less than 10 dBA. Combined with the results from the reference study it questions the benefit of the shields as a means to protect musicians' hearing.

Table 2: Summary of the attenuations.

Shield Type	Mean Attenuation	Standard error
Manhasset	9.2	0.6
Wenger	5.9	0.3
t-Test	0.006	

Table 3: Attenuations measured in this study and by the reference.

	Manhasset	Wenger
This study	9.2	5.9
Reference	2.7	-2.1

4.2 Repeatability

Table 2 shows a reasonable repeatability between the sound levels of the two renditions by the players, something that helps validate the results. Those differences should be the same for both trials, something that didn't show, probably due to variations of the position of the instrument while playing and to directionality pattern of the same. That is quite visible in the case of the trombone, an instrument large enough in comparison to the distance between its bell and the shield.

Acknowledgments

Thanks are due to Leslie Allt, principal flute, Richard Sandals, principal trumpet and David Pell, bass trombone, members of the National Ballet of Canada Orchestra for acting as sound sources for the tests.

Measurements were performed by Lydia Hamata and Wahaj Alam from Ryerson University, Toronto.

The final version was set up by Francesca Copelli from Ryerson University, Toronto.

References

[1] Y. Luo, A. Pham, A. Behar, S. Mosher, and M. Abdoli-Eramaki. Acoustic Shields - A Study of Field Attenuation. Accepted for publication, Canadian Acoustics.



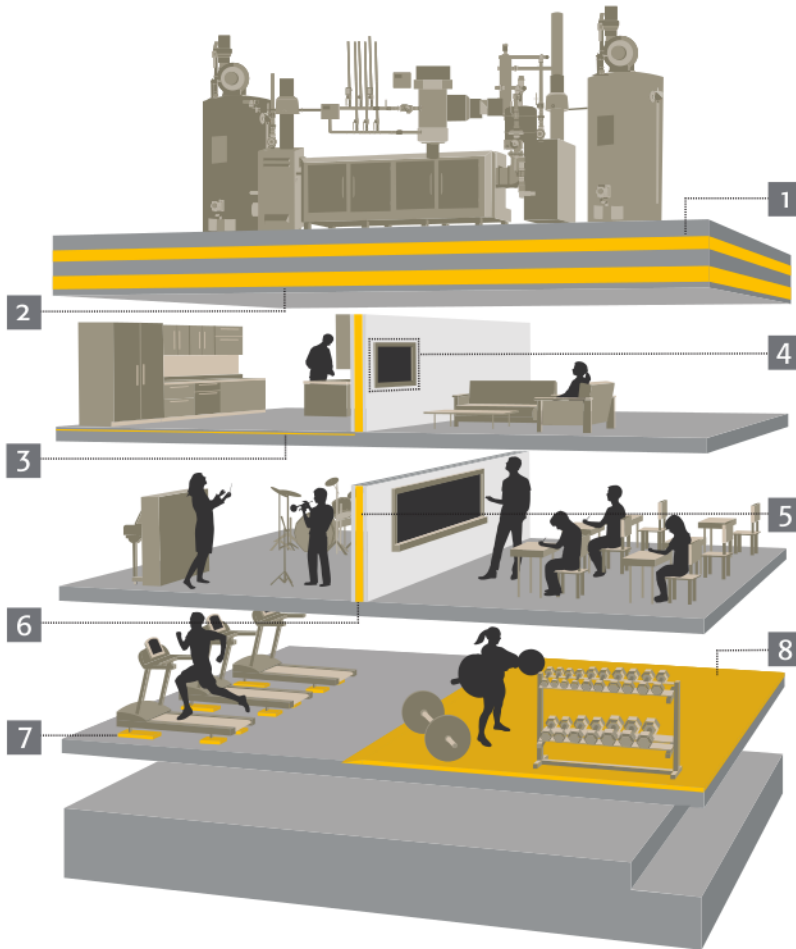
HGC ENGINEERING

- > Noise & Vibration Control in Land-use Planning
- > Noise & Vibration Studies: Residential and Commercial
- > Building Acoustics, Noise & Vibration Control
- > Land-use Compatibility Assessments
- > Third-party Review of Peer Reports
- > Expert Witness Testimony

905-826-4546
 answers@hgcengineering.com
www.hgcengineering.com



It's not magic, it's engineering.®



SOUND AND VIBRATION ISOLATION

We are a team of experienced engineers focused on developing high-performing, cost effective acoustical products to ensure building code is met for sound transmission (STC/IIC).

Innovative by design, simple to install, **GenieClip®** and **GenieMat®** are the trusted brands of architects, builders and acoustical consultants worldwide.



WWW.PLITEQ.COM | 416-449-0049 | INFO@PLITEQ.COM

SIMULATION STUDY OF SUPER-RESOLUTION IN HYDROPHONE MEASUREMENTS OF PULSED ULTRASONIC FIELDS

Wahiba Djerir*¹ and Tarek Boutkedjirt²

¹Research Center in Industrial Technologies (CRTI), Algiers, Algeria

²Faculty of Physics, University of Sciences and Technology Houari Boumediène, Algiers, Algeria

Résumé

Afin de réaliser des mesures fiables du champ ultrasonore impulsionnel, l'utilisation d'un hydrophone piézoélectrique comme récepteur est recommandé. Cependant, en raison de la taille finie de l'ouverture du récepteur, la pression acoustique mesurée est affectée par le moyennage spatial sur sa surface active. Le but de ce travail est de déconvoluer les effets d'ouverture de l'hydrophone récepteur afin de reconstruire le champ ultrasonore impulsionnel avec une bonne résolution spatiale. Pour cela, nous considérons le champ de pression impulsionnel rayonné dans l'eau par des transducteurs à large bande de 19 mm de diamètre, avec des fréquences centrales $f_c = 2,25$ MHz et $f_c = 15$ MHz. Les récepteurs sont des hydrophones à membrane en PVDF de 25 μm d'épaisseur avec des ouvertures rectangulaires et circulaires. Les résultats de cette étude montrent la forte dépendance de la qualité de la reconstruction du rapport signal sur bruit (SNR). Généralement, la qualité de la reconstruction diminue avec la réduction du SNR. Une bonne qualité de reconstruction a été obtenue avec un coefficient de corrélation supérieur à 0,9936 lorsque les signaux "acquis" ne sont pas trop bruités (SNR = 60 dB). Dans ce cas, l'amélioration de la résolution spatiale par un facteur de 5 et 9, respectivement, pourrait être atteinte. La qualité de la reconstruction dépend également des dimensions de l'hydrophone, de la distance axiale par rapport à la source et de la fréquence centrale de l'impulsion ultrasonore ainsi que de sa bande passante spectrale.

Mots clefs : Super-résolution, filtre inverse spatial, filtre de Wiener spatial, hydrophone en PVDF, champ ultrasonore impulsionnel, champ ultrasonore reconstruit

Abstract

In order to carry out reliable measurements of pulsed ultrasonic fields, the use of a piezoelectric hydrophone as receiver is recommended. However, due the finite size of the receiver aperture the measured acoustic pressure is affected by spatial averaging on the surface active face. The aim of this work is to deconvolve the spatial effects of the receiver hydrophone in order to reconstruct the pulsed ultrasonic field with a better spatial resolution. Hereby, the linear pulsed pressure field radiated in water by wideband planar transducers of 19 mm diameter, with central frequencies $f_c=2.25$ MHz and $f_c=15$ MHz are considered. The receivers are PVDF membrane hydrophones of 25 μm - thickness with rectangular and circular apertures. The results of this study show the strong dependency of the reconstruction quality upon the signal-to-noise ratio (SNR). Generally, the quality of the reconstruction decreases with decreasing SNR. Good reconstruction quality has been obtained with correlation coefficient larger than 0.9936 when the "acquired" signals are not too much noisy (SNR=60dB). In this case, improvement of the spatial resolution by a factor of 5 and 9 respectively could be reached. The reconstruction quality depends also upon the hydrophone dimensions, the axial distance to the source, the central frequency and the spectral frequency bandwidth of the pressure pulse.

Keywords: Super-resolution, spatial inverse filter, spatial Wiener filter, PVDF hydrophone, pulsed ultrasonic field, ultrasonic field reconstruction

1 Introduction

In order to carry out reliable measurements of pulsed ultrasonic fields, different techniques are used. However, the most used standardized technique consists in the utilization of piezoelectric PVDF membrane hydrophones as receivers. That is principally because of their advantageous acoustic properties [1-4] and commercial availability. However, when high frequencies are used, spatial averaging due to their finite-size aperture and the variations of their frequency response have to be considered [5-8]. These

spatio-temporal transmission properties may strongly affect the electric signal delivered by these devices.

In this work, and in order to reconstruct the impulse ultrasonic field with a high spatial resolution we propose to deconvolve the spatial effects of the hydrophone. The application of deconvolution methods has already been applied in different fields to signals of various forms [9-10]. Methods for correcting the spatial averaging effect have also been proposed [11-16].

These are however mostly developed by using idealized models. It should be mentioned that a fundamental difference of the work here proposed compared to the works cited above is that these are based on a correction of the

*w.djerir@crti.dz

†tboutkedjirt@usthb.dz

value of the pressure taking into account the general form of the field. The method suggested in this paper allows to find the original value of the pressure, which should be received by a point transducer, by spatial deconvolution of the signal received by a large-size hydrophone and thus permits a super-resolution measurement of this field. Also, the possibility of deconvolving the spatial effects has been shown for harmonic ultrasonic fields only [17-18]. The present contribution is concerned with the study of pulsed ultrasonic fields. In this work, we are interested only in the spatial effects of the hydrophone. It should be noted that the deconvolution of the temporal effect is well established in the literature [19-20].

2 Response of the hydrophone receiving chain to the ultrasonic pressure field

In order to develop appropriate procedures through which the spatial effects of the receiving hydrophone can be inverted, the study of the direct problem is necessary. First, the output signal of the receiving hydrophone, $v(x, y, z_0, t)$, when it is placed in the transverse plane, $z = z_0$, has to be determined; z_0 is the distance from the source.

The receiving system (hydrophone with its receiving chain) being supposed linear and space- and time-invariant, can be characterized by its spatio-temporal impulse response, $h(x, y, t)$. The electric output voltage of the hydrophone chain, $v(x, y, z_0, t)$, can then be obtained by convolving this response with the radiated pressure field. Furthermore, if the signal is assumed to be corrupted by an additive noise, $n(x, y, z_0, t)$, this voltage will be given by:

$$v(x, y, z_0, t) = p(x, y, z_0, t) \otimes_{xyt} h(x, y, t) + n(x, y, z_0, t) \quad (1)$$

Where $p(x, y, z_0, t)$ is the acoustic pressure radiated by the transducer at the field point $M(x, y, z_0, t)$.

\otimes_{xyt} designates the spatio-temporal convolution operator. Since the hydrophone surface vibrates synchronously with the incident wave and as we are only interested in the spatial properties of the hydrophone, equation (1) becomes:

$$\langle p_n(x, y, z_0, t) \rangle = p(x, y, z_0, t) \otimes_{xy} h(x, y) + n_p(x, y, z_0, t) \quad (2)$$

Where \otimes_{xy} designates the spatial convolution operator. $h(x, y)$ represents the two-dimensional spatial impulse response of the hydrophone (its aperture function). In this case, $\langle p_n(x, y, z_0, t) \rangle$ represents the noisy spatially averaged pressure and $n_p(x, y, z_0, t)$ the noise corrupting this pressure. It should be noted that $\langle p_n(x, y, z_0, t) \rangle$ can be obtained by temporal deconvolution of the received voltage $v(x, y, z_0, t)$ by the temporal impulse response $h(t)$ of the hydrophone. This can be derived from its complex receiving transfer function $H(f)$.

2.1 Simulation of the radiated pressure field

For the simulation of the ultrasonic field, the latter is supposed to be radiated in water by a planar circular piston of diameter 19 mm set in a rigid baffle. The pulsed ultrasonic pressure generated at the surface of the transmitter is assumed to be, in a first step of the study, as a gaussian modulated sinusoid of central frequency $f_c = 2.25$ MHz with a wide fractional frequency bandwidth pulse (B=60% at -6dB); f_c corresponds to a wavelength $\lambda_c = 0.67$ mm of the ultrasonic wave in water. In a second step, a transmitted pressure pulse of $f_c = 15$ MHz central frequency ($\lambda_c = 0.1$ mm) with the same fractional frequency bandwidth will be considered. At the axial distance z_0 , the temporal variations of ultrasonic pressure, for different radial positions r , shows the well-known contributions of plane wave and edge waves in the “direct radiation” region ($0 \leq r < a$) and edge wave exclusively in the “shadow region” ($r \geq a$).

2.2 Spatial Impulse Response of the Hydrophone

Our receiver is constituted of a PVDF membrane hydrophone of finite-size aperture. This latter is characterized by the spatial transfer function $\mathcal{H}(f_x, f_y)$ in the corresponding frequency domain. f_x and f_y are the spatial frequencies in the x - and y - directions respectively. Firstly, a hydrophone of rectangular aperture has been chosen with the dimensions $l_x = 1.4$ mm, $l_y = 0.6$ mm, that means $l_x = 2.1\lambda_c$, $l_y = 0.89\lambda_c$, at $f_c = 2.25$ MHz, in order to demonstrate the geometry-dependent averaging effect for both dimensions (the two co-ordinates). The sensitivity is supposed to be constant over the hydrophone aperture (ideal aperture). It should be noted that equation (2) supposes that the ultrasonic field is being scanned by means of the hydrophone in the two orthogonal directions x and y . A scanning step width $\Delta x = \Delta y = 0.2$ mm, that is $\Delta x = \Delta y = 0.3\lambda_c$, at $f_c = 2.25$ MHz, leads to the discretization of the hydrophone aperture in 3×7 square receiving cells. The corresponding spatial transfer function is represented in Figure 1.

The latter was obtained using the two-dimensional spatial Fourier transform of the impulse response of the rectangular aperture $h(x, y)$ defined above.

2.3 Noise of the Measuring System

Noise is an important item when considering any deconvolution problem. Indeed, measured signals are more or less corrupted by noise. Moreover, measurement uncertainties have to be taken into account [21-22]. Therefore, in order to approach real measurement conditions, the acoustic pressure spatially averaged by the

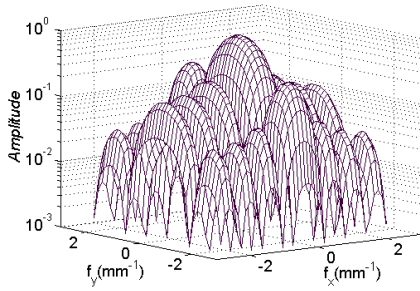


Figure 1: Amplitude of the spatial transfer function of a hydrophone of rectangular aperture ($l_x=1.4\text{mm}=2.1\lambda_c$, $l_y=0.6\text{mm}=0.89\lambda_c$; $\lambda_c=0.67\text{mm}$).

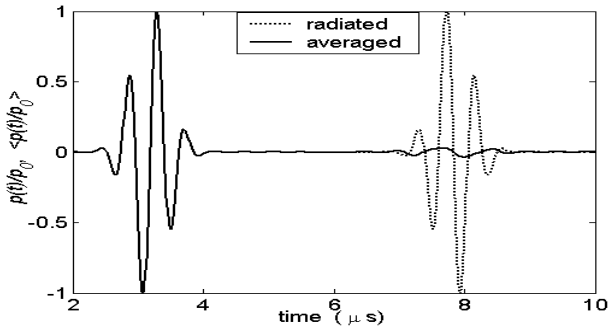


Figure 2: Radiated pressure (dotted curve) and spatially averaged pressure (thick curve) by a hydrophone of a rectangular aperture ($l_x=1.4\text{mm}=2.1\lambda_c$, $l_y=0.6\text{mm}=0.89\lambda_c$; $\lambda_c=0.67\text{mm}$) on transducer axis ($x=0\text{mm}$, $y=0\text{mm}$) at $z_0=3\text{mm}$.

hydrophone is supposed to be corrupted by a stationary and non-correlated noise. In addition, the noise is supposed to be white with a Gaussian distribution. This noise has an average value $n_m = 2.32 \times 10^{-6} P_0$ (in Pa) and a standard deviation $\sigma = 7.1 \times 10^{-3} P_0$ (in Pa). These values correspond to a signal-to-noise ratio (SNR) of 40 dB with a reference level of $1P_0$ (in Pa). P_0 is a reference pressure amplitude taken as the maximal amplitude of the radiated plane wave pressure pulse.

3 Spatial transmission effects of the hydrophone system (Averaging)

By convolving the radiated pressure $p(x, y, z_0, t)$ with the aperture function of the hydrophone $h(x, y)$ the spatially averaged pressure over the receiver face can be obtained. That is:

$$\langle p(x, y, z_0, t) \rangle = p(x, y, z_0, t) \otimes_{xy} h(x, y) \quad (3)$$

Taking account of equations (2) and (3), the output voltage of the receiver hydrophone becomes:

$$\langle p_n(x, y, z_0, t) \rangle = \langle p(x, y, z_0, t) \rangle + n_p(x, y, z_0, t) \quad (4)$$

The effects of hydrophone spatial properties on the “measured” pressure field are illustrated in Figure 2. This figure shows the variations of the radiated and the averaged pressure when the hydrophone is placed on the transducer

axis ($x=0\text{mm}$, $y=0\text{mm}$) at the distance $z_0=3\text{mm}$. It can be noticed that, compared with the radiated pressure field, the plane wave is not affected by spatial averaging. On the contrary, the amplitude of the edge wave is considerably reduced.

4 Deconvolution of the spatial effect of the hydrophone

In order to retrieve the radiated pressure field $\hat{p}(x, y, z_0, t)$ outgoing from the “measurement data”, that is, from the acoustic pressure spatially averaged by the hydrophone after temporal deconvolution $\langle p_n(x, y, z_0, t) \rangle$, a spatial deconvolution method is proposed [17-18]. This method permits the spatial effects to be inverted.

The acquisition system being supposed linear, the estimated value $\hat{p}(x, y, z_0, t)$ of the ultrasonic pressure can be obtained by using a spatial reconstruction filter with the spatial impulse response $h_F(x, y)$, that is:

$$\hat{p}(x, y, z_0, t) = h_F(x, y) \otimes_{xy} \langle p_n(x, y, z_0, t) \rangle \quad (5)$$

As a criterion for the evaluation of the quality of the deconvolution procedure, the normalized correlation coefficient, $r_{\hat{p}p}$, between the reconstructed pressure, $\hat{p}(x, y, z_0, t)$, and the radiated pressure, $p(x, y, z_0, t)$, is used. On transducer axis, this coefficient is given by [23]:

$$r_{\hat{p}p} = A/B \quad (6)$$

With:

$$A = \sum_{k=1}^N p^*(i_0, j_0, k) \hat{p}(i_0, j_0, k) \quad (7)$$

$$B = \sqrt{\sum_{k=1}^N |p(i_0, j_0, k)|^2 \sum_{k=1}^N |\hat{p}(i_0, j_0, k)|^2} \quad (8)$$

Where i_0, j_0 and k are the indices related to the position $x=0$, $y=0$ and, the time t respectively. N is the number of temporal samples.

4.1 Spatial two-dimensional inverse filter

The intuitive method for the reconstruction of the ultrasonic field is the inverse filtering, which simply compensates for the spatial aperture effects. The spatial transfer function of this filter is simply the inverse of that of the hydrophone, that is:

$$\mathcal{H}_F(f_x, f_y) = 1 / \mathcal{H}(f_x, f_y) \quad (9)$$

The pressure field can not be reconstructed from the spatially averaged data by using a spatial inverse filter in the case of an idealized aperture. Indeed, the calculations showed that the obtained acoustic pressure is completely submerged by the system noise. According to equation (9), the zeros of the spatial transfer function of the hydrophone correspond to infinite values of the transfer function of the

inverse filter. In this case, inverting the hydrophone aperture by using this filter may be not possible. This characterizes the ill-posedness of this inverse problem.

Even if the zeros are numerically avoided, the problem remains ill-conditioned [23] because of the drastic amplification of the noise level in the deconvolved signals. In addition to this inverse filter, a low pass filter with a cut-off frequency limited to useful frequencies of the signal has been applied. The deconvolution result, when using this additive filter, is shown in Figure 3, which still exhibits a poor quality of the reconstructed signal.

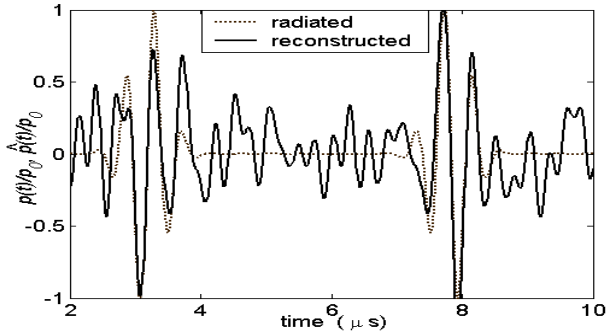


Figure 3: Acoustic pressure reconstructed by using a spatial inverse filter associated to a low pass filter on transducer axis at $z_0=3\text{mm}$. Hydrophone of rectangular aperture: ($l_x=1.4\text{mm}=2.1\lambda_c$, $l_y=0.6\text{mm}=0.89\lambda_c$; $\lambda_c=0.67\text{mm}$, SNR = 40dB).

4.2 Spatial two-dimensional Wiener filter

Because of the ill-posedness of the problem, it is necessary to use a regularization procedure. From a purely mathematical point of view, the principle of the regularization consists in adding to the null or almost null values of the inversion operator a sufficient quantity so that calculation can be carried out with a satisfactory stability [21-22]. From a physical point of view, the aim of the regularization procedure is to lead to a convolved signal, which is a solution of the inverse problem satisfying some physical conditions [24]. The Wiener filter is based on the minimization of the mean square error between the pressure to be reconstructed, $p(x, y, z_0, t)$, and the estimated pressure value, $\hat{p}(x, y, z_0, t)$, (MMSE criterion), that is:

$$E\{[\hat{p}(x, y, z_0, t) - p(x, y, z_0, t)]^2\} \rightarrow \min \quad (10)$$

Where E designates the expected value. Its spatial transfer function is given as follows [26]:

$$\mathcal{H}_F(f_x, f_y) = \frac{\mathcal{H}^*(f_x, f_y) \Phi_{pp}(f_x, f_y, z_0)}{|\mathcal{H}(f_x, f_y)|^2 \Phi_{pp}(f_x, f_y, z_0) + \Phi_{n_p n_p}(f_x, f_y, z_0)} \quad (11)$$

Where $\mathcal{H}^*(f_x, f_y)$ is the complex conjugated of the spatial transfer function of the hydrophone. $\Phi_{pp}(f_x, f_y, z_0)$ and $\Phi_{n_p n_p}(f_x, f_y, z_0)$ are the spatial power spectrum densities (PSDs) of the original acoustic pressure and of the

pressure noise respectively. The use of this procedure permits a simultaneous deconvolution of the hydrophone aperture and the reduction of the noise level. For its implementation two cases have been considered. In the first one, a-priori knowledge of the PSDs of the acoustic pressure and of the pressure noise has been assumed. The filter implemented under these ideal conditions will be next designated as “ideal”. In the second one, as no a-priori knowledge of these quantities was assumed, the PSDs have been estimated from the spatially averaged pressure after temporal deconvolution. The filter implemented under these conditions will be designated by “real”. For both types of the Wiener filter, a supplementary low pass filter is implemented in order to ameliorate the quality of the signal reconstruction.

Wiener filter with a-priori known PSDs

In this case, a-priori knowledge of the PSDs is assumed. The comparison of the reconstructed pressure (Figure 4a) when using this “ideal” Wiener filter with the radiated pressure (Figure 4a) (dotted curve) on transducer axis ($x = 0, y = 0$) shows that, under these ideal conditions, good reconstruction results can be achieved ($|r_{\hat{p}p}|=0.9931$).

Wiener filter with estimated PSDs

Generally, for the investigation of ultrasonic fields, there is no sufficient information on the ultrasonic field to be investigated. In this case, there is no a-priori knowledge of the PSDs, Φ_{pp} and $\Phi_{n_p n_p}$. Therefore, these quantities are replaced in equation (11) by their estimated values, $\Phi_{\hat{p}\hat{p}}$ and $\Phi_{\hat{n}_p \hat{n}_p}$.

For an estimation of these quantities, the following procedure is adopted. First, an estimated mean level of $\Phi_{\hat{n}_p \hat{n}_p}$ for the pressure noise is determined from the spatial spectrum of the spatially averaged pressure. This level is estimated from the high spatial frequencies region of the spectrum, where the useful signal can be considered as negligible. i.e. the region in which no useful signal spectrum can be identified. An estimated PSD of the noiseless spatially averaged pressure, $\Phi_{\langle \hat{p} \rangle_0 \langle \hat{p} \rangle_0}$ is then obtained by subtracting the estimated PSD of the pressure noise, $\Phi_{\hat{n}_p \hat{n}_p}$, from that of the noisy spatially averaged pressure, $\Phi_{\langle p_n \rangle \langle p_n \rangle}$. That is:

$$\Phi_{\langle \hat{p} \rangle_0 \langle \hat{p} \rangle_0} = \Phi_{\langle p_n \rangle \langle p_n \rangle} - \Phi_{\hat{n}_p \hat{n}_p} \quad (12)$$

Finally, an estimated spatial PSD of the acoustic pressure to be reconstructed, $\Phi_{\hat{p}\hat{p}}$, is obtained from the quotient of the PSD of the estimated noiseless spatially

averaged pressure $\Phi_{\langle \hat{p} \rangle_0 \langle \hat{p} \rangle_0}$ and the square of the hydrophone transfer function $\mathcal{H}(f_x, f_y)$. That is:

$$\Phi_{\hat{p}\hat{p}} = \Phi_{\langle \hat{p} \rangle_0 \langle \hat{p} \rangle_0} / |\mathcal{H}|^2 \quad (13)$$

The temporal variations of the pressure so reconstructed on axis at $z_0=3\text{mm}$ are shown in Figure 4b. Though the use of Wiener filter under these “real” conditions leads to results of less quality ($|r_{\hat{p}\hat{p}}|=0.9155$) compared to those obtained in the “ideal” case, the reconstruction results are obviously more significant than those furnished by using a spatial inverse filter.

Effect of axial distance to the source

When studying the direct problem, it has been shown that the effect of spatial averaging decreases while moving the receiver away from the source [23]. That suggests studying the influence of the axial distance on the quality of reconstructed field. In this order, the same pressure field studied previously is considered.

This field is “acquired” by using the hydrophone of the same aperture ($l_x=1.4\text{mm}$, $l_y=0.6\text{mm}$, with $\text{SNR} = 40\text{ dB}$ and at particular axial distances $z = 10\text{ mm}$, $z=15\text{ mm}$ and $z=20\text{ mm}$. The radiated acoustic pressure $p(x, y, z_0, t)$, and the spatially averaged one, $\langle p_n(x, y, z_0, t) \rangle$, which have been obtained at these axial distances are illustrated in Figures 5a, 5c and 5e respectively.

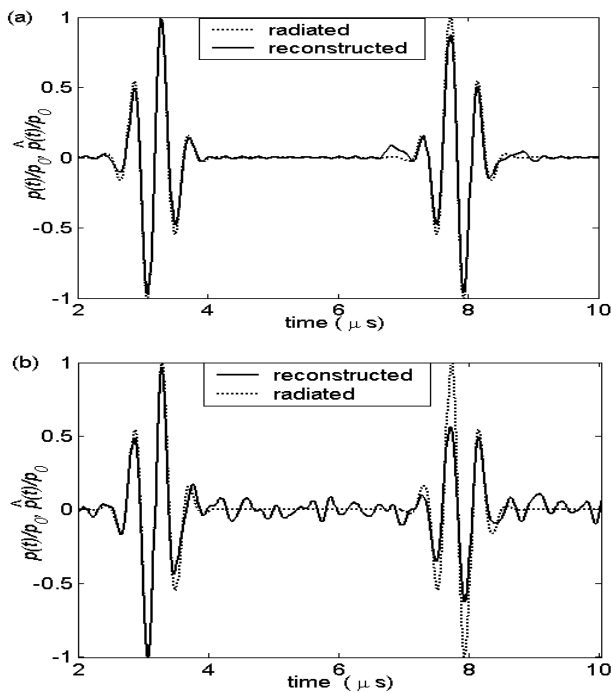


Figure 4: Acoustic pressure reconstructed by means of a spatial Wiener filter on transducer axis at $z_0=3\text{mm}$: (a) “ideal” Wiener filter, (b) “real” Wiener filter. Hydrophone of rectangular aperture: ($l_x=1.4\text{mm}=2.1\lambda_c$, $l_y=0.6\text{mm}=0.89\lambda_c$; $\lambda_c=0.67\text{mm}$, $\text{SNR} = 40\text{dB}$).

Figures 5b, 5d and 5f show the reconstruction results at these distances respectively. These results have been obtained by using a spatial Wiener filter with estimated PSDs. It should be noted that in Figures 5c, 5d, 5e and 5f, the edge wave slightly interferes with the plane wave because of the distance considered and of the pulse width. By comparing these figures to those obtained at $z = 3\text{mm}$ (Figure 4b), one notes that the quality of reconstruction depends upon the axial distance z .

This quality becomes better when moving the receiver away from the source. This improvement is confirmed quantitatively by the calculation of the normalized correlation coefficient between the reconstructed acoustic pressure and the radiated one. The values of this coefficient are $|r_{\hat{p}\hat{p}}|=0.9285$, $|r_{\hat{p}\hat{p}}|=0.9430$ and $|r_{\hat{p}\hat{p}}|=0.9789$ at the distances $z=10\text{ mm}$, 15 mm and 20 mm respectively. This improvement of the reconstruction quality at farther axial distance from the source allows using greater aperture dimensions or higher transducer frequency at these distances before the limits of the procedure are reached.

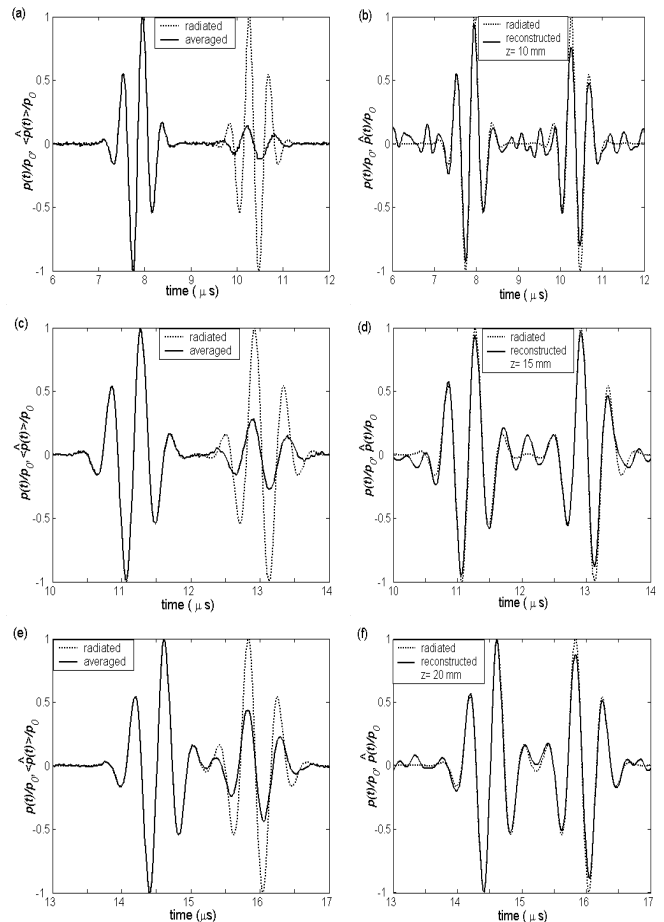


Figure 5: (a, c, e) Spatially averaged pressure and (b, d, f) Acoustic pressure reconstructed by using a “real” Wiener filter on transducer axis at different distances from the source. Hydrophone of rectangular aperture: ($l_x=1.4\text{mm}=2.1\lambda_c$, $l_y=0.6\text{mm}=0.89\lambda_c$; $\lambda_c=0.67\text{mm}$, $\text{SNR} = 40\text{dB}$).

Effect of hydrophone dimensions

Another criterion for the evaluation of the effectiveness of the spatial deconvolution method is the size of the hydrophone aperture.

In this case, the less advantageous reconstruction procedure “Wiener filter with estimated PSDs” has been tested for a hydrophone of greater aperture ($l_x = 1.8 \text{ mm} = 2.7 \lambda_c$, $l_y = 1 \text{ mm} = 1.5 \lambda_c$; $\lambda_c = 0.67 \text{ mm}$), with an SNR = 40 dB at $z = 20 \text{ mm}$. Figure 6a shows the radiated acoustic pressure on axis (dotted curve) as well as the spatially averaged one (solid curve).

The reconstructed pressure by means of the “real” Wiener filter is illustrated in Figure 6b (solid curve). Although the edge wave has clearly greater amplitude than that of the spatially averaged one (Figure 6a), the reconstructed pressure field presents some differences with the original one ($|r_{pp}| = 0.8262$). By comparing the reconstruction results obtained for this hydrophone aperture and those obtained in Figure 5f, it can be noticed that the quality of the reconstruction diminishes with increasing aperture dimensions.

Effect of SNR

Another critical parameter, which influences the quality of the reconstruction, is the signal-to-noise ratio (SNR). In order to investigate its effect, signals delivered by the hydrophone chain with other noise levels (SNR = 60 dB and SNR = 20 dB) are considered.

These signals have been “acquired” at the same axial distance from the source ($z = 20 \text{ mm}$) and for the same aperture dimension ($l_x = 1.8 \text{ mm}$, $l_y = 1 \text{ mm}$).

The curve in Figure 7a is obtained for an SNR = 60 dB. It shows that the “real” Wiener filter furnishes excellent reconstruction results when the “acquired” signals are not too much noisy ($|r_{pp}| = 0.993$).

This result is equivalent to an improvement of the spatial resolution by a factor of 9 in the x-direction and of 5 in the y-direction. On the contrary, for a low SNR (20 dB), the reconstruction results become poor and $|r_{pp}| = 0.302$ (Figure 7b). This result indicates that the limits of the reconstruction procedure are already attained for these aperture dimensions, at this axial distance and for this SNR.

Results for a circular aperture

Hydrophones with circular active area are mostly used. Therefore, the deconvolution procedure described in §4.2 has been also tested for hydrophones of circular aperture. The results presented here are obtained with a hydrophone aperture of diameter $\varnothing = 1 \text{ mm} \cong 1.4 \lambda_c$; $\lambda_c \cong 0.67 \text{ mm}$.

By means of this hydrophone, the ultrasonic pressure field has been scanned in the transverse plane at $z = 20 \text{ mm}$ from the source. The signal has been “acquired” with an SNR = 40 dB.

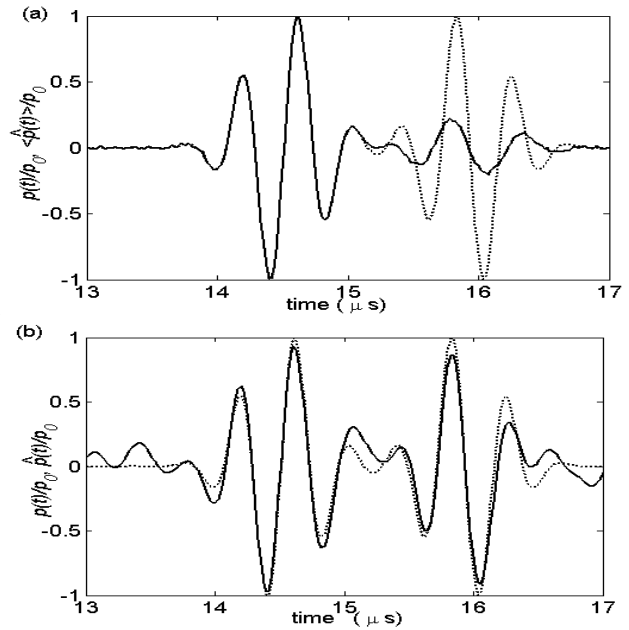


Figure 6: (a) Spatially averaged pressure and (b) Acoustic pressure reconstructed by using a “real” Wiener filter, on transducer axis at $z_0 = 20 \text{ mm}$. Hydrophone of rectangular aperture: ($l_x = 1.8 \text{ mm} = 2.7 \lambda_c$, $l_y = 1 \text{ mm} = 1.5 \lambda_c$; $\lambda_c = 0.67 \text{ mm}$, SNR = 40 dB). Radiated pressure in dotted curve.

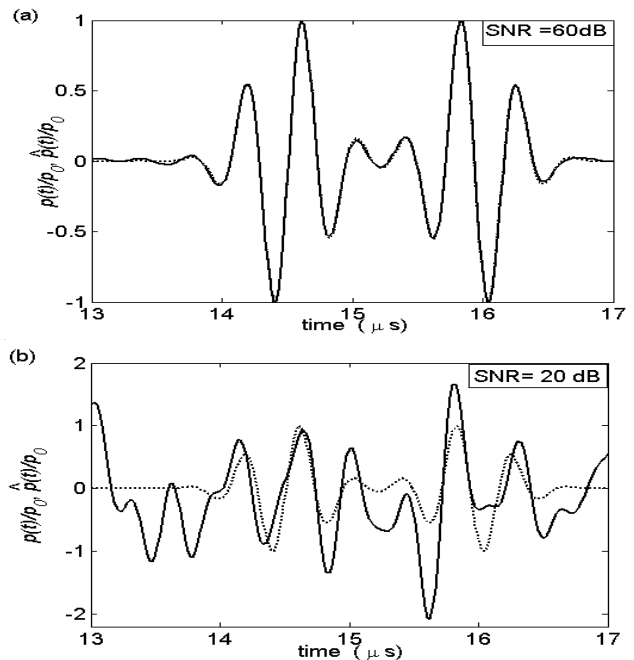


Figure 7: Acoustic pressure reconstructed by means of a “real” Wiener filter on transducer axis at $z_0 = 20 \text{ mm}$ for different SNR a) SNR = 60 dB, b) SNR = 20 dB. (Hydrophone of rectangular aperture: $1.8 \text{ mm} \times 1 \text{ mm}$, SNR = 40 dB). Radiated pressure in dotted curve.

Figure 8a illustrates the spatially averaged pressure (thick curve). The reconstruction result on axis obtained by using a spatial Wiener filter with estimated PSDs is shown in Figure 8b.

The comparison of this result with the radiated acoustic pressure (thin curve in Figure 8a and dotted curve in Figure 8b) shows that, for this aperture, the edge wave, which has been affected by spatial averaging has been correctly reconstructed. This is confirmed by the calculation of the normalized correlation coefficient $|r_{pp}| = 0.9794$. The improvement of the resolution by using this deconvolution procedure has been thus achieved by a factor 5.

Effect of pulse central frequency and bandwidth

In order to study the effect of the signals frequency increase, a radiated pressure with a center frequency 15 MHz and 60% fractional bandwidth has been considered.

The receiver is a hydrophone of circular aperture of 1 mm diameter placed on axis at $z=20\text{mm}$ and the signal is "acquired" with $\text{SNR}=40\text{dB}$. The quality of the spatial deconvolution obtained by the application of the "ideal" Wiener filter (Figure 9a) is still good.

However, the use of a real Wiener filter (Figure 9b) shows that for an excitation with a higher frequency, the limits of the method are quickly reached.

Indeed, when the the center frequency and the bandwidth of the pressure pulse increases, the quality of the spatial deconvolution diminishes.

5 Conclusion

In this study, it has been shown that it is possible to deconvolve the effects of the spatial transmission properties of the receiver hydrophone of a pulsed ultrasonic field. The spatial deconvolution is an ill-posed problem. This has been overcome by using a regularization procedure such as by using a spatial Wiener filtering.

This permitted the pulsed pressure field to be reconstructed from "measurement data" with a better resolution. The spatial deconvolution carried out using the Wiener filter showed that the quality of the reconstruction of the pulsed ultrasonic field depends strongly upon the SNR, the spatial frequencies bandwidth of the field pressure investigated, which is related to the axial distance from the source, and the dimensions of the hydrophone aperture. In all cases, the greater is the SNR, the better are the results.

In addition, the farther is the scanned field region, the greater the aperture dimensions can be considered, before the limits of the reconstruction procedure are reached. The study has been achieved for the field of a circular planar transmitter and receivers of rectangular and circular apertures. It could, however, be generalized to other aperture geometries and any kind of ultrasonic field. Though the showed results concerned the on-axis region, the deconvolution allows the reconstruction of the original pressure at any region of the ultrasonic field, provided SNR is sufficient.

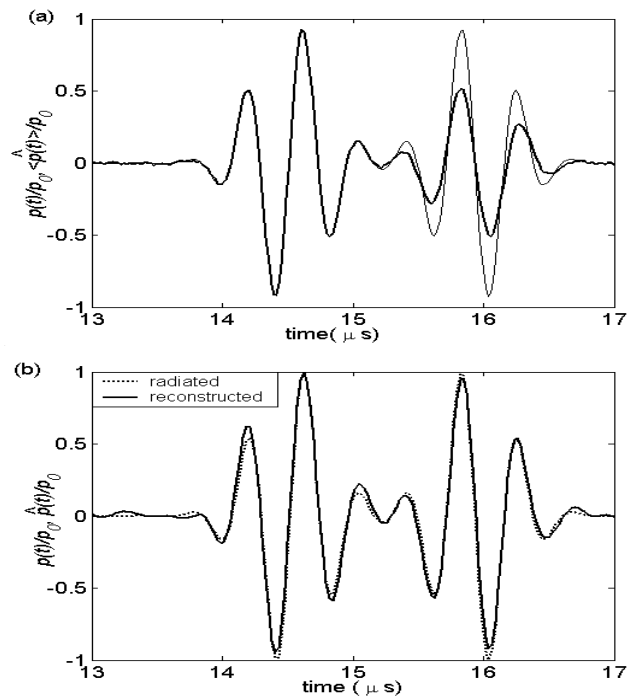


Figure 8: (a) Spatially averaged pressure, (b) Acoustic pressure reconstructed by using a "real" Wiener filter, on transducer axis at $z_0 = 20\text{mm}$. (Hydrophone of circular aperture: $\varnothing=1\text{mm}=1.4\lambda_c$; $\lambda_c=0.67\text{mm}$, $\text{SNR} = 40\text{dB}$). Radiated pressure in dotted curve.

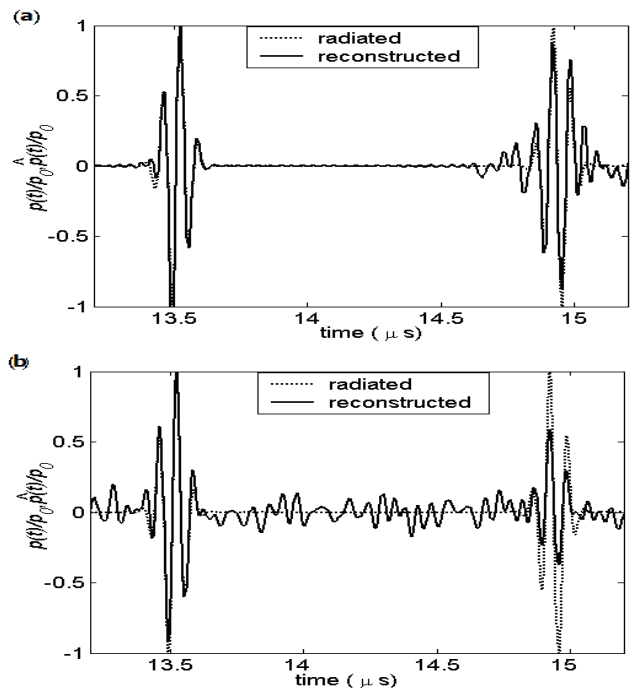


Figure 9: Acoustic pressure reconstructed by means of a spatial Wiener filter on transducer axis at $z_0 = 20\text{mm}$. (a) "ideal" Wiener filter and (b) "real" Wiener filter. (Hydrophone aperture: $\varnothing=1\text{mm}=10\lambda_c$; $\lambda_c=0.1\text{mm}$, $\text{SNR} = 40\text{dB}$). Radiated pressure ($f_c=15\text{MHz}$) in dotted curve.

References

- [1] V. Wilkens, S. Sonntag and O. Georg. Robust spot-poled membrane hydrophones for measurement of large amplitude pressure waveforms generated by high intensity therapeutic ultrasonic transducers. *J. Acoustic. Soc. Am.*, 39 :1319, 2016.
- [2] Nagle et al. Challenges and Regulatory Considerations in the Acoustic Measurement of High-Frequency (>20 MHz) Ultrasound. *J. Ultrasound Med.*, 32 :1897, 2013.
- [3] P. Lum, M. Greenstein, C. Grossman and T.L Szabo. High frequency membrane hydrophones. *IEEE Trans. Ultrason. Ferroelectr. Freq. Control UFFC.*, 34 :536, 1996.
- [4] R.C. Preston, D.R. Bacon, A.J. Livett and K. Rajendran. PVDF membrane hydrophone performance properties and their relevance to the measurement of the acoustic output of medical ultrasonic equipment. *J. Phys. E: Sci. Instrum.*, 16 :786, 1983.
- [5] C.J. Daly and N.A.H.K. Rao. Time-and frequency-domain description of spatially averaged one-way diffraction for an unfocused piston transducer. *Ultrasonics*, 37 :209, 1999.
- [6] R. A. Smith. Are hydrophones of diameter 0.5 mm small enough to characterize diagnostic ultrasound equipment?. *Phys. Med. Biol.*, 34 :1593, 1989.
- [7] K. Beissner. Maximum hydrophone size in ultrasonic measurements. *Acustica*, 59 :61, 1985.
- [8] A. Markiewicz and R.C. Chivers. Typical errors in using finite miniature ultrasonic probes for far field measurements. *Acoust. Lett.*, 6 :142, 1983.
- [9] H. Webster, M. R. Davenport and J.P. Ardouin. 3D Deconvolution of vibration corrupted hyperspectral images. *Spectral Sensing Research for Surface and Air Monitoring in Chemical. Biological and Radiological Defense and Security Applications*, 49 :521, 2009.
- [10] R. Jirik and T. Taxt. Homomorphic deconvolution of ultrasonics image. *Ultrasonic and Advanced Methods for Nondestructive Testing and Material Characterization*, 559 :590, 2007.
- [11] B. Zeqiri, A.D. Bond. The influence of waveform distortion on hydrophone spatial averaging correction: theory and measurement. *J. Acoustic. Soc. Am.*, 92 :1809, 1992.
- [12] E. G. Radulescu, P.A. Lewin, A. Goldstein and A. Nowicki. Hydrophone spatial-averaging corrections from 1-40 MHz. *IEEE Trans. UFFC.*, 48 :1575, 2001.
- [13] E. G. Radulescu, P.A. Lewin, A. Nowicki. 1–60 MHz measurements in focused acoustic fields using spatial averaging corrections. *Ultrasonics*, 40 : 497, 2002.
- [14] M. Yoshioka and T. Kikuchi. Evaluation of Hydrophone Spatial Averaging Effect in Near Field Measurement for Determining Mechanical Index. *The Japan Society of Applied Physics*, 51, 2012.
- [15] C. Koch and W. Molkenstruck. Primary calibration of hydrophones with extended frequency range 1 to 70MHz using optical interferometry. *IEEE Trans. Ultrason. Ferroelectr. Freq. Contr. UFFC.*, 46 : 885, 1999.
- [16] G. Xing, P. Yang, P. Hu, K. H. Lam, L. He and Z. Zhang. "Field characterization of steady state focused transducers using hydrophones based on Fresnel approximation. *Measurement Science and Technology*, 28 :065005, 2017.
- [17] T. Boutkedjirt and R. Reibold. Reconstruction of ultrasonic fields by deconvolving the hydrophone aperture effects. I. Theory and simulation. *Ultrasonics*, 39 :631, 2002.
- [18] T. Boutkedjirt and R. Reibold. Reconstruction of ultrasonic fields by deconvolving the hydrophone aperture effects. II. Experiment. *Ultrasonics*, 39 :641, 2002.
- [19] A. M. Hurrell and S. Rajagopal. The Practicalities of Obtaining and Using Hydrophone Calibration Data to Derive Pressure Waveforms. *IEEE Trans. Ultrason. Ferroelectr. Freq. Control UFFC.*, 64 :126, 2017.
- [20] S. Eichstädt, V. Wilkens, A. Dienstfrey, P. D. Hale, B. Hughes and C. Jarvis. On challenges in the uncertainty evaluation for time-dependent measurements. *Metrologia*, 53 :125, 2016.
- [21] Mario Bertero and Patrizia Boccacci. Introduction to inverse problems in imaging. Institute of Physics Publishing Bristol and Philadelphia. 1998.
- [22] David Colton and Rainer Kress. Inverse acoustic and electromagnetic scattering theory. Applied Mathematical Sciences, 1993.
- [23] W. Djerir and T. Boutkedjirt. Reconstruction of pulsed ultrasonic fields by deconvolution of the spatio-temporal effects of the receiving hydrophone: Theory and simulation. *Proc. 4th European Congress on Acoustics, Forum Acusticum*, 8430, 2005.
- [24] W.K. Pratt. Generalized Wiener filtering computation techniques. *IEEE Transactions on Image Processing*, 21 :636, 1972.



**Have you heard
about the benefits
of Johns Manville
Sound-SHIELD™
Insulation?**

What you won't hear is disturbing household noise. That's because Sound-SHIELD™ insulation actually reduces noise transfer in interior walls and between floors. Which means exceptional sound control throughout your entire home.

Visit www.JM.com/Canada
or email infocanada@jm.com
to learn more.



© 2016 Johns Manville. All Rights Reserved



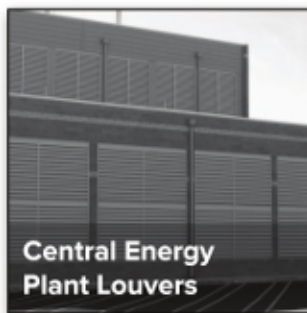
Outdoor Noise Control

Community friendly solutions for chillers and cooling towers

- Customizable solutions featuring independently tested products
- On grade and rooftop applications
- Proven design and performance of noise reduction with low system pressure loss since 1958



Cooling Tower
Barrier Wall System



Central Energy
Plant Louvers



Equipment Yard
Noise Control



1-800-684-2766 | www.kineticsnoise.com | canadiansales@kineticsnoise.com

GRAS Sound & vibration

SINUS

SVS
SOUND & VIBRATION SOLUTIONS CANADA Inc.



Hearing Protection Testing



Multifunction Calibrator



Modified NEW Pinna

New Low-noise KEMAR Manikin



**Rugged Microphone
HALT Tested
IP-67**



**Low Noise
High Sensitivity**



**Type I & II
Low Cost SLM
Longest Battery Life**



**Award Winning
Beam Forming
Acoustic Imaging**

Soundbook™
Designed for You:

- Innovative ✓
- IEC conform ✓
- Inexpensive ✓
- User friendly ✓
- General purpose ✓
- Tough (MIL) ✓
- Reliable ✓

PTB Approved



High Performance Low Cost Acoustic Analysers

Sound & Vibration Solutions Canada Inc.
Integrated Solutions from World Leaders

519-853-4495

ametelka@cogeco.ca

www.svsCanada.ca

PERSPECTIVES ON HOW ACOUSTICAL, NON-ACOUSTICAL, AND USER CHARACTERISTICS SHOULD BE CONSIDERED IN MULTIMODAL VIRTUAL REALITY RESEARCH AND APPLICATION

Jennifer L. Campos ^{*1,2}, Darryl McCumber ^{†3}, Brian Chapnik ^{‡3}, Gurjit Singh ^{*1,4,5}, Sin-Tung Lau ^{°1}, Karen Z. H. Li ^{♠6}, Victoria Nieborowska ^{†6} and M. Kathleen Pichora-Fuller ^{*1,2}

¹Toronto Rehabilitation Institute - University Health Network, Toronto, Ontario

²Department of Psychology, University of Toronto, Toronto, Ontario

³HGC Engineering, Mississauga, Ontario

⁴Department of Speech-Language Pathology, University of Toronto, Toronto, Ontario

⁵Phonak Canada Ltd, Mississauga, Ontario

⁶Department of Psychology, Concordia University, Montréal, Québec

Résumé

L'utilisation des environnements de réalité virtuelle (RV) est de plus en plus répandue dans la recherche et les milieux cliniques/appliqués, y compris dans le contexte de la recherche sur l'audition. Cela est, en partie, dû à la capacité de recréer des défis réalistes et quotidiens. En tant que tel, il devient de plus en plus important de caractériser les différences entre les propriétés acoustiques des sondes traditionnelles et les nouveaux environnements de test en RV. Bien qu'il existe des normes internationales spécifiant les propriétés acoustiques nécessaires aux environnements sonores hautement contrôlés, tels que les cabines de son (*soundbooths*), il n'existe, actuellement, pas de pratiques optimales pour mesurer et contrôler les propriétés acoustiques des systèmes de RV multimodaux. Dans le présent article, nous fournissons une perspective générale sur comment les caractéristiques acoustiques ou non acoustiques (ex. affichages visuels, dispositifs interactifs) et les caractéristiques des utilisateurs (ex. âge) sont importantes à considérer dans la conception et l'utilisation de systèmes en RV multimodaux. Les mesures ont été effectuées dans des conditions dans lesquelles a) aucun équipement de laboratoire ne fonctionnait, b) l'équipement de laboratoire (ordinateurs, ventilateurs, matériel de projection, tapis roulants) fonctionnait, et c) des stimuli expérimentaux (discours cible, parole concurrente et autres bruits de fond tels que des bruits de circulation simulés) étaient présents ou absents. Comme preuve de concept, nous rapportons ici un protocole d'acquisition de mesures acoustiques (c.-à-d. temps de réverbération, niveau de bruit et rapport signal sur bruit) pour caractériser les propriétés acoustiques d'une cabine de son standard en comparaison aux données obtenues dans un laboratoire de RV multimodal représentatif (*StreetLab à l'Institut de réadaptation de Toronto*). Les mesures ont été effectuées dans des conditions dans lesquelles a) aucun équipement de laboratoire ne fonctionnait, b) l'équipement de laboratoire (ordinateurs, ventilateurs, matériel de projection, tapis roulants) fonctionnait, et c) des stimuli expérimentaux (discours cible, parole concurrente et autres bruits de fond tels que des bruits de circulation simulés) étaient présents ou absents. Nous discutons ensuite des conséquences potentielles et uniques de ces résultats sur la perception auditive et la performance chez des jeunes utilisateurs et des personnes plus âgées. Nous considérons également les implications pour la mise en œuvre du contenu auditif dans les systèmes de RV multimodaux de façon plus générale. Dans l'ensemble, il est très utile d'étendre les connaissances acquises par la recherche sur l'audition conduite dans les cabines de son en utilisant des conditions d'évaluation plus écologiques et plus réalistes offertes par les technologies de RV qui progressent rapidement. En effet, de telles technologies pourraient changer le paysage de la recherche auditive et les approches de pratiques en réadaptation en audiologie. Cependant, comme ces opportunités et technologies évoluent, il est nécessaire d'établir des lignes directrices et des normes appropriées pour la conception, la mesure et la comptabilisation des propriétés acoustiques des environnements des évaluations en RV pour la recherche et d'autres applications à travers des populations d'utilisateur diverses.

Mots-clés : simulation, environnements virtuels, audition, auditif, vieillissement, cabine de son, acoustique, réaliste

Abstract

The use of Virtual Reality (VR) environments is becoming more widespread in research and clinical/applied settings, including in the context of hearing research. This is in part due to the ability to recreate realistic, everyday challenges. As such, it is becoming increasingly important to characterize the differences between the acoustical properties of traditional soundbooths and new VR test environments. While there are international standards specifying the necessary acoustical properties of highly controlled sound environments, such as soundbooths, there are no currently specified best practices for the measurement and control of the acoustical properties of multimodal VR systems. In the present paper, we provide a general perspective on how acoustical, non-acoustical (e.g., visual displays, interactive devices), and user (e.g., age) characteristics are important to consider in developing and using multimodal VR systems. As a proof of concept, we report here a protocol for acquiring acoustical measurements (reverberation time, noise level, and signal-to-noise ratio (SNR)) to

characterize the acoustical properties of a standard soundbooth and compare these measurements to a representative multimodal VR laboratory (StreetLab at the Toronto Rehabilitation Institute). Measurements were made under conditions in which a) no lab equipment was operating, b) lab equipment (computers, fans, projection equipment, treadmills) was operating, and c) experimental stimuli (target speech, competing speech and other background noise such as simulated traffic sounds) were present or absent. We subsequently discuss the potential and unique consequences of these results to auditory perception and performance in younger and older user populations. We also consider the implications for implementing auditory content within multimodal VR systems more broadly speaking. Overall, there is great value in extending the knowledge that has been amassed from hearing research conducted in soundbooths by using the more ecological and realistic testing conditions afforded by rapidly advancing VR technologies. Indeed, such technologies could change the landscape of auditory research and approaches to practice in rehabilitative audiology. However, as these opportunities and technologies evolve, there is a need to establish appropriate guidelines and standards for designing, measuring, and accounting for the acoustical and non-acoustical properties of VR testing environments for research and other applications across various user populations.

Keywords: simulation, virtual environments, hearing, auditory, aging, sound booth, acoustics, realistic

1 Introduction

Over the last several decades VR technologies have improved dramatically. Higher quality, more accessible (i.e., more widely available and easier to use), and less expensive systems now provide novel ways in which to create realistic, controlled, and safe testing conditions [1-4]. Current VR systems also offer the opportunity to create more integrated multimodal simulations in which multiple sensory inputs can be presented with high fidelity and can be controlled systematically. Here we refer to multimodal VR systems as those that include simulated content presented via two or more sensory inputs. For instance, VR systems can be comprised of an immersive visual display (e.g., a large-screen projection display or a head-mounted display), a method of presenting auditory stimuli (e.g., headphones or loudspeakers), and/or interactive devices (e.g., treadmill, haptic glove, joystick, vehicle consoles in driving simulators, cockpits in flight simulators).

The content of the virtual environments and unique testing scenarios can be highly customized to the research question of interest. These systems allow investigators to evaluate human perception and performance under complex, multisensory conditions that more closely resemble conditions encountered in real world environments and interactions. They also permit control over the environmental content and the presence/absence and properties of individual sensory stimuli as might be done in more traditional lab-based experiments conducted in simpler and more artificial, unisensory test environments. While there have been marked improvements in the quality and implementation of visual displays and interactive devices, less careful consideration has been given to the widespread implementation and incorporation of realistic auditory

displays within many multimodal VR systems [5-7]. There is great utility in considering the importance of acoustical and auditory stimulus properties across all VR applications for which they are implemented. VR could provide a unique tool for research and applications focused on auditory perception in complex environments.

1.1 Hearing research: Moving out of the soundbooth

Traditionally research in fields such as psychoacoustics and audiology has been conducted in sound-attenuating booths or anechoic rooms where it is possible to precisely control environmental conditions. Specifically, experimental conditions have been considered ideal if they minimize acoustical interference (e.g., reverberation or background noise), distracting multisensory stimulation (e.g., complex or dynamic visual or motor inputs), and attentional distractions (e.g., multi-tasking). Limiting these factors has many advantages if the tester wants to precisely evaluate the abilities of individuals to detect, perceive, and interpret auditory stimuli as a function of the physical properties of sound signals, to define neurophysiological responses to auditory stimuli, to characterize different types and magnitudes of hearing loss, and/or to evaluate some basic benefits of using technologies such as hearing aids. Nevertheless, questions may be raised as to the functional significance of the results obtained in such artificial testing environments that lack the typical demands of the multisensory (e.g., auditory, visual), mobility-related, and cognitive conditions that people often encounter in the real world. Thus, researchers are beginning to develop new methods to move from testing *hearing* in acoustically ideal soundbooth conditions to testing *listening* in more realistic and often adverse conditions [8, 9]. These new approaches could enable researchers to study the complex interactions among sensory and cognitive processes that have functional implications for listening in daily life [10]. Therefore, in the context of hearing research, multimodal VR systems can offer a valuable middle ground between controlled laboratory/clinical soundbooth environments and the real world.

*jennifer.campos@uhn.ca

†dmccumber@hgcengineering.com

‡bchapnik@hgcengineering.com

♦gurjit.singh@phonak.com

◊sin-tung.lau@uhn.ca

✧karen.li@concordia.ca

†victoria.nieborowska@alum.utoronto.ca

•k.pichora.fuller@utoronto.ca

Several decades ago, methods were developed to simulate purely auditory scenes using loudspeaker arrays within acoustically controlled lab settings. By the mid-1990's, investigators began adapting commercially available signal processing software using head-related transfer functions (HRTFs) to simulate spatial displays of sound sources, with the idea being that VR could be applied in rehabilitative audiology (e.g., [11]). The early auditory VR simulations were typically implemented without corresponding simulated visual inputs (or any other concomitant sensory inputs). These simulated audio techniques were subsequently adopted to test auditory perceptual processes, assess the nature of hearing loss, and evaluate new hearing aid technologies [12]. Such algorithms have continued to become more and more sophisticated [13]. There has been a growing awareness and interest in these techniques (see Figure 1 for a historical timeline), including explorations of how they can be applied in clinical settings. For example, VR holds promise as a tool for optimizing hearing aid fittings by testing different hearing aid functions in more realistic scenes [14, 15].

Currently, auditory simulations are being incorporated into even more complex, multimodal VR systems developed to represent specific sensory-cognitive-motor interactions during tasks like those encountered in everyday life, such as in walking simulators and driving simulators [16-19]. From the perspective of hearing researchers, there is a growing awareness that testing the performance of people who have hearing loss within these contexts is very important given that hearing loss affects not only speech intelligibility, but also non-auditory domains such as cognition and mobility [48]. Testing in simulated VR environments could provide new knowledge regarding the effects of hearing loss on perception and performance in everyday environments. For instance, hearing loss is associated with higher rates of falls [20, 48] and driving errors, particularly when individuals are distracted [21, 48]. Importantly, being on the brink of

potentially widespread implementation of multimodal VR systems, it is now a critical time for investigators to establish standards and guidelines surrounding the design, measurement, and implementation of auditory simulations within multimodal VR applications. Such guidelines should include considerations of the acoustics of the VR environment (e.g. reverberation time, noise level), the characteristics of the user (here we focus on age), and the nature of additional sensory inputs (e.g., visual environment). Below we reflect on why each of these factors is important to consider in the context of the development of multimodal VR and we describe a proof of concept approach by characterizing the acoustics of a representative multimodal VR research laboratory and the potential consequences to auditory performance across different user populations. Indeed, we have been motivated by our own experiences in attempting to use a listening task traditionally conducted in a soundbooth [22] within a multimodal, VR environment [17, 23]. In order to understand the reasons underpinning the clear differences in word recognition accuracy we observed within these two spaces for younger and older adults, we needed to compare the acoustical properties of the two test environments.

1.2 Auditory displays and acoustical factors

Acoustical considerations are important because a potential limitation of using multimodal VR systems for some hearing research is that simulations of auditory scenes may be contaminated by other background sounds inside or outside the test environment (e.g., computers, fans, interactive devices), especially if there is inadequate attenuation of ambient noise provided by the walls of the test room. There may also be excessive reverberation within the test environment. Even with these shortcomings, VR may still be more advantageous than artificial soundbooth testing conditions for some research and clinical purposes.

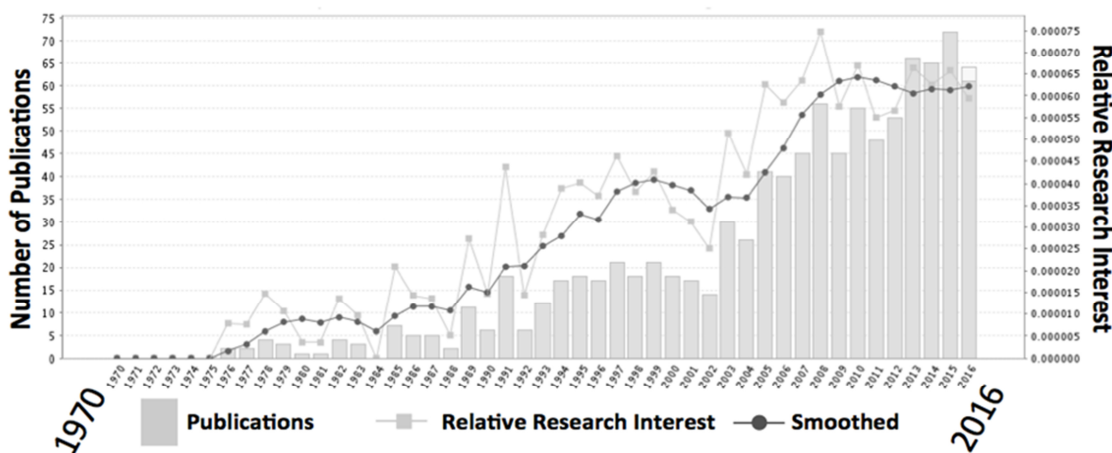


Figure 1: A historical timeline reflecting the growing interest in auditory simulations. Values based on a GoPubMed search in December, 2016, using search terms (((((((auralization*) OR auditor*) ((hearing AND loss*)) OR Audiology[MeSH Terms]) OR Hearing Loss[MeSH Terms]) OR "Head-Related Transfer Function*")) AND (((computer simulation[MeSH Terms]) OR Virtual realit*) OR Simulation*). Bar graphs represent the total number of publications and the line graphs represent the relative research interest (i.e. the relative growth in comparison to the growth of whole PubMed).

In audiology, progress has been made using HRTFs to simulate spatialized sound in clinical tests conducted under headphones (e.g., the Listening in Spatialized Noise-Sentences; [24, 25]). Simulated auditory displays presented over headphones, however, cannot be used to test performance when conventional hearing aids are worn. In future, methods using computational corrections to overcome limitations in acoustical simulations presented over loudspeakers could provide important new tools that would enable VR to be used more extensively in rehabilitation applications [15].

1.3 Age of the user

Another factor that is rarely considered in the context of VR system development, application, and evaluation, is the unique characteristics of the users or research participants. Well-documented sensory and cognitive changes occur over the lifespan [26]. Age-related changes may affect performance across a range of basic behavioral tasks, and may interact with the characteristics of the testing environment. Specifically, when considering the effects of auditory and cognitive aging, differences in the acoustical and non-acoustical properties of test environments will likely lead to differences on task performance that may be proportionally greater for older compared to younger adults. For instance, in terms of acoustical properties, highly controlled soundbooth environments allow for better control over parameters such as reverberation, sound level, and signal-to-noise ratio (SNR). In VR environments (and in the real world), these parameters are often more difficult to control, and the consequences to performance may be more apparent in older than in younger adults [18]. It is not uncommon for VR laboratories to have additional sources of noise (e.g., interactive devices such as treadmills, computers, safety devices and ventilation systems). These types of sounds that are not designed as part of the simulation may have differential effects on performance outcomes depending on the abilities of the listener. For example, it may be important to customize acoustical stimuli to individuals or groups of listeners to ensure audibility and minimize disproportionate masking effects. Investigators developing and using these systems must be cognizant of the potential need to adjust the level and other characteristics of the presentation of acoustical signals according to listeners' abilities to compensate for unwanted or unintended interactions between the person and the test environment that are introduced in the VR simulation but that would not be present in the real world conditions being simulated (e.g., the noise of the computers used to produce the VR simulation).

1.4 Multisensory and multimodality factors

A non-acoustical property that can differ between soundbooth and VR environments is the presence and complexity of visual input. Visual input that is deliberately incorporated into simulated VR content can be physically or semantically related to the auditory input (e.g., the coupling of dynamic visual and auditory inputs such as wind, tire,

engine sounds generated during simulated driving), or unrelated (e.g., the simultaneous presentation of a dynamic visual driving scene with non-informative or even distracting auditory input such as music, radio commentary, or telephone communication). The former case may be beneficial, while the latter case may be detrimental to performance. For some tasks, older adults are thought to demonstrate a heightened integration of redundant and congruent sensory inputs compared to younger adults [27-29], such that congruent multisensory conditions may provide proportionally greater benefit than reduced sensory conditions for older compared to younger adults. In contrast, older adults may be less able to inhibit irrelevant or incongruent multisensory inputs [30], suggesting that the presence of non-informative and potentially distracting multisensory feedback may be more disruptive for older adults.

In summary, testing perception and performance under ecological and realistic simulated conditions using VR may have advantages depending on the question at hand. However, performance will vary with the properties of the stimuli (e.g., unisensory versus multisensory), the testing environment (e.g., impoverished versus enriched), the task, and the age of the user/participant. Thus, it is important to account for and report these factors in VR research and applications. While it is common practice to thoroughly describe and compare test stimuli and user characteristics across studies, testing environments are seldom compared. Hearing researchers typically comply with acoustical standards for auditory testing environments [31], but VR researchers who are not focused on audition per se are more likely to employ highly variable, non-standardized, and poorly characterized auditory testing environments. Thus, standards for auditory VR developed by experts in acoustics and hearing will need interdisciplinary adoption.

1.5 Objectives of the current study

In this exploratory study, we characterize the acoustical properties (e.g., noise level, SNR, reverberation time) of a standard soundbooth and compare these measured properties to those of a representative, high-fidelity, immersive VR environment (StreetLab at the Toronto Rehabilitation Institute's Challenging Environment Assessment Laboratory (CEAL)). Measurements were made for the following conditions: a) without any lab equipment operating (i.e., computers, fans, projection equipment, interactive devices), b) with the lab equipment operating, and c) with auditory stimuli (target speech, competing speech and other background noise such as simulated traffic sounds) present or absent. We subsequently discuss the potential consequences of these results to auditory perception and performance across different user populations and the broader implications of implementing auditory content within multimodal VR systems.

2 Method

2.1 Stimuli and Apparatus

Stimuli

The speech stimuli present during some acoustical measurement conditions (see below) were the Coordinate Response Measure (CRM) sentences developed for research concerning listening in multi-talker displays [32].

Soundbooth

The soundbooth used to collect benchmark acoustical measurements was a 3.3 m (l) x 3.3 m (w) x 2.01 m (h) (21.89 m³) single-walled sound-attenuating booth (Industrial Acoustics Company, New York) located at the Human Communication Lab at the Mississauga Campus of the University of Toronto. An array of three Grason-Stadler loudspeakers (No. 1761-9630) was used to present the speech stimuli. The stimuli were presented from each loudspeaker at 60 dB A. The three loudspeakers were positioned in the soundbooth at approximately the head height of a seated person and at a distance of 1.6 meters, with one loudspeaker in front (0° azimuth), one to the right, and one to the left (+/-90° azimuth). All loudspeakers were activated when speech stimuli were presented.

Multimodal VR Laboratory

Acoustical measurements were collected in StreetLab located within Toronto Rehabilitation Institute's CEAL (Figure 2).



Figure 2: StreetLab Virtual Reality environment within the Challenging Environment Assessment Laboratory (CEAL) at the Toronto Rehabilitation Institute.

In StreetLab, an array of seven loudspeakers (Meyersound MP-4XP, Meyersound Laboratories, Inc.) and a subwoofer (Meyersound MP-10XP) were located behind a curved visual projection screen (the screen is made of a thin, sound-permeable material). The center loudspeaker is positioned at 0° azimuth at approximately head height for a standing person and the other six loudspeakers are distributed in an array in the same horizontal plane at +/-28° (right front and left front), +/-90° (right side and left side), and +/-127° (right rear and left rear). The subwoofer is

located under the floor, below the center loudspeaker, in front of a treadmill. Each loudspeaker was positioned at a distance of 2.14 m from the listener. StreetLab is teacup shaped and the interior spatial volume is 31.66 m³. Visual simulations within StreetLab were presented using a high-resolution, 240° field-of-view horizontal x 110° field-of-view vertical projection screen with a calibrated six projector system (Eyevis ESP, Reutlingen, Germany). Sound dampening foam panels are installed behind the screen surface, on the surrounding walls, and on parts of the floor and ceiling to provide sound attenuation (BasoTect Melamine sound insulation foam). For this study, the simulated scene was a six-lane, two-directional traffic intersection in downtown Toronto (see Figure 2), which was simulated using a customized OpenSceneGraph application (<http://www.openscenegraph.org>). The sentence stimuli used for the speech recordings (described above) were presented with no corresponding visible talker in the simulated visual scene. All loudspeakers were activated when speech stimuli and traffic stimuli were presented. StreetLab also has the capability of introducing mobility-related tasks, such as walking on a treadmill, balancing on a force platform, driving a car, or maneuvering a wheelchair. In this study, acoustical measurements were also made during the operation of the treadmill device.

2.2 Procedures

Acoustical measurements were conducted in the soundbooth at the Human Communication Lab and in StreetLab by the same acoustical engineer (DM). The sound measurements were conducted using a Norsonic NOR140 sound level meter, serial number 1405033. The measurements were conducted at a height and location approximating the head height and position of a typical participant in the two testing environments. Measurements and analyses included reverberation times (RT), background sound levels, SNR calculations and speech intelligibility calculations.

The criteria discussed below have been developed based on the guidelines provided in the ANSI S12.60 [33] American National Standard, "Acoustical Performance Criteria, Design Requirements, and Guidelines for Schools", which provides guidelines for the acoustical design of teaching spaces. This well-known standard was chosen as a benchmark for evaluating the VR environment because classrooms are real-world communication environments that are expected to meet strict acoustical criteria to enable listeners to achieve acceptable performance when confronting the cognitive demands of verbal communication during learning. This is therefore an important benchmark with respect to acceptable *minimal* standards when simulating realistic, but quiet listening conditions. For simulations that require noisier conditions (e.g., city street), it is easier to titrate up from the minimal standards for a quiet space than it is to attempt to make an unavoidably noisy environment quieter.

Reverberation time

Reverberation is characterized by the time it takes sound to decay by 60 dB (RT_{60}). In this study, RT_{60} was measured over the entire frequency range from 100 to 5,000 Hz in each test environment. While reverberation can be measured across all frequencies, the RT_{60} measured in the octave band around 500 Hz is often referenced as a simple comparative measure. For example, in teaching spaces, the RT_{60} at mid-frequencies (e.g., at 500 Hz) should be kept below 0.5 seconds and values greater than 0.5 seconds can reduce speech intelligibility, especially for individuals with hearing loss [34].

Background noise levels

Background sound can reduce speech intelligibility. The most widely accepted criteria for recommended levels of background sound are based on overall A-weighted sound levels and/or Noise Criterion (NC) curves [35]. ANSI S12.60 [33] indicates that core teaching spaces should have background sound levels of approximately 35 dB A (or less), corresponding to roughly NC-30. Higher background sound levels may be acceptable if the level of the speech is high enough, but this range is considered reasonable to ensure good intelligibility of source signals at normal voice output levels in a typical space.

Signal-to-Noise ratio

Once reverberation is reasonably well controlled, the main acoustical factor contributing to speech intelligibility is the SNR; that is, the levels of speech reaching a listener (and particularly the speech peaks) relative to the background sound levels at the listener's position. To illustrate this, calculations can be performed to determine the Speech Intelligibility Index (SII), as described by ANSI/ASA S3.5 [36], Standard Methods for Calculation of the Speech Intelligibility Index. In these calculations, the measured background sound levels are compared to the measured speech peaks. An SII value of 1 indicates that all speech cues reach the listener, whereas an SII value of 0.0 indicates no intelligibility. A value of 0.5 indicates that half of the speech cues are intelligible.

Conditions tested

In the present study, background sound levels were measured in each of the testing environments under several different conditions that varied as a function of the additional sources of background sounds that could be generated in the test environments during experiments. Specifically, the soundbooth was measured with a) no equipment operating and b) equipment operating (lights, computer, touch screen monitor). StreetLab was measured with a) no equipment operating, b) equipment operating (lights, projectors), c) treadmill on, but not moving, d) treadmill on, moving at 1m/s, e) traffic noise simulation added with no additional equipment operating, f) traffic noise added with the treadmill moving at 1 m/s. Speech stimuli were introduced during Conditions b (soundbooth

and StreetLab), c and d (StreetLab only) to measure signal-to-noise ratios and the SII.

3 Results

The RT_{60} was lower in the soundbooth than in StreetLab at all frequencies (Figure 3). Nevertheless, the RT_{60} was less than 0.5 seconds for all but the lowest frequencies in StreetLab, which is considered acceptable for communication and unlikely to result in reduced speech intelligibility in an environment such as a classroom [34]. Figure 4 shows the noise levels across frequencies and Table 1 shows the average sound levels for the selected sample of possible testing conditions that could be used during experiments conducted in StreetLab.

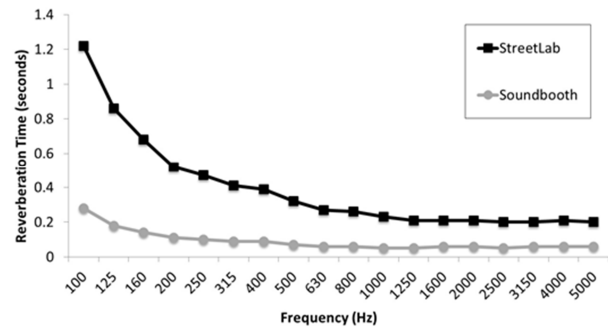


Figure 3: Reverberation times (RT_{60}) measured from 100 Hz to 5 kHz in both the soundbooth and StreetLab testing environments.

In the soundbooth, when no equipment was operating, the background sound level (23 dB A) was well within the targets specified in ANSI standard S12.60 [33] for classroom environments. As expected, the levels across frequencies also approximated the stricter criteria concerning permissible levels for audiometric testing specified in ANSI S3.1 [37]. In StreetLab, when no equipment was operating, the background sound level (43 dB A) was higher than in the soundbooth and higher than the targets referenced for ANSI S12.60 [33]. Turning on the basic equipment in Condition b in the soundbooth made very little difference to the measured sound levels (1 dB), whereas turning on the basic equipment in StreetLab resulted in a greater increase in the sound level (8 dB). Furthermore, as shown in Figure 4, the frequency response of the noise produced by turning on basic equipment differed between the two environments, with higher noise levels at the mid-high frequencies in StreetLab than in the soundbooth. While simply turning on the treadmill in StreetLab introduced no additional increase in sound level (Condition c), the sound level increased by an additional 6 dB when the treadmill motors were operating (Condition d), and another 5 dB when simulated traffic noise was added (Condition e). Therefore, it would be expected that speech intelligibility performance would be poorer in StreetLab than in a conventional soundbooth because of the elevated levels of background noise, with the differences being greater as more realistic conditions were used in StreetLab (e.g., walking on a moving treadmill or adding traffic noise).

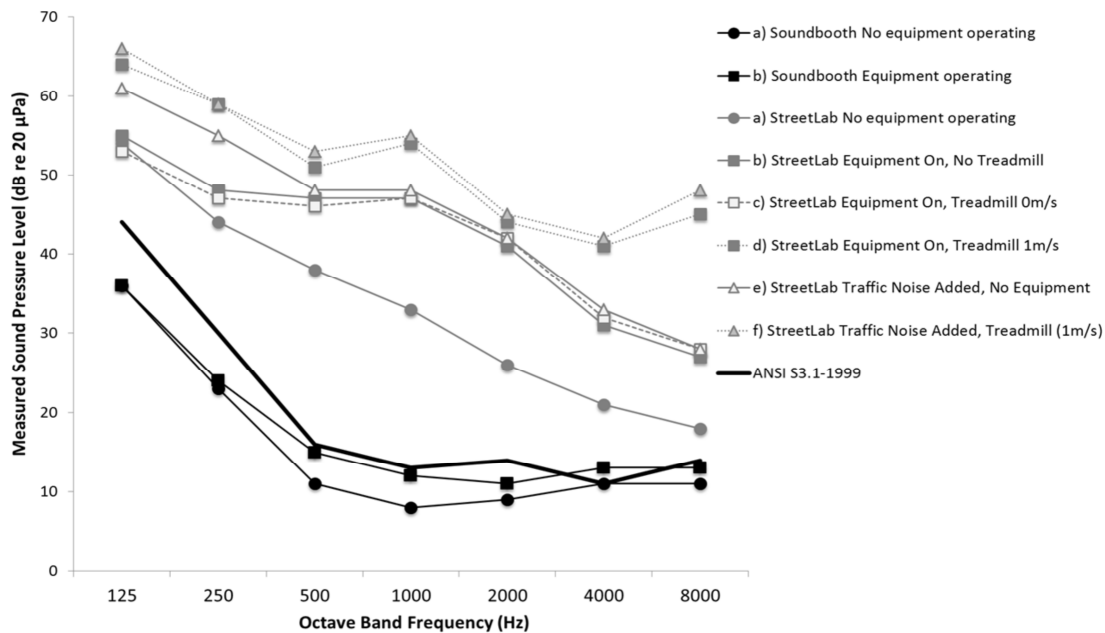


Figure 4: Octave-band sound levels measured in the soundbooth and in StreetLab. Results are shown for conditions without and with basic equipment operating in each test environment (Condition a and b respectively). Results are also shown for four additional possible test conditions in StreetLab, including: treadmill on but not moving (Condition c), treadmill moving at 1m/s (Condition d), with traffic noise but no equipment on (Condition e), or with traffic noise and the treadmill moving at 1 m/s (Condition f). The corresponding maximum permissible background sound levels for audiometric testing specified in ANSI S3.1-1999 are also shown for comparison.

Table 1: Average background sound levels across a sample of different testing conditions in dB A and NC.

Location	Condition	Background Sound Level	
		dB A	NC
Soundbooth	a) No equipment operating	23	15
	b) Equipment operating	24	17
StreetLab	a) No equipment operating	43	37
	b) Equipment operating	51	46
	c) Equipment On, Treadmill 0 m/s	50	46
	d) Equipment On, Treadmill 1 m/s	57	53
	e) Traffic Noise Added, No Equipment	56	65
	f) Traffic Noise Added, Treadmill (1 m/s)	60	65

Speech intelligibility calculations were conducted for the CRM sentences presented in the soundbooth and StreetLab under some of the background noise conditions listed in Table 1 (Condition b in both environments and Conditions c and d in StreetLab). In addition to the conditions listed in Table 1, another condition was evaluated in which the intensity level of the CRM sentences was strategically increased in an attempt to bring the SNR in StreetLab closer to the recommended target SNR for classrooms. The speech peaks of the CRM sentences were

measured as characterized by the 10th percentile, L₁₀, of the sound level in each band occurring over each sentence. Notably, as shown in Figure 5, the frequency responses of the speech stimuli differed between the two test environments, with higher levels of speech in the mid-high frequencies in the soundbooth than in StreetLab. The speech peak measures were used in conjunction with the background sound levels occurring at the same time to calculate the SII.

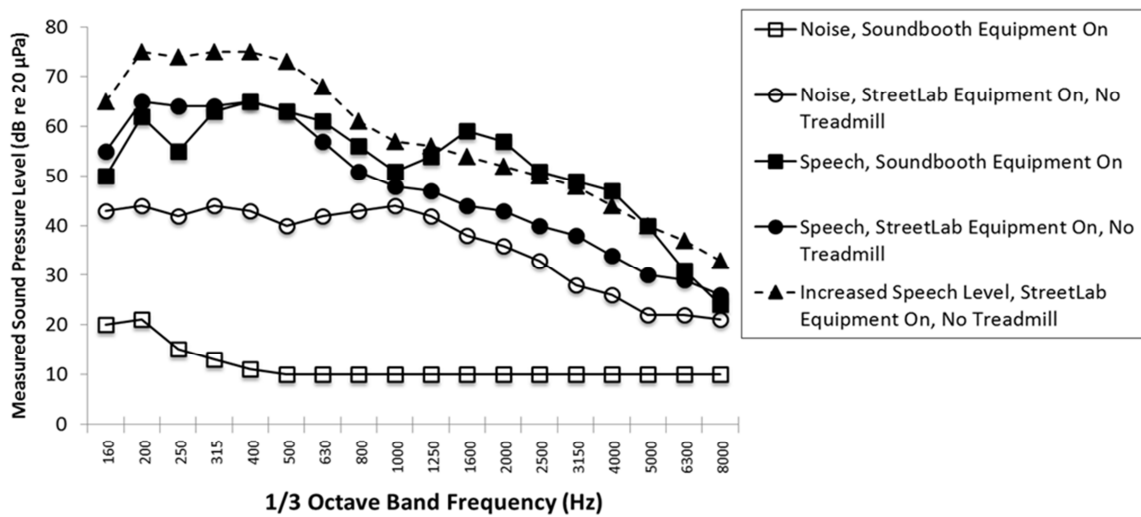


Figure 5: 1/3 octave-band sound levels measured in the soundbooth and in StreetLab as used for calculating the SII. Results are shown for noise measured with basic equipment operating (Condition b) in each test environment. Results are also shown for speech stimuli in each environment and at an increased level in StreetLab.

Table 2: Comparison of speech peak to background sound and calculated SII.

Location	Condition	Background Sound Level (dB A, L _{EQ})	Level of Speech Peaks (dB A, L ₁₀)	SNR	Speech Intelligibility Index (SII)
Soundbooth	Equipment Operating	24	61	37	0.98
StreetLab	Equipment Operating	51	66	15	0.74
	Equipment On, Treadmill 0 m/s	50	66	16	0.73
	Equipment On, Treadmill 1 m/s	57	66	9	0.64
	Increased Speech Peaks	51	76	25	0.96

The overall A-weighted levels and the corresponding calculated SII results are summarized in Table 2. The SII in the soundbooth was .98. In contrast, there were much poorer SII values in StreetLab; e.g., with basic equipment operating the SII value was .74, with the treadmill on but not moving it was .73, and when the treadmill was moving it was even lower (.64). These SII values reflect the slightly lower average speech peak levels in StreetLab compared to the soundbooth (5 dB difference) and the much higher noise levels (28 dB difference) in StreetLab with basic equipment operating compared to the soundbooth. However, increasing the level of the speech was successful in achieving an SII value (.96) that was closer to that achieved in the soundbooth.

4 Discussion

There were several clear differences between the acoustical properties of the soundbooth and StreetLab, including reverberation, background noise level, and the SNR under different experimental conditions. Below we discuss how these differences in acoustical properties might affect

listening performance depending on the nature of the task and the population tested.

4.1 Acoustical properties

Reverberation times

StreetLab was more reverberant than the soundbooth. The reverberation level within StreetLab, however, was still within the range deemed to be acceptable according to the ANSI 12.60 [33] standards for a classroom environment. The effects of increased reverberation on perceptual and behavioral outcomes largely depend on the scenario being tested. For instance, when simple identification tasks are the main outcome of interest, increased reverberation may be less consequential; however, if precise sound localization or speech intelligibility in noise is being evaluated, more reverberant testing environments may be more deleterious [6]. Such deleterious consequences would likely be greater for older compared to younger adults given that age and pure-tone thresholds are independently correlated with ability to recognize words in reverberant and noisy environments (e.g., [38]).

Background sound levels

The background sound levels in StreetLab were higher than those in the soundbooth, even in the most acoustically controlled condition (i.e., no equipment operating, no interactive devices activated, and no simulated ambient traffic sounds). When no equipment was operating, the noise level in StreetLab was 8 dB higher than the maximum recommended average level for good speech intelligibility (35 dB A; [34]). Furthermore, the maximum recommended background sound level was exceeded by 16 dB when the basic equipment was operating, by 15 dB when the treadmill was also operating, and by 25 dB when all equipment was operating and the simulated street and traffic noise was turned on. Clearly, for experiments requiring a quiet environment, it would be more appropriate to test in a soundbooth than in a multimodal simulation lab like StreetLab. For controlled experiments examining performance under realistic noisy conditions, sound levels should be matched to those of the naturalistic conditions of interest. For example, with the simulated traffic noise turned on, the sound level in StreetLab (60 dB A) was still significantly lower than real world background sound levels under city traffic conditions (approximately 80 dB A, [39]), but could be systematically increased as appropriate if the purpose of the test was to evaluate performance in higher levels of traffic noise as might be encountered in the real world. Thus, it would be feasible and justifiable to test behavior during non-quiet conditions in StreetLab.

SNR

The lower background sound levels in the soundbooth resulted in a higher SNR compared to the SNRs found in StreetLab across all conditions with the various types of equipment and devices operating and/or with street sounds. By intentionally increasing the level of the sentence stimuli from 66 to 76 dB A (typical of increasing speech from a raised to a loud voice; [40], pg. 35), we were able to increase the SNR to 25 dB in StreetLab. This SNR is not as large as the SNR measured within the soundbooth (37 dB), but it is an SNR at which speech intelligibility would be very high for most people ($SII = .96$). Importantly, when using a VR lab such as StreetLab, the presentation level of target sounds such as speech may need to be adjusted to compensate for the additional extraneous noise introduced by equipment (e.g., interactive devices such as the treadmill included here). In general, appropriate adjustment of the SNR necessitates the acoustical measurement of both the intended experimental target stimuli, as well as the intended and unintended background sound levels. Calibration based on room properties would be warranted given the differences in the frequency responses of the speech and the noise in the two test environments. Furthermore, the absolute and relative levels of the target and background sounds may need to be adjusted based on audiometric thresholds when participants with hearing loss are tested (see [41]). While these considerations would be obvious and intuitive to most hearing researchers, they may not be commonly considered by many researchers who are using

simulated auditory scenes, but who are not expert in acoustics.

4.2 Factors to consider in developing more naturalistic multimodal testing protocols

The present study demonstrates the need to describe the acoustical properties of test environments and take them into account when designing studies and comparing results across studies in which testing environments differ along a continuum that varies from the highly artificial, controlled and standardized environment of the soundbooth to more realistic and less standardized VR environments and natural environments. While there are standards for audiometric testing and soundbooths used for audiometry, no such standards exist for VR environments or when testing is conducted in more natural environments. It is encouraging that some researchers are starting to develop well-documented, calibrated naturalistic auditory stimuli for auditory research using naturalistic background sounds (e.g., ICRA Natural Sound Library; <https://tspace.library.utoronto.ca/handle/1807/66299>). As the use of VR becomes more widespread in hearing research, aging research, and beyond, standards should evolve to characterize the properties of testing environments in a systematic manner.

When developing multimodal VR protocols, appropriate baseline perceptual tasks should be incorporated because individuals and groups of listeners (e.g., younger vs. older listeners; listeners with normal hearing vs. listeners who are hard of hearing) may differ in their SNR thresholds or in their auditory processing abilities that are critical for listening in reverberant or complex scenes (for a review see [42]). The presentation of stimuli can then be adjusted according to the properties of the environment in relation to the abilities of the participants if the research question depends on equating the difficulty of listening conditions for all participants. This approach avoids the risks associated with making assumptions about equivalence across environmental conditions and participants without explicitly addressing these factors (e.g., to isolate differences due to age from differences due to hearing loss). A better understanding of the effects of environmental factors on performance and their interactions with individual factors such as age and hearing loss is needed to advance theories pertaining to how people listen in adverse environments (e.g., [8]). Such knowledge of the effects of environmental factors could also be applied by rehabilitative audiologists in training clients on how to reduce listening effort, as well as to improve architectural and engineering designs of communication spaces and technologies for special subpopulations of listeners [10].

4.3 Implications for hearing rehabilitation

In the real world, not only are there multiple and changing visual and auditory environmental inputs, but people are typically dynamic (standing, walking, reaching, turning, etc.) and are performing more than one task at any given time (e.g., listening, talking, walking and remembering past

experiences, planning what to do next). Compared to testing in a typical soundbooth, conducting studies using a multimodal VR system provides a controlled, yet more proximate estimate of how these factors might be associated with real-world performance. To fully take advantage of the possibility of manipulating aspects of the VR environment that could not be controlled in real-world testing conditions, procedures for measuring and adjusting for the acoustical properties of VR test environments need to be developed.

In the context of hearing rehabilitation, when evaluating the effectiveness of hearing aid technologies, a disconnect has been reported between the benefits observed during laboratory testing (e.g., measuring word-recognition accuracy on speech-in-noise tests administered in soundbooths) and self-reported benefit and satisfaction in everyday usage of hearing aids [43]. It is possible that results obtained in soundbooths may lead to overestimations or misinterpretations of the benefits associated with using hearing aids in the real world because in everyday life observers perform activities with much more complex auditory stimulation, additional sensory stimulation (e.g., visual, tactile, kinesthetic), and with varying cognitive task demands. Therefore, while improvements associated with hearing aid technologies may be observed in highly controlled, but artificial lab environments, the magnitude of this advantage may not necessarily generalize to functioning in everyday life.

In the real world, listeners use their hearing for purposes other than understanding speech. Auditory abilities (e.g., localization) can support mobility and navigation [48]. Indeed, individuals with hearing loss have identified their most commonly reported limitations to be related to “mobility” and “agility” (65%) compared to communication (12%), memory (12%), or learning (11%) [44]. Introducing controlled VR testing conditions that also allow for common, mobility-related tasks to be conducted (e.g., walking), may provide additional insights into the effects of hearing loss and the benefits of hearing aids in more realistic and demanding conditions compared to testing conditions that are limited to standing or sitting in place. There are also many types of hearing aid technologies that introduce a variety of signal processing options and control features (e.g., directional microphones, multichannel compression, noise reduction, bilateral information exchange, etc.). Each of these variations may differentially benefit everyday, real-world behaviors in unique ways. For example, it is possible that specific features of hearing aids (e.g., microphone directionality) may work particularly well when having a conversation with a dinner partner in a noisy restaurant, but may not be as useful (or may possibly be detrimental) when navigating a busy intersection in heavy traffic. Comparing performance with hearing aid technologies across a range of challenging and realistic conditions simulated by VR could provide a richer understanding of their advantages and limitations.

The effects of age-related changes in auditory processing can also be compounded by an increased prevalence of other sensory, motor and cognitive declines that affect older adults. Specifically, much more needs to be

learned about how age-related auditory declines interact with age-related declines in other domains of functioning (e.g., vision, mobility, cognition), especially when complex and cognitively demanding tasks are performed in realistic conditions that are often unfavorable, if not adverse. Introducing novel VR methods that allow for the systematic manipulation of sensory inputs and the strategic modification of perceptual and cognitive demands can help to further our understanding of how these factors interact with age. Immersive, multisensory, VR technologies show great promise in addressing these gaps.

VR may also provide an opportunity to improve or extend the possible range of outcome measures. The outcome measures most commonly used to assess auditory abilities and hearing aid effectiveness in the soundbooth are not necessarily the same outcome measures that would be most relevant for everyday listening. Many older adults who have normal or near-normal audiograms have little difficulty in ideal listening conditions. Amplification can restore the audibility of speech for those who have hearing loss. Nevertheless, older adults, regardless of their audiometric thresholds, report poorer functioning in everyday listening conditions than younger adults [45]. Some of the variation across individuals in speech understanding in noise can be explained by measures of supra-threshold auditory temporal processing and cognitive processing [46]. Furthermore, once speech or other sounds have been heard, cognitive resources are required for the person to comprehend, evaluate, remember and respond appropriately to sound input and to integrate it with other incoming signals and stored knowledge. Cognitive measures such as working memory can be used to assess inter-individual differences in the cognitive capacity deployed in specific listening situations and to assess intra-individual differences in the allocation of cognitive capacity in response to varying demands across changing listening environments [47]. The growing interest in how to conceptualize and measure listening effort and aspects of auditory cognition (memory and attention) reflects recognition by audiologists that both auditory and cognitive processing contribute to everyday listening experiences [10]. As behavioral and physiological measures of listening effort continue to be developed, the complex and demanding conditions that can be simulated using VR may be extremely useful for the evaluation of performance across a range of conditions more representative of those encountered in everyday life.

Acknowledgments

We thank Bruce Haycock, Susan Gorski, and Larry Crichlow for their technical assistance and Jessica Babineau for constructing the historical timeline of auditory VR.

References

- [1] Campos JL, Bülhoff HH. Multisensory integration during self-motion. In: Ed. Wallace M, Murray M, *Front Neural Bases Multisensory Processes*, pages 603-628. London: Taylor and Francis, 2012.

- [2] Rizzo A, Parsons TD, Buckwalter, J. Using virtual reality for clinical assessment and intervention. In *Handbook of Technology in Psychology, Psychiatry, and Neurology: Theory, Research, and Practice*, pages 277-318. Nova Science Publishers Inc, 2012.
- [3] Hale KS, Stanney KM. *Handbook of Virtual Environments: Design, Implementation, and Applications, Second Edition*. CRC Press, Taylor and Francis, Florida, 2015.
- [4] Parsons TD. Virtual reality for enhanced ecological validity and experimental control in the clinical, affective and social neurosciences. *Front Hum Neuro*. 2015;11(9):660.
- [5] Shilling RD, Shinn-Cunningham BG. Virtual auditory displays. In *Handbook of Virtual Environments Technology*, K. Stanney (ed.), pages 65-92. Erlbaum, 2002.
- [6] Vorlander M, Shinn-Cunningham BG. Virtual auditory displays. In *Handbook of Virtual Environments, 2nd edition: Design, Implementation, and Applications*, K Hale, K Stanney (Eds), pages 87-114. Erlbaum, 2012.
- [7] Carlile S, Leung J. The perception of auditory motion. *Trends Hear*. 2016;20:1-19.
- [8] Mattys SL, Davis MH, Bradlow AR et al. Speech recognition in adverse conditions: A review. *Lang Cogn Process*. 2012;27(7-8):953-978.
- [9] Keidser G. Introduction to special issue: Towards ecologically valid protocols for the assessment of hearing and hearing devices. *J Am Acad Audiol*. 2016;27(7):502-503.
- [10] Pichora-Fuller MK, Kramer SE, Eckert M et al. Hearing impairment and cognitive energy: The Framework for Understanding Effortful Listening (FUEL). *Ear Hear*. 2016;37(Suppl 1):S5-S27S.
- [11] Pichora-Fuller MK, Hodgson M, Schneider BA et al. Potential applications of auralization in audiological rehabilitation. *Proc Int Symp Simulation, Visualization and Auralization for Acoustic Research and Education*, pages 393-394. Tokyo, Japan, 1997.
- [12] Seeber BU, Kerber S, Hafter ER. A system to simulate and reproduce audio-visual environments for spatial hearing research. *Hear Res*. 2010;260(1-2):1-10.
- [13] Mihelj M, Novak D, Begus S. Acoustic modality in virtual reality. In *Virtual Reality Technology and Applications*, pages 131-159. Springer, Netherlands, 2014.
- [14] Punch JL, Robb R, Shovels, AH. Aided hearing aid user preferences in laboratory versus real-world environments. *Ear Hear*. 1994;15:50-61.
- [15] Oreinos C, Buchholz JM. Evaluation of loudspeaker-based virtual sound environments for testing directional hearing aids. *J Amer Acad Audiol*. 2016;7:541-556.
- [16] Wu Y-H, Nazan A, Rizzo M et al. (2014). Measuring listening effort: driving simulator vs. simple dual-task paradigm. *Ear Hear*. 2014;35(6):623-632.
- [17] Lau ST, Pichora-Fuller MK, Li KZH et al. Effects of hearing loss on dual-task performance in an audiovisual virtual reality simulation of listening while walking. *J Amer Acad Audiol*. 2016;27(7):567-587.
- [18] Ramkhalawansingh R, Keshavarz B, Haycock B et al.. Age differences in visual-auditory self-motion perception during a simulated driving task. *Front Psych*. 2016;7(595):1-12.
- [19] Campos JL, Bédard M, Classen S, Delparte JJ, Hebert DA, Hyde N, Law G, Naglie G, and Yung S. Guiding framework for driver assessment using driving simulators. *Front Psychol*. 2017;8: 1428,
- [20] Lin FR, Ferrucci L. Hearing loss and falls among older adults in the United States. *Arch Intern Med*. 2012;172(4): 369-371.
- [21] Hickson L, Wood J, Chaparro A et al. Hearing impairment affects older people's ability to drive in the presence of distractors. *J Amer Geriatrics Soc*. 2010;58: 1097-1103.
- [22] Singh G, Pichora-Fuller MK, Schneider BA. Auditory spatial attention in conditions of real and simulated spatial separation by younger and older adults. *J Acous Soc Amer*. 2008;124:1294-1305.
- [23] Nieborowska V, Lau ST, Campos JL et al. Effects of age on dual-task walking while listening. *J Mot Beh*. (in press) .
- [24] Cameron S, Dillon H. Development of the Listening in Spatialized Noise-Sentences Test (LISN-S). *Ear Hear*. 2007;28:196-211.
- [25] Cameron S, Dillon H. *Listening in Spatialized Noise-Sentences test (LiSN-S)*, Murten, Switzerland: Phonak Communications AG, 2009.
- [26] Albers MW et al. At the interface of sensory and motor dysfunctions and Alzheimer's disease. *Alzheim Demen*. 2015; 11:70-98.
- [27] Laurienti PJ, Burdette JH, Maldjian JA et al. Enhanced multisensory integration in older adults. *Neurobio Aging*. 2006;27(8):1155-1163.
- [28] Mozolic JL, Hugenschmidt CE, Peiffer AM et al. Multisensory integration and aging. In Murray MM & Wallace MR (Eds), *The Neural Bases of Multisensory Processes* (Chapter 20). Boca Raton (FL): CRC Press, 2012.
- [29] Freiherr J, Lundström JN, Habel U et al. Multisensory integration mechanisms during aging. *Front Hum Neuro*. 2013;7:863.
- [30] Weeks JC, Hasher L. The disruptive - and beneficial - effects of distraction on older adults' cognitive performance. *Front Psych*. 2014;5:133.
- [31] Frank T. ANSI update: maximum permissible ambient noise levels for audiometric test rooms. *Am J Audiol*. 2000;9(1);3-8.
- [32] Bolia RS, Nelson WT, Ericson MA et al. A speech corpus for multitalker communications research. *J Acous Soc Amer*. 2000;107:1065-1066.
- [33] American National Standards Institute. Acoustical Performance Criteria, Design Requirements, and Guidelines for Schools, Part 1: Permanent Schools (ANSI 12.60 I). New York, 2010.
- [34] Bradley JS. Acoustical design of rooms for speech. Construction Technology Update No. 51, Institute for Research in Construction, National Research Council of Canada: Ottawa, 2002.
- [35] Beranek LL, Blazier WE, Figwer JJ. Preferred Noise Criterion (PNC) curves and their application to rooms. *J Acous Soc Amer*. 1971;50:1223-1228.
- [36] American National Standards Institute. Standard Methods for Calculation of the Speech Intelligibility Index (ANSI/ASA S3.5 (R2012)). New York, 2012.
- [37] American National Standards Institute. Maximum Permissible Ambient Noise Levels for Audiometric Test Rooms (ANSI S3.1). New York, 1999.
- [38] Helfer KS, Wilber LA. Hearing loss, aging, and speech perception in reverberation and noise. *J Speech Hear Res*. 1990;33(1);149-155.
- [39] National Institute on Deafness and other Communication Disorders
<http://www.nidcd.nih.gov/staticresources/health/education/teachers/CommonSounds.pdf>

[40] Pearson KS, Bennett RL, Fidell S. Speech levels in various noise environments. Environmental Health Effects Research Series. EPA-600/1-77-025. Report from the Office of Health and Ecological Effects, U.S. Environmental Protection Agency, Washington, 1977.

[41] Humes LE, Dubno JR. Factors affecting speech understanding in older adults. In Gordon-Salant S, Frisina RD, Popper AN and Fay RR (Eds), Aging Audit Syst., *Springer Handbook of Auditory Research*, pages 211–257. Springer, New York, 2010.

[42] Pichora-Fuller MK, Alain C, Schneider B. Older adults at the cocktail party, pages 227-259. In Middlebrooks J, Simon J, Popper A, Fay RR (Eds), *The auditory system at the cocktail party*, Springer Handbook of Auditory Research. Springer: Berlin, 2017.

[43] Gnewikow D, Ricketts T, Bratt GW et al. Real-world benefit from directional microphone hearing aids. *J Rehab Res and Devol.* 2009;46:603-618.

[44] Statistics Canada. Participation and activity limitation survey: Facts on hearing limitations. 2006.

[45] Banh J, Singh G, Pichora-Fuller MK. Age affects responses on the Speech, Spatial, and Qualities of Hearing Scale (SSQ) for adults with minimal audiometric loss. *J Amer Acad Audiol.* 2012;23: 81-91.

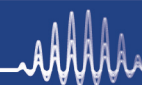
[46] Humes LE. The contributions of audibility and cognitive factors to the benefit provided by amplified speech to older adults. *J Am Acad Audiol.* 2007;18(7):590-603.

[47] Smith S, Pichora-Fuller MK, Alexander G. Development of the Word Auditory Recognition and Recall Measure (WARRM): A working memory test for use in rehabilitative audiology. *Ear Hear.* 2006;37(6):e360-e376.

[48] Campos JL, Ramkhalawansingh R, Pichora-Fuller MK. Hearing, self-motion perception, mobility and aging. *Hear Res.* 2018. <https://doi.org/10.1016/j.heares.2018.03.025>

Scantek, Inc.

Calibration Laboratory



Scantek offers traceable, high quality and prompt periodic calibration of any brand of sound and vibration instrumentation

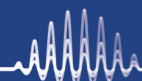
Calibration and Service Capabilities:

- Microphones
- Preamplifiers
- Acoustical Calibrators
- Sound Level Meters & Analyzers
- Accelerometers & Vibration Meters
- Vibration Calibrators and more

ISO 17025:2005 and ANSI/NCSL Z-540-1: 1994 Accredited Calibration Laboratory

Scantek, Inc.

Sales, Rental, Calibration

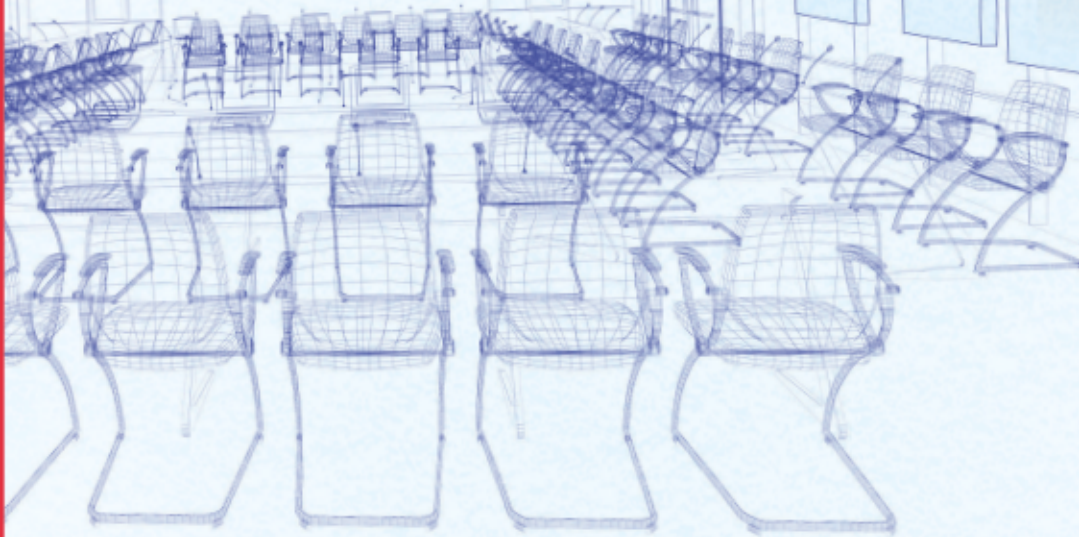


www.ScantekInc.com/calibration

800-224-3813

WE CAN MAKE WHATEVER YOU MAKE

BETTER. SAFER. QUIETER.



Custom insulation solutions for acoustical panels start here.

Made from basalt rock, ROXUL® Core Solutions (OEM) insulation provides excellent acoustical dampening and fire resistant properties. So whether you're designing acoustical panels, a music studio or modular office – our team of experts will work with you before, during and after fabrication to create the custom sound solution you're looking for.

Visit us at roxul.com/oem



Part of the ROCKWOOL Group



EFFECTIVE
SOUND
MASKING

Don't miss your **TARGET**

Simply put, poor tuning equals poor masking. In fact, each decibel decrease in overall volume can reduce performance by 10%. Failing in just one key frequency can reduce it by 5%. LogiSon TARGET rapidly adjusts the masking sound to meet the specified spectrum with unequalled accuracy, reducing tuning time while maximizing benefits.

logison.com

© 2018 K.R. Moeller Associates Ltd. LogiSon is a registered trademark of 777388 Ontario Limited.



LogiSon[®]
ACOUSTIC NETWORK

TRUE NORTH: A COMPARISON OF MEASURED VS MODELLED NOISE LEVELS WITH INOISE

Henk de Haan ^{*1} and Virgini Senden ^{†1}
¹dBA Noise Consultants Ltd, Okotoks, Alberta, Canada

1 Introduction

Standard ISO 9613-2 [1] is a widely used standard in noise predictions for industrial noise. Various jurisdictions in Canada recommend or require the use of ISO 9613-2. The standard has been implemented in several commercially available software suites that are in use in Canada today, e.g. CadnaA, Predictor and Soundplan. It has been noted that the translation of ISO 9613-2 in software algorithms can be open to interpretation [3], [4]. As a consequence, different software suites may produce different results for the same modelled situation. To help remedy this unwanted situation, Standard ISO/TR 17534-3 [2] was introduced in 2015. Recently, a new software suite has been introduced to the Canadian market, iNoise. iNoise looks and feels very similar to Predictor and is being marketed as a suite that strictly confirms to ISO 9613-2 in combination with ISO/TR 17534-3. Time for a reality check: how do noise levels that were predicted using iNoise compare to measured noise levels?

2 ISO 9613-2

2.1 General

ISO 9613-2 specifies an engineering method for calculating the noise propagation outdoors from a variety of sources with a known noise emission to receptors at a distance under meteorological conditions that are favorable for noise propagation (downwind from source to receptor, wind speed between 1-5 m/s, or a well-developed moderate ground-based temperature inversion). The estimated accuracy of ISO 9613-2 for broadband noise is ± 3 dB for distances up to 1 km and a mean height of source and receiver of less than 30 m, not taking effects from screening or reflections into account. The stated accuracy only applies to the propagation and not to the source description.

2.2 Ambiguities and clarifications in ISO/TR 17534

ISO 9613-2 is not completely unambiguous and some clauses are open to different interpretations. An example of ambiguous text in ISO 9613-2 (page 9, chapter 7.4 Screening) is “*Assume that only one significant sound-propagation path exist from the sound source to the receiver. If this assumption is not valid, separate calculations are required for other propagation paths*”.

* henk@dbanoise.com

† virgini@dbanoise.com

There is no further definition given for ‘significant’ and no unambiguous guidance on the number and construction of other propagation paths.

3 Proofing the Pudding

3.1 Predicted vs. Measured Results

It can be useful to compare predicted results with measured results to verify the accuracy of noise models. Several conditions apply:

- The measurements used for calibration should be conducted such that the results apply only to the measured noise sources and are only marginally influenced by e.g. ambient noise levels;
- In order to compare apples to apples, measurements should be conducted under conditions (both operational and meteorological) that resemble modelled conditions (e.g. downwind) or vice versa.

3.2 Test Case

A newly constructed natural gas plant is located in northern British Columbia in a mostly undisturbed (by other noise sources) environment. The regulatory approval for the facility included a condition that mandated a post-construction noise survey. dBA Noise Consultants was retained for the post construction survey.

The facility includes equipment typically found in natural gas plants such as large combustion engines, compressors, electric motors, air coolers and condensers, generators, heaters, vessels and pressure valves. Part of the equipment is housed in industrial buildings with several openings (both silenced and unsilenced louvres, forced ventilation, combustion air intakes, open roof ridges). Some significant noise sources are located outdoors (e.g. coolers and condensers). The buildings are situated in several parallel rows – noise levels at receptors located at the fenceline could be screened by multiple buildings. The ground was sandy and unpaved, but not compacted throughout. It was therefore considered to have a low porosity. ISO 9613-2 recommends a ground factor of 0 (hard) for such a surface.

3.3 Near-field Measurements

During the summer of 2017, we conducted near-field measurements around individual pieces of equipment and in openings to assess sound power levels in accordance with e.g. ISO 3744 [5] If possible, noise sources were

approached as point sources, but for most surface-enveloping measurements were used. We also recorded location, height, dimensions, specific operating conditions such as rpm etc. For buildings, we recorded location, height, location, size and number of openings.

3.4 Fenceline Measurements

We also conducted a total of 11 fenceline measurements on several different days at a receptor height of approximately 3.5 m, and at a distance of approximately 140 – 250 m from the nearest dominant noise sources. The locations were at the north, east and south side of the plant. Measurements were conducted under mild downwind ($\pm 45^\circ$) conditions, with some cloud cover (up to 7/8). These meteorological conditions were considered to be in accordance with ISO conditions. Other noise sources than the plant were not audible during the measurements. Measurement duration was sufficiently long for the Leq to settle well before the conclusion of each individual measurement. Thus, the measurements were considered to be suitable for a comparison to modelled results. The measured noise levels varied from 61 dBA to 65 dBA.

3.5 Modelling

We modelled the plant in iNoise and compared the calculated noise levels at the fenceline receptors to the measured results. Model settings of note were a ground factor of 0.2 respectively and 0.0 (hard ground). This comparison stems from our preferred general settings using the Predictor software suite (a ground factor of 0 only for surfaces like water or paved, open surfaces, 0.8 for soft ground and 0.2 for hard ground).

3.6 Comparison Measured vs Calculated

The average, highest and lowest differences are included in Table 1. A detailed comparison for the differences between measured and calculated noise levels is included in Figure 1.

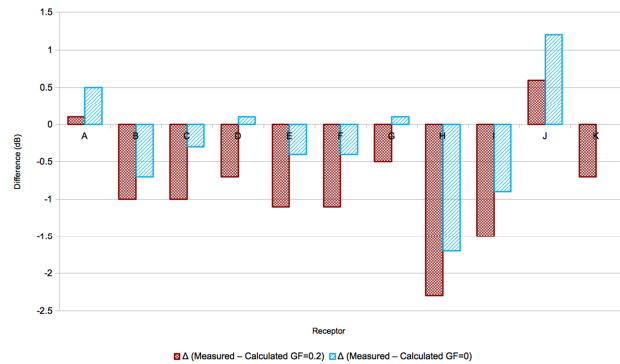
4 Discussion

Results for both comparisons are well within the margin of ± 3 dB that is included in ISO 9613. Average results are slightly below the measured results. A modelled ground factor of 0 for ground surfaces resembles measured noise levels more closely than a ground factor of 0.2. Using a ground factor of 0 follows ISO 9613-2 more closely. iNoise therefore seems capable of accurately predicting noise levels within the accuracy of ISO 9613-2. It is recommended to strictly follow ISO 9613-2 when modelling. Future comparisons could involve measured noise levels over soft (absorbing) ground near the receptor.

Table 1: Comparison Difference Measured vs Calculated Noise Levels (dB).

Description	Ground Factor 0.2	Ground Factor 0.0
Average 11 receptors	-0.8	-0.2
Highest Difference	0.6	1.2
Lowest Difference	-2.3	-1.7

Figure 1: Comparison Measured vs Calculated Noise Levels (dB).



References

- [1] ISO-9613-2, Acoustics – Attenuation of sound during propagation outdoors – General method of calculation, ISO, 1996.
- [2] ISO/TR 17534-3, Acoustics – Software for the calculation of sound outdoors – Recommendations for quality assured implementation of ISO 9613-2 in software, ISO, 2015.
- [3] Hartog van Banda, S.E. and Stapelfeldt, H., Implementing prediction standards in calculation software – the various sources of uncertainty, Forum Acusticum, 2005.
- [4] Hartog van Banda, S.E. and Manvell, D., Implementing noise prediction standards in software – challenges and experiences, *Internoise*, 2013.
- [5] ISO 3744, Acoustics — Determination of sound power levels and sound energy levels of noise sources using sound pressure — Engineering methods for an essentially free field over a reflecting plane, 3rd edition, 2010.

There's a lot of noise out there.

Rockfon® ceilings provide the style architects want and the high sound absorption you need. Get the facts at www.Rockfon.com.



The Passing Whistler

The Gum Smacker

The Loud Talker

The Coffee Slurper

The Click-Clacker

The Squeaky Roller



Part of the ROCKWOOL Group



SYSTEMS FOR RESEARCH & DEVELOPMENT



MEET YOUR NEW SOUNDADVISOR



SoundAdvisor Model NMS044

NOISE MONITORING SOLUTIONS | Models 831C & NMS044

SoundAdvisor from Larson Davis sets a new standard for connectivity, access, and control of your noise monitoring using a network connection

- Connect over cellular, WiFi, or wired networks
- Control meter and view data via web browser
- Receive real-time alerts on your mobile device
- Monitor continuously with a solar powered outdoor system

www.dalimar.ca | info@dalimar.ca | 450.424.0033



EDITORIAL BOARD - COMITÉ ÉDITORIAL

Aeroacoustics - Aéroacoustique

Anant Grewal (613) 991-5465 anant.grewal@nrc-cnrc.gc.ca
National Research Council

Architectural Acoustics - Acoustique architecturale

Jean-François Latour (514) 393-8000 jean-francois.latour@snclavalin.com
SNC-Lavalin

Bio-Acoustics - Bio-acoustique

[Available Position](#)

Consulting - Consultation

Tim Kelsall 905-403-3932 tkelsall@hatch.ca
Hatch

Engineering Acoustics / Noise Control - Génie acoustique / Contrôle du bruit

Joana Rocha Joana.Rocha@carleton.ca
Carleton University

Hearing Conservation - Préservation de l'ouïe

Alberto Behar (416) 265-1816 albehar31@gmail.com
Ryerson University

Hearing Sciences - Sciences de l'audition

Olivier Valentin 514-885-5515 m.olivier.valentin@gmail.com
ÉTS, Université du Québec

Musical Acoustics / Electroacoustics - Acoustique musicale / Électroacoustique

Annabel J Cohen acohen@upei.ca
University of P.E.I.

Physical Acoustics / Ultrasounds - Acoustique physique / Ultrasons

[Available Position](#)

Physiological Acoustics - Physio-acoustique

Robert Harrison (416) 813-6535 rvh@sickkids.ca
Hospital for Sick Children, Toronto

Psychological Acoustics - Psycho-acoustique

Jeffery A. Jones jjones@wlu.ca
Wilfrid Laurier University

Shocks / Vibrations - Chocs / Vibrations

Pierre Marcotte marcotte.pierre@irsst.qc.ca
IRSST

Signal Processing / Numerical Methods - Traitement des signaux / Méthodes numériques

Tiago H. Falk (514) 228-7022 falk@emt.inrs.ca
Institut national de la recherche scientifique (INRS-EMT)

Speech Sciences - Sciences de la parole

Michael Kieft +1 902 494 5150 mkieft@dal.ca
Dalhousie University

Underwater Acoustics - Acoustique sous-marine

[Available Position](#)

Special Issue: Audiology and Neurosciences - Numéro spécial: audiologie et neurosciences

Olivier Valentin, M.Sc., Ph.D. 514-885-5515 m.olivier.valentin@gmail.com
Université de Sherbrooke

Technical Notes - Exposés techniques

Umberto Berardi 416 979 5000 (3263) uberardi@ryerson.ca
Ryerson University



The network of research organizations
Le réseau des organismes de recherche

An information system with academic CV management, expertise inventory and networking capabilities for research institutions and associations.

Un système d'information avec gestion de CV académique, un inventaire de l'expertise interne et des capacités de réseautage pour des organismes de recherche.

With UNIWeb, researchers can:

Avec Uniweb, les chercheurs peuvent:

Streamline

funding applications with Canadian Common CV integration

Simplifier

les demandes de financement grâce à l'intégration au CV commun canadien

Reuse

CCV data to generate academic CVs and progress reports

Réutiliser

les données du CVC pour générer des CV académiques et des rapports de progrès

Mobilize

knowledge by creating engaging webpages for research projects

Mobiliser

les connaissances en créant des pages Web attrayantes pour les projets de recherche

<http://uniweb.network>

CALL FOR PAPERS!



Special Issue: Audiology & Neurosciences

Acoustics is a broad subject matter that currently employs hundreds of us across Canada in fields as different as teaching, research, consulting and others. To reflect such diversity the Canadian Acoustics has been regularly publishing over the last 40 years a series of special journal issues to highlight thematic topics related to acoustics.

Therefore, the Canadian Acoustics journal is currently inviting submissions for the next special issue programmed for March 2019. **The focus of manuscripts submitted to this Special Issue may include (but are not restricted to) topics related to audiology and neurosciences such as:**

- Acoustics applications in electrophysiology (e.g. EEG, EOG, ECOG...)
- Hearing assessment (e.g. audiometry, DPOAE...)
- Any other topics in audiology/neurosciences related to acoustics.

HOW TO BE PART OF IT?

To contribute to these special “audiology and neuroscience” journal issues, authors are invited to submit their manuscript under the “Special Issue” section through the online system at <http://jcaa.caa-aca.ca> **before November 15th 2018.**

Each manuscript will be reviewed by the Canadian Acoustics Editorial Board that will enforce the journal publication policies (original content, non-commercialism, etc., refer to the Journal Policies section online for further details).

A UNIQUE SPECIAL ISSUE YOU WANT TO APPEAR IN!

This special issue of the journal can be considered as a true directory for audiology and neuroscience in Canada. They will be published in hardcopies and sent to all CAA national and international members, while electronic copies will be made available in open-access on the journal website. The content of these issues will be entirely searchable and comprehensively indexed by scholar engines as well as by major internet search engines (Google, Bing, etc.). Authors are invited to carefully select their keywords to maximize the visibility of their articles.

If you have any questions, please contact Mr. Olivier Valentin (olivier.valentin@etsmtl.ca). To secure an advertisement for this special issue, please contact Mr. Bernard Feder (advertisement@caa-aca.ca).

**SUCH AN OFFER WILL ONLY APPEAR EVERY 7 OR 9 YEARS,
SO MAKE SURE TO TAKE ADVANTAGE!**

APPEL À SOUMISSIONS !



Numéro Spécial: Audiologie & Neurosciences

L'acoustique est un vaste domaine qui offre des centaines d'emplois à travers le Canada, et ce, dans différents secteurs tels que l'éducation, la recherche, la consultation professionnelle, etc... Afin de bien refléter cette diversité, l'Acoustique Canadienne a publié régulièrement au cours des 40 dernières années une série de numéros spéciaux pour souligner les divers champs d'applications de l'acoustique

L'Acoustique Canadienne fait donc un appel à soumettre une série d'articles pour le prochain numéro spécial planifié pour mars 2019. **Ce numéro spécial inclura principalement (mais ne se limitera pas à) des contributions dont le sujet est en lien avec l'audiologie et les neurosciences, tel que :**

- Applications de l'acoustique en électrophysiologie (EEG, EOG, ECOG, etc...)
- Évaluation de l'audition et de la surdité (audiométrie, DPOAE, etc...)
- Tout autre sujet en audiologie/neurosciences en lien avec l'acoustique.

COMMENT EN FAIRE PARTIE?

Pour contribuer à ce numéro spécial « audiologie et neurosciences », les auteurs sont invités à soumettre un article, sous la rubrique « Numéro spécial » dans notre système en ligne au <http://jcaa.caa-aca.ca> **avant le 15 novembre 2018**. Il est possible de soumettre un même article dans les deux langues officielles.

Chaque article sera révisé par le comité éditorial de l'Acoustique canadienne qui veillera à ce que les politiques de publications de la revue soient respectées (contenu original, contenu non commercial, etc. – voir les politiques de la revue pour de plus amples détails).

UN NUMÉRO UNIQUE DANS LEQUEL VOUS VOULEZ PARAÎTRE!

Ce numéro spécial « audiologie et neurosciences » peut être considéré comme un véritable répertoire à propos de l'audiologie et des neurosciences au Canada. Ils sont publiés en format papier et envoyés à tous les membres nationaux et internationaux de l'ACA. Une version électronique est aussi disponible en ligne sur le site internet de la revue. Le contenu de ces numéros est indexé, donc facilement trouvable au moyen de moteurs de recherche classiques, tels que Google, Bing, etc... Les auteurs sont invités à bien choisir les mots clefs pour maximiser la visibilité de leur article.

Pour toutes questions, vous pouvez communiquer avec Mr. Olivier Valentin (olivier.valentin@etsmtl.ca). Pour réserver un espace de publicité dans un de ces numéros spéciaux, veuillez communiquer avec Bernard Feder (advertissement@caa-aca.ca).

**UNE TELLE OPPORTUNITÉ NE SE REPRODUIRA PAS AVANT 7 OU 9 ANS,
ASSUREZ-VOUS D'EN PROFITER MAINTENANT!**

VIBRATION MONITORING TERMINAL – TYPE 3680

GOOD VIBRATIONS



Reliably take real-time measurements with our new Vibration Monitoring Terminal. The robust device enables you to:

- Protect against structural damage risks in construction and mining
- Assess human response to road and rail traffic vibration
- Monitor background vibration to avoid sensitive machinery disturbance

The Vibration Monitoring Terminal includes metrics for a wide range of applications. The system provides continuous, uninterrupted, real-time monitoring 24/7. Alerts are based on level and time of day. It contains a single tri-axial geophone for full coverage of vibration levels, and built-in remote access so you don't need to visit a site to retrieve data.

Use the unit with our Sentinel environmental monitoring service or as a stand-alone device.

See more at www.bksv.com/VMT

Brüel & Kjær 
BEYOND MEASURE



Brüel & Kjær North America Inc.
3079 Premiere Parkway, Suite 120
Duluth, GA 30097
Tel: 770 209 6907

bkinfo@bksv.com
www.bksv.com/VMT

Sound and Vibration Instrumentation

Scantek, Inc.



Sound Level Meters

Selection of sound level meters for simple noise level measurements or advanced acoustical analysis



Building Acoustics

Systems for airborne sound transmission, impact insulation, STIPA, reverberation and other room acoustics measurements



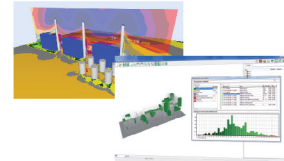
Vibration Meters

Vibration meters for measuring overall vibration levels, simple to advanced FFT analysis and human exposure to vibration



Sound Localization

Near-field or far-field sound localization and identification using Norsonic's state of the art acoustic camera



Prediction Software

Software for prediction of environmental noise, building insulation and room acoustics using the latest standards



Monitoring

Temporary or permanent remote monitoring of noise or vibration levels with notifications of exceeded limits

Scantek, Inc.

Sales, Rental, Calibration

www.ScantekInc.com

800-224-3813

www.arcacoustics.com

ARCACOUSTICS
ARCHITECTURAL AND INTERIOR ACOUSTICS

877-337-9312



Contact us for the Right Solution for your Space

One Stop Shop for all your Interior and Building Noise Control Solutions

Home Theaters and Music Rooms
Commercial and Retail Spaces
Gyms and Athletic Centers
Basements

Isolation Clips for Walls and Ceilings
Soundproof Windows and Doors
Sound Impact Underlayments
Acoustical Panels

CANADIAN ACOUSTICS ANNOUNCEMENTS - ANNONCES TÉLÉGRAPHIQUES DE L'ACOUSTIQUE CANADIENNE

Looking for a job in Acoustics?

There are many job offers listed on the website of the Canadian Acoustical Association!

You can see them online, under <http://www.caa-aca.ca/jobs/>

August 5th 2015

ICSV26 to be held in Montreal, July 2019

The 26th International Congress on Sound and Vibration (ICSV26) will be held in Montreal, Canada, from 07 - 11 July 2019 at Hotel Bonaventure.

The local organizing committee and scientific committees are currently being formed. Please contact us if you are interested to be part of the adventure! :-)) - You can also check out our website at www.icsv26.org - Jeremie Voix (conference-chair@icsv26.org) - Franck Sgard (technical-chair@icsv26.org) -

October 12th 2017

AWC18 in Victoria, BC

The 176th Meeting of the Acoustical Society of America (ASA) will be held jointly with the Acoustics Week in Canada 2018 of the Canadian Acoustical Association (CAA) in Victoria, BC, Canada, on 5-9 November 2018.

The conference will be organized by the Acoustical Society of America using their guidelines and procedures, while the Canadian Acoustical Association will organize some special sessions and handle its regular business and core activities, such as standards committee, student awards, etc. - For more information, visit <http://acousticalso-ciety.org/meetings> - To contact Dr. Roberto Racca, AWC2018 conference coordinator, please send an email to: conference@caa-aca.ca

November 24th 2017

ASA Fall 2018 meeting/2018 Acoustics Week in Canada

The joint 176th Meeting of the Acoustical Society of America (ASA) and 2018 Acoustics Week Canada of the Canadian Acoustical Association (CAA) will be held Monday through Friday, 5-9 November 2018 at the Victoria Conference Centre, Victoria, British Columbia, Canada. The headquarters hotel is the Fairmont Empress. - -

Blocks of rooms have been reserved at the Fairmont Empress and the Victoria Marriott Inner Harbour Hotel at discounted rates. Please refer to the Victoria meeting website for the call for papers and instructions for submitting abstracts and making hotel reservations. - The deadline for receipt of abstracts is Tuesday, 29 May 2018. - - The call for papers describes the special sessions that will be organized by the ASA Technical and Administrative Committees and the CAA and other events such as a hot topics session, short course, and tutorial lecture. Social events will include the Social Hours, Women in Acoustics Luncheon, the Society Luncheon and Lecture, and the Jam session. - - Special events include the Undergraduate Research Exposition and Early-Career Speed-Networking. - - Student events, organized by the Student Council, will include a Student Orientation, a Meet and Greet, and the Student Reception. See the Student Information section of the meeting announcement for details including information about the Students Meet Members for Lunch program. - - Funding opportunities are offered including Student Transportation Subsidies, Dependent Care Subsidies, Young Investigator Travel Grants, Early Career Travel Subsidies, and Best Paper Awards for Students and Early Career Acousticians. - - Accompanying persons are welcome at the meeting and a program of activities will be organized. - - We hope that you will consider presenting a paper or attending the meeting to participate in the exchange of ideas and the latest research developments in acoustics and to meet with your colleagues in the ASA. -

April 19th 2018

À la recherche d'un emploi en acoustique ?

De nombreuses offre d'emploi sont affichées sur le site de l'Association canadienne d'acoustique !

Vous pouvez les consulter en ligne à l'adresse <http://www.caa-aca.ca/jobs/>

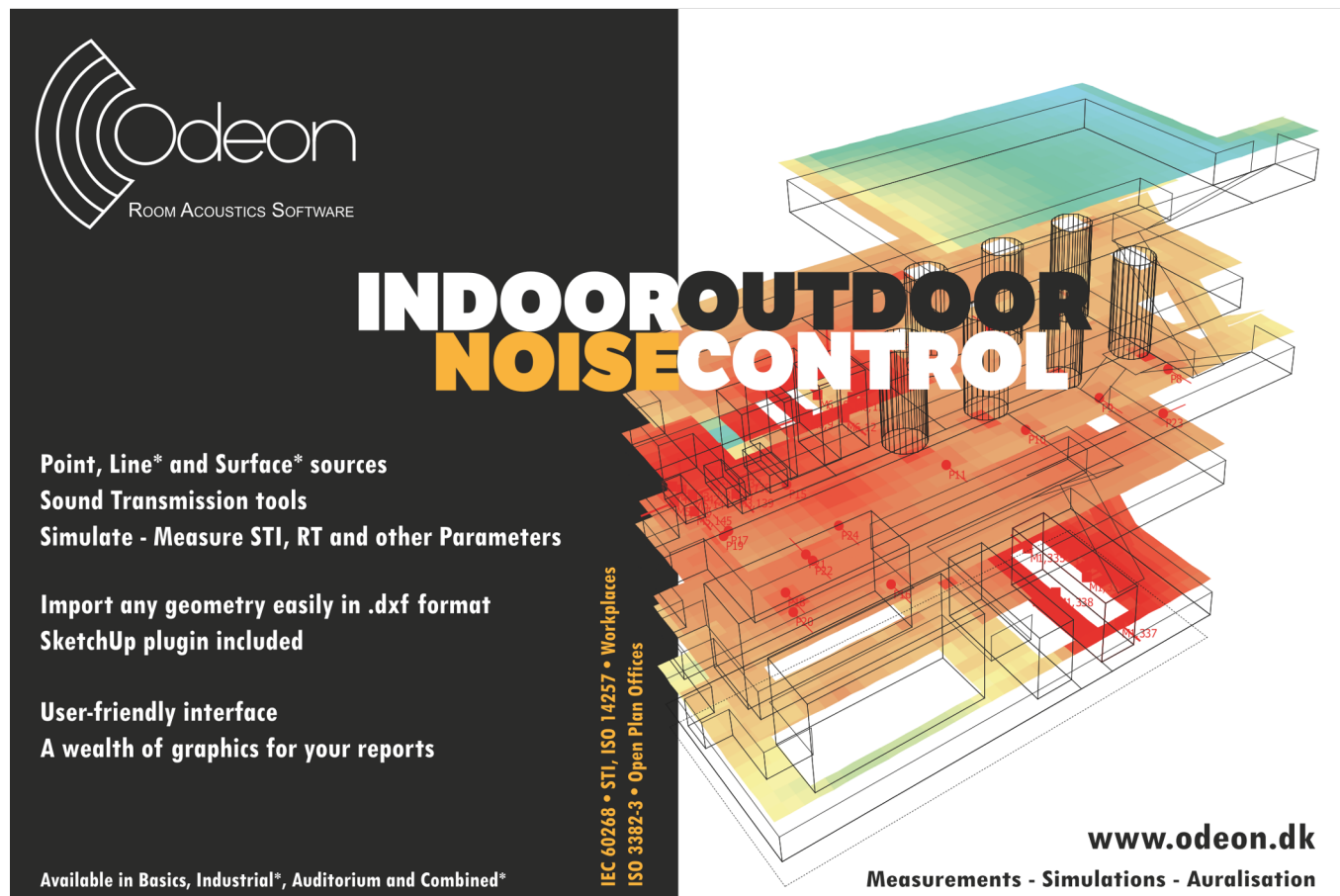
August 5th 2015

AWC18 à Victoria, B.-C.

La 176e rencontre de l'Acoustical Society of America (ASA) se tiendra conjointement avec la Semaine canadienne d'acoustique 2018 de l'Association canadienne d'acoustique à Victoria, C.-B., du 5 au 9 novembre 2018.

La conférence sera organisée par l'Acoustical Society of America selon leurs méthodes et procédures, tandis que l'Association canadienne d'acoustique y organisera des sessions spéciales et tiendra ses rencontres régulières ainsi que ses activités propres, telles la rencontre des comités de normalisation, le programme de prix pour les étudiants, etc. - - Pour plus d'information, visiter <http://acousticalsociety.org/meetings> - - Pour contacter Dr Roberto Racca, le coordinateur du congrès AWC2018, merci d'écrire un courriel à : conference@caa-aca.ca

November 24th 2017



Odeon
ROOM ACOUSTICS SOFTWARE

INDOOR OUTDOOR NOISE CONTROL

Point, Line* and Surface* sources
Sound Transmission tools
Simulate - Measure STI, RT and other Parameters

Import any geometry easily in .dxf format
SketchUp plugin included

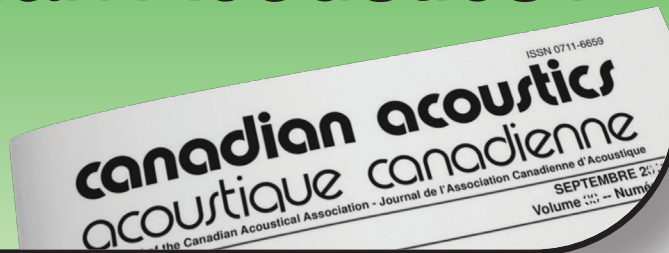
User-friendly interface
A wealth of graphics for your reports

Available in Basics, Industrial*, Auditorium and Combined*

IEC 60268 • STI, ISO 14257 • Workplaces
ISO 3382-3 • Open Plan Offices

www.odeon.dk
Measurements - Simulations - Auralisation

Why publish in Canadian Acoustics?



Because, it is...

- A respected scientific journal with a 40-year history uniquely dedicated to acoustics in Canada
- A quarterly publication in both electronic and hard-copy format, reaching a large community of experts worldwide
- An Open Access journal, with content freely available to all, 12 months from time of publication
- A better solution for fast and professional review providing authors with an efficient, fair, and constructive peer review process.

Pourquoi publier dans Acoustique canadienne ?



ISSN 0711-6659
canadian acoustics
acoustique canadienne
The Canadian Acoustical Association - Journal de l'Association Canadienne d'Acoustique
SEPTEMBRE 2018
Volume ... - Numéro ...

Parce que, c'est...

- Une revue respectée, forte de 40 années de publications uniquement dédiée à l'acoustique au Canada
- Une publication trimestrielle en format papier et électronique, rejoignant une large communauté d'experts à travers le monde
- Une publication "accès libre" dont le contenu est disponible à tous, 12 mois après publication
- Une alternative intéressante pour une évaluation par les pairs, fournissant aux auteurs des commentaires pertinents, objectifs et constructifs

Application for Membership

CAA membership is open to all individuals who have an interest in acoustics. Annual dues total \$110.00 for individual members and \$50.00 for student members. This includes a subscription to *Canadian Acoustics*, the journal of the Association, which is published 4 times/year, and voting privileges at the Annual General Meeting.

Subscriptions to *Canadian Acoustics* or Sustaining Subscriptions

Subscriptions to *Canadian Acoustics* are available to companies and institutions at a cost of \$110.00 per year. Many organizations choose to become benefactors of the CAA by contributing as Sustaining Subscribers, paying \$475.00 per year (no voting privileges at AGM). The list of Sustaining Subscribers is published in each issue of *Canadian Acoustics* and on the CAA website.

Please note that online payments will be accepted at <http://jcaa.caa-aca.ca>

Address for subscription / membership correspondence:

Name / Organization _____
 Address _____
 City/Province _____ Postal Code _____ Country _____
 Phone _____ Fax _____ E-mail _____

Address for mailing Canadian Acoustics, if different from above:

Name / Organization _____
 Address _____
 City/Province _____ Postal Code _____ Country _____

Areas of Interest: (Please mark 3 maximum)

- | | | |
|--|---|---|
| 1. Architectural Acoustics | 5. Psychological / Physiological Acoustic | 9. Underwater Acoustics |
| 2. Engineering Acoustics / Noise Control | 6. Shock and Vibration | 10. Signal Processing / Numerical Methods |
| 3. Physical Acoustics / Ultrasound | 7. Hearing Sciences | 11. Other |
| 4. Musical Acoustics / Electro-acoustics | 8. Speech Sciences | |

For student membership, please also provide:

 (University) (Faculty Member) (Signature of Faculty Member) (Date)

I have enclosed the indicated payment for:
 CAA Membership \$ 110.00
 CAA Student Membership \$ 50.00

Corporate Subscriptions (4 issues/yr)
 \$110 including mailing in Canada
 \$118 including mailing to USA,
 \$125 including International mailing

Sustaining Subscription \$475.00
 (4 issues/yr)

Please note that the preferred method of payment is by credit card, online at <http://jcaa.caa-aca.ca>

For individuals or organizations wishing to pay by check, please register online at <http://jcaa.caa-aca.ca> and then mail your check to:

**Executive Secretary, Canadian Acoustical:
 Dr. Roberto Racca
 c/o JASCO Applied Sciences
 2305-4464 Markham Street
 Victoria, BC V8Z 7X8 Canada**

Formulaire d'adhésion

L'adhésion à l'ACA est ouverte à tous ceux qui s'intéressent à l'acoustique. La cotisation annuelle est de 105.00\$ pour les membres individuels, et de 50.00\$ pour les étudiants. Tous les membres reçoivent *L'Acoustique Canadienne*, la revue de l'association.

Abonnement pour la revue *Acoustique Canadienne* et abonnement de soutien

Les abonnements pour la revue *Acoustique Canadienne* sont disponibles pour les compagnies et autres établissements au coût annuel de 105.00\$. Des compagnies et établissements préfèrent souvent la cotisation de membre bienfaiteur, de 475.00\$ par année, pour assister financièrement l'ACA. La liste des membres bienfaiteurs est publiée dans chaque issue de la revue *Acoustique Canadienne*.

Notez que tous les paiements électroniques sont acceptés en ligne <http://jcaa.caa-aca.ca>

Pour correspondance administrative et financière:

Nom / Organisation _____
Adresse _____
Ville/Province _____ Code postal _____ Pays _____
Téléphone _____ Téléc. _____ Courriel _____

Adresse postale pour la revue *Acoustique Canadienne*

Nom / Organisation _____
Adresse _____
Ville/Province _____ Code postal _____ Pays _____

Cocher vos champs d'intérêt: (maximum 3)

- | | | |
|---|-------------------------------|--|
| 1. Acoustique architecturale | 5. Physio / Psycho-acoustique | 9. Acoustique sous-marine |
| 2. Génie acoustique / Contrôle du bruit | 6. Chocs et vibrations | 10. Traitement des signaux / Méthodes numériques |
| 3. Acoustique physique / Ultrasons | 7. Audition | 11. Autre |
| 4. Acoustique musicale / Électro-acoustique | 8. Parole | |

Prière de remplir pour les étudiants et étudiantes:

_____ (Université) (Nom d'un membre du corps professoral) _____ (Signature du membre du corps professoral) _____ (Date)

Cocher la case appropriée:

- Membre individuel 110.00 \$
 Membre étudiant(e) 50.00 \$

Abonnement institutionnel

- 110 \$ à l'intérieur du Canada
 118 \$ vers les États-Unis
 125 \$ tout autre envoi international
 Abonnement de soutien 475.00 \$
(comprend l'abonnement à
L'acoustique Canadienne)

Merci de noter que le moyen de paiement privilégié est le paiement par carte crédit en ligne à <http://jcaa.caa-aca.ca>

Pour les individus ou les organisations qui préféreraient payer par chèque, l'inscription se fait en ligne à <http://jcaa.caa-aca.ca> puis le chèque peut être envoyé à :

Secrétaire exécutif, Association canadienne d'acoustique :

Dr. Roberto Racca
c/o JASCO Applied Sciences
2305-4464 Markham Street
Victoria, BC V8Z 7X8 Canada

BOARD OF DIRECTORS - CONSEIL D'ADMINISTRATION

OFFICERS - OFFICIERS

PRESIDENT
PRÉSIDENT

Jérémie Voix
ÉTS, Université du Québec
president@caa-aca.ca

EXECUTIVE SECRETARY
SECRÉTAIRE

Roberto Racca
JASCO Applied Sciences
secretary@caa-aca.ca

TREASURER
TRÉSORIER

Dalila Giusti
Jade Acoustics Inc.
treasurer@caa-aca.ca

EDITOR-IN-CHIEF
RÉDACTEUR EN CHEF

Umberto Berardi
Ryerson University
editor@caa-aca.ca

DIRECTORS - ADMINISTRATEURS

Alberto Behar
Ryerson University
albehar31@gmail.com

Michael Kieft
Dalhousie University
mkieft@dal.ca

Mehrzad Salkhordeh
dB Noise Reduction Inc.
mehrza@dbnoisereduction.com

Bill Gastmeier
HGC Engineering
bill@gastmeier.ca

Andy Metelka
SVS Canada Inc.
ametelka@cogeco.ca

Bryan Gick
University of British Columbia
gick@mail.ubc.ca

Hugues Nelisse
Institut de Recherche Robert-Sauvé
en Santé et Sécurité du Travail
(IRSST)
nelisse.hugues@irsst.qc.ca

UPCOMING CONFERENCE CHAIR
DIRECTEUR DE CONFÉRENCE (FUTURE)

Roberto Racca
JASCO Applied Sciences
conference@caa-aca.ca

PAST PRESIDENT
PRÉSIDENT SORTANT

Frank A. Russo
Ryerson University
past-president@caa-aca.ca

WEBMASTER
WEBMESTRE

Philip Tsui
RWDI
web@caa-aca.ca

PAST CONFERENCE CHAIR
DIRECTEUR DE CONFÉRENCE (PASSÉE)

Peter VanDelden
peter.vandelden@rwdi.com

AWARDS COORDINATOR
COORDINATEUR DES PRIX

Joana Rocha
Carleton University
awards-coordinator@caa-aca.ca

SOCIAL MEDIA COORDINATOR
COORDINATEUR MÉDIA SOCIAUX

Huiwen Goy
Ryerson University
huiwen.goy@psych.ryerson.ca

[Available Position](#)

SUSTAINING SUBSCRIBERS - ABONNÉS DE SOUTIEN

The Canadian Acoustical Association gratefully acknowledges the financial assistance of the Sustaining Subscribers listed below. Their annual donations (of \$475 or more) enable the journal to be distributed to all at a reasonable cost.

L'Association Canadienne d'Acoustique tient à témoigner sa reconnaissance à l'égard de ses Abonnés de Soutien en publiant ci-dessous leur nom et leur adresse. En amortissant les coûts de publication et de distribution, les dons annuels (de 475\$ et plus) rendent le journal accessible à tous les membres.

Acoustec Inc.

J.G. Migneron - 418-496-6600
info@acoustec.qc.ca
acoustec.qc.ca

Acoustex Specialty Products

Mr. Brian Obratoski - 2893895564
Brian@acoustex.ca
www.acoustex.ca

AcoustiGuard-Wilrep Ltd.

Mr Peter Harper - 416-471-3166
peter@wilrep.com
acoustiguard.com

AECOM

Alan Oldfield - 9057127058
alan.oldfield@aecom.com
aecom.com

Aercoustics Engineering Ltd.

Nicholas Sylvestre-Williams - (416) 249-3361
NicholasS@aercoustics.com
aercoustics.com

Bruel & Kjaer North America Inc.

Andrew Khoury - 514-695-8225
andrew.khoury@bksv.com
bksv.com

CDMca Ltd.

Jonas Salkauskis - 647-317-0692
jonas.salkauskis@cdmca.com
www.cdm.eu

Dalimar Instruments Inc

Monsieur Daniel Larose - 450-424-0033
daniel@dalimar.ca
www.dalimar.ca

dB Noise Reduction

Mehrzaad Salkhordeh - 519-651-3330 x 220
mehrzaad@dbnoisereduction.com
dbnoisereduction.com

FFA Consultants in Acoustics and Noise Control

Clifford Faszer - 403.508.4996
info@ffaacoustics.com
ffaacoustics.com

GHD

Michael Masschaele - +1 519 340 3818
michael.masschaele@ghd.com
ghd.com

H.L. Blachford Ltd.

Duncan Spence - 905-823-3200
amsales@blachford.ca
blachford.ca

HGC Engineering Ltd.

Bill Gastmeier -
bill@gastmeier.ca
hgcengineering.com

Integral DX Engineering Ltd.

Gregory Clunis - 613-761-1565
greg@integraldxengineering.ca
integraldxengineering.ca

Jade Acoustics Inc.

Ms. Dalila Giusti - 905-660-2444
dalila@jadeacoustics.com
jadeacoustics.com

JASCO Applied Sciences (Canada) Ltd.

Roberto Racca -
roberto.racca@jasco.com
jasco.com

Pyrok Inc.

Howard Podolsky - 914-777-7770
mrpyrok@aol.com
pyrok.com

ROCKFON

Dr. Gary S. Madaras - 708.563.4548
gary.madaras@rockfon.com
rockfon.com

RWDI

Mr. Peter VanDelden - 519-823-1311
peter.vandelden@rwdi.com
rwdi.com

Scantek Inc.

Steve Marshall - 1-410-290-7726
S.Marshall@scantekinc.com
scantekinc.com

West Caldwell Calibration Labs

Mary Richard - 905-554-8005
wcclca@gmail.com
wccl.com